INFORMATION TO USERS

This manuscript has been reproduced from the microfilm master. UMI films the text directly from the original or copy submitted. Thus, some thesis and dissertation copies are in typewriter face, while others may be from any type of computer printer.

The quality of this reproduction is dependent upon the quality of the copy submitted. Broken or indistinct print, colored or poor quality illustrations and photographs, print bleedthrough, substandard margins, and improper alignment can adversely affect reproduction.

In the unlikely event that the author did not send UMI a complete manuscript and there are missing pages, these will be noted. Also, if unauthorized copyright material had to be removed, a note will indicate the deletion.

Oversize materials (e.g., maps, drawings, charts) are reproduced by sectioning the original, beginning at the upper left-hand corner and continuing from left to right in equal sections with small overlaps.

ProQuest Information and Learning
300 North Zeeb Road, Ann Arbor, MI 48106-1346 USA
800-521-0600

Partial Oxidation of Methanol to Formaldehyde over Mo-Sn Oxide Catalysts

by

Rowaida George Zoumot

A thesis submitted to
the school of Graduate Studies
in partial fulfillment of the requirements for the
degree of Master of Applied Science
in
Chemical Engineering

DEPARTMENT OF CHEMICAL ENGINEERING
UNIVERSITY OF OTTAWA
OTTAWA, ONTARIO,

Dedication

TO MY PARENTS

Abstract

The vapor phase air oxidation of methanol to formaldehyde was investigated over molybdenum oxide, tin oxide and their mixtures in an integral flow reactor at atmospheric pressure between temperature of 513 and 573 K, a space time of 10-40 hr g-cat/g-mol methanol and a molar ratio of 0.04-0.1 mol CH_3OH/mol air. Experiments were done under such conditions that the effects of internal and external heat and mass transfer effects were negligible.

The effects of several process variables, temperature, space time and methanol/air ratio on the conversion of methanol and the selectivity of the catalyst for formaldehyde production were determined. The results indicated that the impact of the process variables on the conversion, selectivity and yield of formaldehyde were in the following decreasing order T > W/F > R.

A screening study indicated the optimum catalyst composition to be 50% SnO_2 and 50% MoO_3, while conversion increased with temperature and W/F selectivity decreased. This catalyst proved to be highly active and selective to formaldehyde production. Selectivity and yield of up to about 100% were obtained at 100% conversion at a temperature of 553 K, a space time (W/F) of 40 g-cat/g-mol methanol per hour and a molar ratio (R) of 0.04 mol CH_3OH/mol air.

The rate expression

$$r = \frac{k_1 P_M^2}{1 + \frac{k_1 P_M^2}{2k_2 P_{O_2}}}$$

was deduced assuming a steady-state involving two-stage irreversible oxidation-reduction process. It represented the experimental data satisfactorily. Arrhenius plots of the two rate constants gave activation energies of 31.7 and 18.1 kcal/g-mol.

Acknowledgement

I wish to express my sincere gratitude to my thesis advisor, Prof. R. S. Mann for his continuous encouragement and his invaluble guidance during the course of this investigation. I would like also to express my sincere thanks to the Jordan University of Science and Technology for its scholarship program.

Finally my deepest appreciation goes to all my professors and fellow graduate students for their assistance and friendliness.

Notation

Various symbols, superscripts, subscripts, and abbreviations used frequently in this work are summarized below. All notation is fully defined where it first arises in the text.

Symbols

a_m	area of the particle per unit mass, m^2/kg
A_o	defined as per Equation 7.9 and Table 4.2
A_1	defined as per Equation 7.9 and Table 4.2
C_p	constant pressure heat capacity per unit mass of fluid, J/gmol K
D	molecular diffusivity of the species being transferred into the system of interest, m^2/s
D_{AB}	bulk diffusivity, m^2/s
D_c	combined diffusivity (Knudsen and molecular diffusion), m^2/s
D_e	effective diffusivity, m^2/s
D_K	Knudsen diffusivity, m^2/s
D_p	catalyst particle diameter, m

$E(Y)$ expected value of the random variable Y,

F_i molar flow rate of component i, g-mol/hr

G mass velocity based on the total cross-sectional area of the reactor, kg/m^2 s

G_m mass velocity based on the total (superficial) cross-sectional area of the reactor, kg/m^2 s

h heat transfer coefficient between the catalyst particle and the bulk fluid, g sec^{-3}/K

j_D mass transfer factor

j_H heat transfer factor

J_i molar flux of species i towards the surface relative to molar average velocity, mol/m^2 s, Equation 3.16

k thermal conductivity of the fluid, g cm sec^{-3}/K

k_i reaction rate constant, Equation 3.7

M molecular weight of the gas mixture

N_{Pr} Prandtl number $= \frac{D_p G C_p}{k}$

N_{Re} Reynolds number $= \frac{D_p G}{\mu}$

N_{Sc} Schmidt number $= \frac{\mu}{\rho D}$

N'_{Re} modified Reynolds number $= \frac{D_p G}{\mu(1-\varepsilon_B)}$

$P_{f,i}$	film pressure factor of species i, Pa
P_i	partial pressure of species i, Pa
$P_{i,b}$	partial pressure of species i in the bulk, Pa
$P_{i,s}$	partial pressure of species i at the surface, Pa
r	reaction rate, mol/s g-catalyst
r_{mA}	molal reaction rate of component A, mol/s g-catalyst
$\overline{r}$	pore radius, m
$\overline{r}$	parameter as per Equation 2.67
R_g	gas constant, J/ mol K
$\overline{R}$	molar ratio of reactants, g-mol CH_3OH/g-mol air multiplied by 100
R	molar ratio of reactants, g-mol CH_3OH/g-mol air
S_g	catalyst specific surface area, m^2/kg
t	time of reaction, hr, Equation 2.3
T	temperature, K
T_b	temperature in the bulk fluid, K
T_s	temperature at the catalyst surface, K
W	weight of catalyst, g

W/F space time, hr g-cat/g-mol methanol

X_1, X_2, X_3, X_4 temperature, space time, reactants' molar ratio, and catalyst's composition, respectively, Equation 4.6

x_i fractional conversion of component i

Superscripts

$^{m}, ^{n}$ order of the reaction

Subscripts

$_0$ condition at reactor inlet

Greek Symbols

α defined as per Equation 3.5

β_i parameter associated with the independent variable x_i, Equation 4.1

δ_A ratio of stoichiometric coefficients, Equation 3.22

ΔG molal free energy of the reaction, J/mol

ΔH molal heat of reaction, J/mol

ΔY pressure gradient, Pa, Equation 2.46

ε catalyst porosity

ε_p porosity of the pellet

η effectiveness factor

θ_j	fraction of available sites occupied by j
λ	mean free path, cm, Equation 3.28
μ	fluid viscosity, kg/m s
Π	total pressure, Pa
ρ	fluid density, kg/m^3
ρ_p	apparent density of catalyst particle (mass per total particle volume), kg/m^3
τ	pressure-dependent residence time, hr g-cat atm/g-mol
τ	tortuosity factor (takes care of length and shape factors)
ϕ	shape factor, assumed 0.9 for irregular granules
Φ	Thiele-type modulus given by Equation 3.31

Abbreviations

C	conversion of methanol
ESR	Electron Spin Resonance
F	formaldehyde
M	methanol
S	selectivity of the catalyst
T	total liquid product

W	water
Y	yield of formaldehyde

Contents

List of Tables

List of Figures

Chapter 1

Introduction

The subject of chemical kinetics is concerned with the quantitative study of the rates of chemical reactions and of factors upon which they depend. It includes empirical studies of the effects of concentration, temperature and hydrostatic pressure on reactions of various types. Such studies may be of practical value in connection with technical processes. Kinetic studies of chemical reactions in which the objective is to arrive at a reaction mechanism are of fundamental interest.

The aim of any kinetic study is to attain a high yield and good selectivity. The use of an empirical rate expression is adequate in order to design the equipment for such reactions. However, it is desirable to obtain a model that would accurately predict the reaction behavior, since then it may be safe to extrapolate outside the range of experimental data.

The discovery of solid catalysts and their application to chemical processes in the early years of this century has led to breakthroughs in the chemical industry. Since then, this industry has diversified and grown in a spectacular way through the development of new or the rejuvenation of established processes, mostly based

on the use of solid catalysts. Because of the importance of catalysts in modifying the economics of chemical synthesis, a considerable amount of research activity has been directed towards improving the existing catalysts or discovering new ones.

For thermodynamically feasible reactions, catalysts help increasing the rate of reaction because they provide an alternate mechanism, each step of which has a lower free activation energy . This suggests that an intermediate substance might be formed by one or more of the reactants and the catalyst surface.

Catalytic reactions are classified according to the number of phases in which they occur. Homogeneous reactions are those that occur when only a single phase is involved in the process, whereas heterogeneous reactions are those associated with two or more phases, and occur at the interphase.

These reactions are very important in industry. One such reaction is the partial oxidation of methanol to formaldehyde, which is widely used as an intermediate chemical in a large variety of organic compounds. Because of its relatively low cost, higher impurity and reactivity, it has become one of the world's most important industrial and research chemicals. More than 3.0×10^6 tons of H_2CO are produced from CH_3OH annually in the U.S. alone [40]. There are two catalytic processes for converting methanol to formaldehyde. One uses Ag as a catalyst at temperature range between 870 and 920 K. It is essentially an oxidative dehydrogenation process [46]. The process operates on the fuel-rich side of the explosion limit, e.g., 30-40% CH_3OH vapor in air, and leads to a selectivity of 90% for H_2CO at 90% CH_3OH conversion [46]. The main by-products are CO, CO_2, H_2 and $HCOOH$. The second commercial process utilizes an iron-promoted MoO_3 catalyst and much lower temperature, i.e., 620 K. The feed typically contains

6-9 mole percent CH_3OH vapor in air. Selectivity to formaldehyde is typically 90% at near complete methanol conversion. It has been known that metal oxide catalysts containing molybdenum trioxide give better yield for the production of formaldehyde.

There are three stages of practical importance in the pyrolytic oxidation of methanol:

$$\frac{1}{2}O_2 + CH_3OH_{(g)} \longrightarrow HCHO_{(g)} + H_2O_{(g)} \quad \Delta H \text{ @ } 298\ K = -37\ kcal$$

$$\frac{1}{2}O_2 + HCHO_{(g)} \longrightarrow CO + H_2O_{(g)} \quad \Delta H \text{ @ } 298\ K = -56\ kcal$$

$$\frac{1}{2}O_2 + CO \longrightarrow CO_2 \quad \Delta H \text{ @ } 298\ K = -68\ kcal$$

At ambient temperatures, the rates of these reactions are insignificant. Since the rate of a chemical process is normally an exponential function of the temperature, the logical course is to operate at high temperatures. Unfortunately, the first and second oxidation stages occur in temperature ranges that overlap; the result is that under ordinary operating conditions, formaldehyde is destroyed almost as quickly as it is formed. Pure formaldehyde vapor begins to decompose at 573 K, so it would be convenient to find a way to induce the primary oxidation of methanol to take place at a lower temperature level. This calls for the use of catalyst.

However, with the aid of a catalyst, the aim of the straight oxidation of methanol is to induce the primary oxidation to take place rapidly at temperatures below those at which the second stage occurs at an appreciable rate. This is possible because the primary stage becomes a heterogeneous reaction whereas the

second stage occurs homogeneously in the gas phase and its rate will depend on the rate at which heat can pass into, and spread through, a poor heat-conductor. Thus although the thermodynamic conditions favor the decomposition of formaldehyde [26], the poor conductivities of both catalyst and gas tend to retard this reaction and so preserve the formaldehyde.

In studying such systems several devices are available to measure the reaction rate either in a differential or in an integral reactor. In the differential method the reactor operates at a low conversion so that the reaction rate may be assumed constant. The integral method is carried out with a steady-state process making the experimental accuracy greater. However, the latter method presents difficulties in the integration of the rate equation because there are several hidden parameters. In this investigation, a fixed-bed integral reactor operating at atmospheric pressure was used.

Since 1931 when Adkins and Peterson [2] discovered the high activity of the mixed Fe_2O_3-MoO_3 catalyst for oxidation of methanol to formaldehyde, most patents and fundamental research dealing with this process have been concerned with the Fe_2O_3-MoO_3 system. The activity may be substantially ascribed to MoO_3. However, it is only recently that the importance of tin-oxide based catalytic systems has begun to be recognized. These catalysts occur in many forms and are used in a wide range of application from electrolysis to gas-phase reactions [23].

This study focuses on the oxidation of methanol over oxide catalysts containing MoO_3 and SnO_2 and their mixtures. The motivation of such study is the lack of information regarding the use of tin oxide with molybdenum trioxide as a catalyst for this reaction.

The objectives of this research were :

- to study the effect of process variables, i.e. temperature (T), space time (W/F), methanol to air molar ratio (R), and catalyst composition on the conversion, selectivity, and yield of the methanol oxidation reaction;
- to study the kinetics and postulate a possible mechanism for the catalytic oxidation of methanol to formaldehyde;
- and to develop a suitable rate expression, which would satisfactorily represent the experimental data.

Chapter 2

Literature Review

A great deal of interest exists for the study of new or modified form of solid catalysts for existing processes and new applications. Development has often been realized by improvement in the experimental characterization techniques. In broad sense characterization includes chemical surface and bulk composition, physicochemical properties manifested in adsorption and reaction kinetics. For years several metal catalysts had been used for the production of formaldehyde. Recently the metal oxide catalyst process has assumed increased importance since it has proven to give better yield.

2.1 Development of Formaldehyde Production

As previously mentioned in chapter one, the first comprehensive study for the oxidation of methanol to formaldehyde on a metal oxide catalyst, MoO_3, Fe_2O_3 and their mixtures was carried out by Adkins and Peterson in 1931 [2]. Since then several other researchers have studied the use of other metal oxides as catalyst for this particular reaction. It is observed that MoO_3 has proven to be an extremely good catalyst with high selectivity for this reaction. The other metal oxide added

to it in most cases act as a promoter. Its purpose is to enhance conversion without sacrificing the selectivity gained by the MoO_3. Details about metallic catalysts can be found in a comprehensive bibliographic review on formaldehyde research published by Walker [54] . Also details about metal oxides catalysts can be found in Dosi [16], Jain [24], and Diaz [15]. The most recent research works related to formaldehyde production including catalysts properties, reaction kinetics and reaction mechanism are summarized below:

Bliznakov et al. [8] proposed that the selectivity of V_2O_5 catalyst for conversion of methanol to formaldehyde increased by adding TeO_2 and MoO_3. They found that the binary system $V_2O_5 - TeO_2$ gave an unsatisfactory degree of conversion, while the three component $V_2O_5 - MoO_3 - TeO_2$ catalyst had a stable activity and oxidized methanol with a specific rate comparable with the industrial iron-molybdenum catalyst.

Gasser and Baiker [19] studied methanol oxidation on vanadium oxide catalyst. The results indicate that amorphous vanadium undergoes structural changes more easily than its crystalline counterpart and may thus be an interesting catalyst precursor.

The mechanism of partial oxidation of methanol over MoO_3 was studied by Chung et al. [13]. The reaction can be represented by a mechanism involving methoxy intermediate chemisorbed on oxygen vacancy sites. Formaldehyde and CO are mainly produced from methoxy on terminal oxygen (Mo=O) vacancy sites.

Louis et al. [31] studied two types of MoO_3 on SiO_2 catalyst for the oxidation of methanol, one prepared by the classical impregnation method, the other by the grafting method. They found that there is a dependence of the formation of

formaldehyde and methyl formate. This could not be clearly for the impregnated catalyst. They proposed a mechanism which involves the formation of formaldehyde from methanol by its migration on silica, where it further reacts with methoxy groups to form methyl formate.

Yang and Lunsford [57] found that molybdenum oxide supported on high surface area silica to be an active catalyst for methanol oxidation to formaldehyde, but at high conversion the selectivity is considerably less than that reported for commercial catalysts. Kinetic isotopes studies confirmed an ealier observation that the breaking of C-H bonds in the methyl group was slow in the catalytic cycle.

To increase the yield of formaldehyde obtained with the industrial catalyst, Estevey et al. [17] proposed that the addition of chromium (III), even in small quantities, produced a lower Mo/Fe atomic ratio and increased the specific surface area.

Methanol oxidation over nonprecious transition metal oxide catalysts supported on 1/8-in $\gamma - Al_2O_3$ tablets was studied by Ozkan et al. [43]. The catalyst oxides of (Cr, Mn, Fe, N, Cu) were prepared using the incipient wetness technique. All the catalysts exhibited similar activities for methanol conversion. However, formaldehyde was observed only on non-copper catalysts in small quantities. Dimethyl ether was the major reaction product over these catalysts.

The kinetics of the vapor-phase air oxidation of methanol to formaldehyde over MoO_3 and Sb_2O_4 catalysts and their mixtures was studied by Diaz [15]. On the basis of his study a catalyst containing 67% $Sb_2O_4 - 33\%$ MoO_3 proved to be highly active and selective to formaldehyde formation.

Recently, Neophytides and Vayenas [40] investigated a new process for formalde-

hyde production. They studied the anodic oxidation of methanol in the solid electrolyte fuel cell CH_3OH, H_2CO, CO, CO_2, H_2, H_2O $Ag|ZrO_2(8\%Y_2O_3)|Ag$, air operating at atmospheric pressure. It was found that methanol can be selectively oxidized to formaldehyde with simultaneous production of electrical energy. Selectivity to formaldehyde was of the order 90% at methanol conversions exceeding 30%. The main by-products were CO and CO_2.

Formaldehyde production from methanol using a porous vycor glass membrane reactor was studied by Song and Hwang [49]. They investigated the reaction kinetics in a fixed bed differential reactor over 99.998% silver needle catalyst. The membrane reactor performance was experimentally analyzed at atmospheric pressure to study the effect of changing operating variables such as temperature, space velocity, air/methanol feed ratio and membrane surface area.

Klissurski et al. [28] studied the activity and selectivity of multicomponent oxide catalysts containing Co, Ni, Fe, and Bi molybdates. The unsupported and silica-supported catalysts, some of them promoted with phosphorus and thallium, have been characterized by x-ray diffraction, infrared spectroscopy, Moessbauer spectroscopy, surface area and porous structure measurements. The selectivity of the investigated catalyst towards the oxidation of methanol to formaldehyde remains extremely high over a wide temperature interval (350-390 degree C). Significant difference in thermal stability of the catalyst during exploitation has been observed and attributed to the presence of a support and promoters.

Sohrabi et al. [48] put forward a two-step mechanism for the oxidation of methanol using a mixture of ferric and molybdenum oxides as catalyst. According to this mechanism, methanol is first oxidized to formaldehyde, accepting an oxygen

molecule from the catalyst and changing the latter into the reduced form. In the second step, the reduced catalyst is transformed into the original form on obtaining an oxygen molecule from the gas phase.

Anhydrous formaldehyde is required for many syntheses and therefore its production is of potential interest. Meyer and Renken [37] found that catalysts based on alkali compounds are active in the dehydrogenation of methanol in absence of oxygen. Sodium carbonate doped with indium shows a selectivity of up to 75% for methanol conversion not exceeding 60%.

2.2 Characterization and Properties of Tin Oxide

It is possible for tin to be present in various forms including metallic oxide as either stable oxide SnO or SnO_2. Tin oxide is an n-type, wide-gap, semiconducting oxide material which is transparent to visible light. Consequently, it is important as an electrode material, in solar cell applications, as a sensor material and as a transparent conductor in electronic displays.

The chemical activity of tin oxide and particularly its redox properties make it an important catalytic material in both pure and mixed oxide forms for gas phase reactions and for electrocatalytic or photoelectrocatalytic reactions. Although tin oxide functions as an oxidative catalyst in most studies, it can also function in a reductive manner.

Complete review of tin oxide-based catalytic systems can be found in Hoflund [23]. It describes some important aspects relating to these catalytic systems.

Buiten [9] studied the oxidation of propylene with molecular oxygen at 370°C

and atmospheric pressure by means of $SnO_2 - MoO_3$ catalysts. SnO_2 showed some catalytic activity. However, SnO_2 covered with a monolayer of molybdenum oxide is 5 to 10 times more active in the oxidation of propylene than SnO_2 alone, and gives a completely different product distribution. On the basis of this study, it was concluded that although MoO_3 did not form a bulk compound with SnO_2 surface, it could be bound to the SnO_2 surface, which then exhibited a peculiar catalytic activity.

Based on this study, Tan et al. [51] studied the oxidation of olefin to ketone over SnO_2-MoO_3 catalysts. They found that propylene is converted to acetone at 100-160°C with more than 90% selectivity over SnO_2-MoO_3. They proposed that the active site seems to involve an acetic point, which is formed by the combination of tin oxide with molybdenum trioxide.

The mechanism of methanol oxidation over $SnO_2 - MoO_3$ catalyst from the viewpoint of the active molybdenum site was investigated by Niwa et al. [38]. They examined the activities of various mixed oxides, including $Fe_2O_3 - MoO_3$, and found higher activities over $SnO_2 - MoO_3$ and $TiO_2 - MoO_3$ catalysts than over $Fe_2O_3 - MoO_3$ catalyst. In the case of mixed $SnO_2 - MoO_3$ catalysts, formaldehyde was formed selectively at 180°C.

The catalytic activity of antimony oxide catalyst dispersed on SnO_2 for propene oxidation was studied by Ono et al. [42]. They proposed that the formation of CO and CO_2 is dominant on SnO_2 catalysts. This gives an indication that tin oxide catalysts play an important role in giving the catalyst high oxidation activity. Kinetic features obtained using simple redox mechanism indicate that the reoxidation step is the rate-determining step over SnO_2.

Reddy et al. [45] reported the direct correlation between low-temperature oxygen chemisorption (LTOC) capacity of a series of SnO_2 supported V_2O_5 and MoO_3 catalysts and their catalytic activity for the partial oxidation of methanol. They found that the amount of oxygen chemisorbed at $-78°C$ on V_2O_5/SnO_2 and MoO_3/SnO_2 correlate directly with the conversion of methanol at 175°C. These catalysts have shown high selectivity for the formation of formaldehyde. Selectivity was over 95% for V_2O_5/SnO_2 and 90% for MoO_3/SnO_2.

Chapter 3

Theoretical Aspects

The relationship between reaction rate and operating variables is an important factor in the design of any catalytic process. This chapter gives a general outlook about the types of mechanisms that are used for kinetic analysis and their characteristics. It also deals with heat and mass transfer related properties on catalyst surface.

3.1 Kinetic Analysis

Chemical kinetics deals with the quantitative studies of the rates at which chemical processes occur, the factors on which these rates depend, and the molecular acts involved in reaction processes. A description of a reaction in terms of its constituent molecular acts is known as the mechanism of the reaction. The term *mechanism* [7] describes all the individual collisional or elementary processes involving molecules (atoms, radicals and ions included) that take place simultaneously or consecutively in producing the observed overall rate. Heterogeneous catalytic reactions consist of at least three single steps: adsorption, surface reaction, and desorption. Considerable simplification results when there is a single

rate-determining step. However, only when surface reaction is the rate-limiting step are overall kinetics governed by the kinetics of the reaction step. On the other hand, if desorption of product is the rate-limiting step, then overall kinetics measured in the gas phase do not reflect the kinetics of the surface-reaction rate [14].

3.1.1 Mechanistic Steps in Heterogeneous Catalytic Reactions

The sequence of physical and chemical steps which occur in an heterogeneous catalytic reaction is as follows [10]:

1. Mass transfer of reactant from the main body of the fluid to the gross exterior surface of the catalyst particle.
2. Molecular diffusion and/or Knudsen flow of reactants from the exterior surface of the catalyst particle into the interior pore structure.
3. Chemisorption of at least one of the reactants on the catalyst surface.
4. Reaction on the surface. (this may involve several steps).
5. Desorption of (chemically) adsorbed species from the surface of the catalyst.
6. Transfer of the products from the interior catalyst pores to the gross external surface of the catalyst by ordinary molecular diffusional/or Knudsen diffusion.
7. Mass transfer of the products from the exterior surface of the particle into the bulk of the fluid.

Steps 1, 2, 6, and 7 are physical processes, while steps 3 to 5 are basically chemical in character. The rates of the various steps depend on a number of factors in addition to the concentration profiles of the reactants and product species.

Steps 1 and 7 are highly dependent on the fluid flow characteristics of the system. Hence, the rate of these steps depends on the mass velocity of the fluid stream, the particle size, and the diffusional characteristics of various molecular species. These steps limit the observed rate only when the catalytic reaction is very rapid and the mass transfer is slow. Steps 2 and 6 depend on the degree of porosity of the catalyst, the dimensions of the pores, the degree to which the pores are interconnected, the gross dimension of the catalyst particle itself, the rate at which the reaction occurs at the catalyst surface, and the diffusional characteristics of the reaction mixture. In order to derive a true rate equation, the preceding factors, which may affect the mechanism significantly, must be minimized as much as possible. It is convenient to employ the concept of a rate-limiting step in the treatment of these processes so that the reaction rate becomes equal to that of the slowest step.

3.1.2 Kinetic Model

In heterogeneous catalysis it is desirable to derive the rate expression based on the Langmuir-Hinshelwood theory [29].

Langmuir-Hinshelwood Mechanism

This type of mechanism assumes that adsorption and desorption processes are in equilibrium at constant pressure and that the reaction takes place between either an adsorbed molecule and a gaseous reactant molecule or between two

chemisorbed molecules on adjacent sites. Rate equation is derived by assuming a rate mechanism and selecting the slowest step as rate-controlling. Further details are given by Smith [47] and by Yang and Hougen [56].

Modified Langmuir-Hinshelwood Mechanism

When the rate of adsorption of reactants offers significant resistance, the assumption of adsorption equilibrium in the original Langmuir-Hinshelwood theory is not valid.

The modified mechanism considers that reactants adsorbed on the surface increase by adsorption and decrease by reaction. When the two rates are equal, the equilibrium conditions are established. This mechanism is generally termed redox mechanism. Oxidation of oxygenated hydrocarbons can be treated as irreversible two- or three-stage oxidation-reduction reaction. A three-stage mechanism has been reviewed by Diaz [15]. A two-stage mechanism is briefly described here.

Two-stage redox mechanism

The oxidation of methanol to formaldehyde taking place by a two-stage redox mechanism can be visualized to occur through the following two steady-state steps, with the equilibrium shifted to the right side

$$CH_3OH + S_{ox} \xrightarrow{k_1} HCHO_{(g)} + H_2O + S_{red} \tag{3.1}$$

$$O_{2(g)} + S_{red} \xrightarrow{k_2} S_{ox} \tag{3.2}$$

The rates of the above reactions are given by:

$$r_1 = k_1 P_M^m \theta \tag{3.3}$$

$$r_2 = k_2 P_{o_2}^n (1 - \theta) \tag{3.4}$$

$$\alpha r_1 = r_2 \tag{3.5}$$

where θ is defined as the fraction of catalyst surface covered by adsorbed or lattice oxygen and α the number of oxygen molecules required to convert one molecule of methanol. It is equal to 0.5 in the present case. Based on Equations 3.3, 3.4 and 3.5, the following expressions can be derived:

$$\theta = \frac{1}{1 + \frac{\alpha k_1 P_M^m}{k_2 P_{O_2}^n}} \tag{3.6}$$

$$r = r_1 = \frac{k_1 P_M^m}{1 + \frac{\alpha k_1 P_M^m}{k_2 P_{O_2}^n}} \tag{3.7}$$

where r is the rate of oxidation of methanol to formaldehyde. The integrated forms of the rate equation with different values of m and n are given in Table 3.1, where

$$P_M = P_{M_o}(1 - x) \tag{3.8}$$

$$P_{O_2} = P_{O_2^o} - \frac{1}{2} P_{M_o} x \tag{3.9}$$

and

P_M = partial pressure of methanol at time t

P_{M_o} = partial pressure of methanol in the feed

P_{O_2} = partial pressure of oxygen at time t

$P_{O_2^o}$ = partial pressure of oxygen in the feed

x = conversion of methanol to formaldehyde

Table 3.1: Two-stage redox mechanism

No.	Reaction Order		Integrated Rate Equation
	m CH_3OH	n O_2	
1	0.5	0	$\frac{W}{F}\frac{1}{x} = -\frac{2}{k_1}\frac{(1-x)^{0.5}-1}{xP_{M_o}^{0.5}} + \frac{\alpha}{k_2}$
2	0.5	0.5	$\frac{W}{F}\frac{P_{M_o}^{0.5}}{2[(1-x)^{0.5}-1]} = -\frac{1}{k_1} - \frac{2\alpha}{k_2}[\frac{(P_{O_2^o}-0.5P_{M_o}x)^{0.5}-(P_{O_2^o})^{0.5}}{P_{M_o}^{0.5}[(1-x)^{0.5}-1]}]$
3	1	0	$\frac{W}{F}\frac{P_{M_o}}{ln(1-x)} = -\frac{1}{k_1} + \frac{\alpha}{k_2}\frac{xP_{M_o}}{ln(1-x)}$
4	1	0.5	$\frac{W}{F}\frac{P_{M_o}}{ln(1-x)} = -\frac{1}{k_1} - \frac{4\alpha}{k_2}\frac{(P_{O_2^o}-0.5P_{M_o}x)^{0.5}-(P_{O_2^o})^{0.5}}{ln(1-x)}$
5	1	1	$\frac{W}{F}\frac{P_{M_o}}{ln(1-x)} = -\frac{1}{k_1} - \frac{2\alpha}{k_2 ln(1-x)}ln[\frac{P_{O_2^o}-0.5P_{M_o}x}{P_{O_2^o}}]$
6	1.5	0	$\frac{W}{F}\frac{1}{x} = \frac{2}{k_1 P_{M_o}^{1.5}(1-x)^{0.5}} + \frac{\alpha}{k_2}$
7	1.5	0.5	$\frac{W}{F}\frac{P_{M_o}^{1.5}}{2[(1-x)^{-0.5}-1]} = \frac{1}{k_1} - \frac{2\alpha P_{M_o}^{0.5}}{k_2}[\frac{(P_{O_2^o}-0.5P_{M_o}x)^{0.5}-(P_{O_2^o})^{0.5}}{[(1-x)^{-0.5}-1]}]$
8	1.5	1	$\frac{W}{F}\frac{P_{M_o}^{1.5}}{2[(1-x)^{-0.5}-1]} = \frac{1}{k_1} - \frac{\alpha P_{M_o}^{0.5}}{k_2[(1-x)^{-0.5}-1]}[ln\frac{(P_{O_2^o}-0.5P_{M_o}x)}{P_{O_2^o}}]$
9	2	0	$\frac{W}{F}\frac{1}{x} = \frac{1}{k_1 P_{M_o}^2(1-x)} + \frac{\alpha}{k_2}$
10	2	0.5	$\frac{W}{F}P_{M_o}^2(\frac{1-x}{x}) = \frac{1}{k_1} - \frac{4\alpha P_{M_o}(1-x)}{k_2 x}[(P_{O_2^o}-0.5P_{M_o}x)^{0.5} - (P_{O_2^o})^{0.5}]$
11	2	1	$\frac{W}{F}P_{M_o}^2(\frac{1-x}{x}) = \frac{1}{k_1} - \frac{2\alpha P_{M_o}(1-x)}{k_2 x}ln[\frac{(P_{O_2^o}-0.5P_{M_o}x}{P_{O_2^o}}]$

3.2 Plug-Flow Reactors

The operation of catalytic reactors is defined by a number of parameters. For instance, a change in mass defines whether the reactor is a batch or a flow reactor. Exchange of temperature defines whether the reactor is adiabatic or isothermal. There are other important parameters in defining the operation of the catalytic reaction such as reactor volume, residence time, and space time. The experimental study of catalytic kinetics usually involves measuring the extent of conversion of the gas passing in steady flow through a batch of solids [30].

For a heterogeneous catalytic reaction, the rate must be expressed per unit weight or per unit area of the catalyst. A material balance for any species, j, over a differential element of the reactor (Figure 3.1) gives the following:

$$\text{input} + \text{generation by reaction} = \text{output} + \text{accumulation}$$

At steady state the accumulation is equal to zero, hence

$$(F_j) + (r_j dW) = (F_j + dF_j) \tag{3.10}$$

The rate of formation of species j in terms of the catalyst weight, W, is given by

$$r_j = \frac{dF_j}{dW} \tag{3.11}$$

where

F_j = molar flow rate of j, g-mol j/hr

W = mass of catalyst, g

r_j = net rate of formation of j, g-mol j/hr g-catalyst

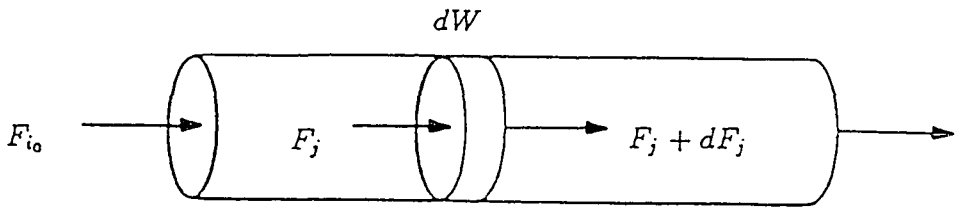

Figure 3.1: Notation for plug flow reactor

Defining the fractional conversion of reactant compound, i, into species j as:

$$x_j = \frac{F_j}{F_{i_o}} \tag{3.12}$$

therefore

$$F_j = F_{i_o} x_j \tag{3.13}$$

and

$$dF_j = F_{i_o} dx_j \tag{3.14}$$

where F_{i_o} is the molar flow rate of reactant compound i, g-mol i/hr.

Substituting the above differential rate expressions over the entire plug-flow reactor gives the plug flow performance equation

$$\frac{W}{F_{i_o}} = \int_{x_{j_o}}^{x_j} \frac{dx_j}{r_j} \tag{3.15}$$

3.2.1 Initial Rate Equation

All the results of this study were derived from a steady, plug-flow, integral reactor. The reaction rate and the concentration vary significantly in the axial direction of a plug-flow reactor. There are several assumptions that are made before deriving the corresponding rate equation:

1. The velocity profile in the reactor is flat, i.e. plug-flow exists. This can be verified by the small size of the catalyst particles and due to the presence of the fine porous plate at the inlet of the reactor.

2. The reactor operates isothermally, i.e. there are no thermal gradients in the reactor. This ideal state can be approximated by inserting the reactor in a fluidized sand bed and by having catalyst dilution, i.e. adding inert solids to the catalyst bed.

3. There is no change in the total molar flow rate during the course of the reaction. This assumption can be verified by the large excess of air which consists of 78.5 mol percent (inert) nitrogen.

4. There is no pressure drop across the reactor.

After the effects of heat and mass transfer and diffusion have been minimized, selection of the rate-determining chemical step is in order. For gaseous reactions catalyzed by solid surfaces, each separate molecular change usually consists of one or two rate-controlling chemical steps such as chemisorption with or without association of one or both reactants; surface reaction between adsorbed reactants and products, and impact of non adsorbed reactant with one that is adsorbed.

Rate expressions may be expressed by a combination of three terms; the kinetic term, the potential term and the adsorption term. Detailed expressions for these general rate equations can be found in a paper by Yang and Hougen [56]. In this paper there are several curves that in a general way show the effects of total pressure and feed composition on initial rates (rates at zero percent conversion). Each curve would be of a similar shape to the parent curve at zero conversion but would drop progressively with increase in percentage conversion and reach a zero-rate curve at equilibrium. In general where adsorption is controlling, the rate curve plotted against conversion at constant pressure and temperature is concave downwards whereas when surface reaction is controlling it is concave upwards.

3.3 Mass and Heat Transfer

A catalyst particle can be effective only if the reactants can reach the catalytic surface. The transfer of reactant from the bulk fluid to the outer surface of the catalyst particle requires a driving force, the concentration difference. Whether this difference in concentration between bulk fluid and particle size is significant or negligible depends on the velocity pattern in the fluid near the surface, the physical properties of the fluid, and the intrinsic rate of the chemical reactions at the catalyst; that is, it depends on the mass-transfer coefficient between fluid and surface and the rate constant for the catalytic reaction.

There will be also a temperature difference between bulk fluid and catalyst surface. Its magnitude will depend on the heat-transfer coefficient between the fluid and catalyst surface, the reaction-rate constant, and heat of reaction.

3.3.1 External Mass Transfer in Fixed Bed Reactors

Average transport coefficients between the bulk stream and particle surface can be correlated in terms of dimensionless groups which characterize the flow conditions. In the gas phase system, it is convenient to define a mass transfer coefficient based on a partial pressure driving force ($k_{P,i}$) as

$$k_{P,i} = \frac{J_i}{P_{i,b} - P_{i,s}} \tag{3.16}$$

The mass transfer coefficient based on a concentration driving force ($k_{C,i}$) therefore is

$$k_{C,i} = k_{P,i} R_g T \tag{3.17}$$

It is common practice to correlate mass transfer data in terms of the well-known Chilton-Colburn j_D factor [12]

$$j_D = \frac{k_{C,i}\rho}{G_m} N_{Sc}^{2/3} \tag{3.18}$$

where N_{Sc} is the Schmidt number and is given by

$$N_{Sc} = \frac{\mu}{\rho D} \tag{3.19}$$

and:

J_i = molar flux of species i towards the surface relative to molar average velocity, mol/m^2 s

$P_{i,b}$ = partial pressure of species i in the bulk, Pa

$P_{i,s}$ = partial pressure of species i at the surface, Pa

R_g = gas constant, J/gmol K

ρ = fluid density, kg/m^3

μ = fluid viscosity, kg/m s

D = molecular diffusivity of the species being transferred into the system of interest, m^2/s

G_m = mass velocity based on the total (superficial) cross- sectional area of the reactor, kg/m^2 s

The j_D factor can be expressed in terms of the film pressure factor for species A, $P_{f,A}$, as

$$P_{f,A} = \frac{(\Pi + \delta_A P_A) - (\Pi + \delta_A P_{A,s})}{ln \frac{\Pi + \delta_A P_A}{\Pi + \delta_A P_{A,s}}} \tag{3.20}$$

then j_D can be expressed as

$$\frac{k_{P,A} P_{f,A}}{G_m} N_{Sc}^{2/3} \tag{3.21}$$

where:

Π = total pressure, Pa

P_A = partial pressure of species A, Pa

$P_{A,s}$ = pressure of species A at the catalyst surface, Pa

and δ_A is given by

$$\delta_A = \frac{r + s + ... - a - b}{a} \tag{3.22}$$

where a,b,r,s,... are the stoichiometric coefficients of the reaction

$$aA + bB + ... \rightleftharpoons rR + sS + ...$$

The effect of mass transfer can be determined from the following relation

$$r_{mA} = k_{G,A} a_m \phi (P_A P_{A,s}) \tag{3.23}$$

where:

r_{mA} = molal reaction rate of component A, gmol s g-catalyst

a_m = area of the particle per unit mass, cm^2/g

ϕ = shape factor, assumed 0.9 for irregular granules

The pressure gradient, ΔY, can be determined from the equations proposed by Yoshida et al. [58]. The pressure gradient is given by the equation

$$\Delta Y_A = \frac{\Delta P_A}{P_A} = \frac{r_{mA}}{a_m \phi G_m} (j_D)^{-1} \frac{P_{A,s}}{\Pi} (N_{Sc})^{2/3} \tag{3.24}$$

Further details can be found in Ajaka [3]. Calculations and estimations for the external and internal mass transfer effects are shown in Appendix E.

3.3.2 Heat Transfer

Heat transfer to or from a fixed bed of catalyst often represents a significant problem. In laboratory studies aimed at a determination of the rate expression for the intrinsic chemical reaction, external gradients in temperature and concentration can be made negligible by operating under the following constraints [10]:

1. Using a reactant stream that is diluted with inerts to reduce the reaction rate so that the energy evolved per unit volume is greatly reduced below that encountered in the absence of inerts.

2. Employ high mass velocities to minimize resistance to heat and mass transfer.

Heat transfer between a fluid and particle surface occurs by the same molecular and convective processes which describe mass transfer. For heat transfer the equation analogous to Equation 3.18 is

$$j_H = (\frac{h}{C_p G})N_{Pr}^{2/3} \tag{3.25}$$

where N_{Pr} is the Prandtle number and is given by:

$$N_{Pr} = \frac{C_p \mu}{k} \tag{3.26}$$

where

μ = fluid viscosity, g/cm s

C_p = constant pressure heat capacity per unit mass of fluid, J/gmol K

k = thermal conductivity of the fluid, g cm sec^{-3}/K

G = mass velocity based on the total cross-sectional area of the reactor, g/cm^2 s

h = heat transfer coefficient between the catalyst particle and the bulk fluid, g sec^{-3}/K

The effect of heat can be verified from the difference between the temperatures of the bulk fluid and that of the catalyst surface. This is given by the following relation

$$T_s - T_b = \frac{r_{mA}(-\Delta H_A)}{\phi h a_m} \tag{3.27}$$

where:

T_s = temperature at the catalyst surface, K

T_b = temperature in the bulk fluid, K

ΔH_A = molal heat of reaction of A, J/gmol

Calculations for the heat transfer effects are shown in Appendix E.

3.4 Diffusion

External surface area of porous catalysts constitutes a small fraction of the total surface area on which the reaction takes place. One or more of several different mechanisms may be responsible for the mass transfer process. For the majority of catalysts and conditions used in industrial practice, the only significant mechanisms are bulk diffusion and Knudsen diffusion. The relative importance of these two processes depends on the relative values of the mean free path and the pore dimensions.

3.4.1 Molecular or Bulk Diffusion

If the mean free path of the diffusing molecule is small with respect to the pore radius, the collisions between molecules control diffusion and the molecular or bulk diffusion is applicable. The mean free path (λ) is the average distance a molecule travels between intermolecular collisions. A rough equation for λ is given by Wheeler [55]:

$$\lambda = \frac{10^{-5}}{\Pi} \tag{3.28}$$

where Π is the pressure in atm and λ in cm.

The effective diffusivity is independent of the pore diameter, and within a given

catalyst pore ordinary bulk diffusion coefficient may be used in Fick's law to evaluate the rate of mass transfer and the concentration profile in the pore.

The effect of molecular diffusion is minimized by using high velocity of gas stream passing through the catalyst bed, and the space time is kept constant.

3.4.2 Knudsen Diffusion

Knudsen diffusion prevails whenever the mean free path between collisions is large compared with the pore diameter. It depends on the molecular velocity and the pore radius, and it is independent of pressure. The molecules hitting the walls are momentarily adsorbed and then are given off in random directions (diffusely reflected). After a collision with the pore wall, the molecule will usually fly to another spot on the wall before having a collision with a second gas phase molecule. Many collisions with the walls will take place for each collision between gas phase molecules.

The effective Knudsen diffusivity is given as:

$$D_K = 19400 \frac{\varepsilon^2}{\tau S_g \rho_p} \sqrt{\frac{T}{M}} \tag{3.29}$$

where

$D_K =$ Knudsen diffusivity, cm^2/s

T = temperature, K

$\varepsilon =$ catalyst porosity

$\tau =$ catalyst tortuosity

$S_g =$ catalyst specific surface area, cm^2/g

ρ_p = catalyst particle density, g/cm^3

M = molecular weight of the gas mixture, g/gmol

The relation between the bulk diffusivity and Knudsen diffusivity is given by

$$\frac{\lambda}{2\overline{r}} = \frac{D_{AB}}{D_K} \tag{3.30}$$

where $\overline{r}$ is the pore radius, cm.

3.4.3 Effectiveness Factor

The effectiveness factor indicates the relative importance of diffusion and reaction limitations. Quantitative analytical treatment of the effects of mass transfer and reaction within the porous structure were first carried out by Thiele [52], Wheeler [55], and Aris [5]. Emphasis was on the development of a technique that can be used to analyse quantitatively the factors that determine the effectiveness with which the surface area of a porous catalyst is associated. Hence, the effectiveness factor, η, for a catalyst is defined as the ratio of the actual rate for the entire catalyst particle to the rate evaluated at the exterior surface conditions.

The intrinsic chemical reaction rate expression can be determined by the proper choice of experimental conditions that eliminate both external and intraparticle mass transfer resistance. By evaluating the effectiveness factor η, the true reaction rate can be calculated.

With the assumption that the reaction is first-order, a new Thiele-type module is defined as:

$$\Phi_S = \overline{r}\sqrt{\frac{k_1' \rho_p S_g}{D_e}} \tag{3.31}$$

where

$\bar{r}$ = radius of catalyst particle, cm

k_1' = rate constant for first order reaction

ρ_p = apparent density of catalyst particle (mass per total volume), g/cm^3

S_g = surface area per gram of catalyst, cm^2/g

D_e = effective diffusivity given by

$$D_e = \frac{D_c \varepsilon_p}{\tau} \tag{3.32}$$

where

D_c = combined diffusivity (Knudsen and molecular diffusion), cm^2/s

ε_p = porosity of the pellet

τ = tortuosity factor (takes care of length and shape factors)

At equimolar counter-diffusion, D_c is given by the equation

$$\frac{1}{D_c} = \frac{1}{D_{AB}} + \frac{1}{D_K} \tag{3.33}$$

then the effectiveness factor is

$$\eta = \frac{3}{\Phi_s}[\frac{1}{tanh(\Phi_s)} - \frac{1}{\Phi_s}] \tag{3.34}$$

For large values of Φ_s(>30), $tanh(\Phi_s)$ approaches unity and the effectiveness factor approaches $3/\Phi_s$, hence the reaction is diffusion-limited within the pellet. At low values of Φ_s, the effectiveness factor approaches unity and hence the reaction is surface-reaction limited.

3.5 Catalyst

A catalyst is defined as a substance that affects the rate or the direction of a chemical reaction, but the amount that is consumed by the reaction is negligible compared to the consumption of reactants [10].

The major factor that determines the catalyst activity is its chemical composition. However, with constant chemical composition, the catalytic characteristics may vary over a wide range depending on the conditions and method of catalyst preparation.

The catalytic properties of a catalyst are measured by the following characteristics:

1. Catalytic activity which is defined as the ratio of the rate of reaction at any time to the rate of reaction with a fresh catalyst..
2. Selectivity characterized by the ratio of formation of desired product to the overall rate of conversion of the initial product.
3. Stability includes thermal stability, resistance to poisoning, and reproducibility in its behavior.
4. Mechanical strength.
5. Hydrodynamic characteristics which are determined by the size, shape and density of the catalyst grains.

The optimum combination of these properties will provide high quality of a catalyst for a particular reaction.

3.5.1 Reaction Mechanisms for $SnO_2 - MoO_3$

The mixed $SnO_2 - MoO_3$ catalyst has been known for its peculiar activity in the oxidation of propylene [9,51] and ethyl benzene [4]. Catalytic activities are much enhanced by mixing these oxides. However, detailed investigation of the structure of the mixed oxide did not detect a new compound consisting of SnO_2 and MoO_3 [9,4]. It was believed that active sites could be attributed essentially to the boundary surface of SnO_2 and MoO_3.

The concentartion of Mo^{5+} is very stable and is not oxidized to Mo^{6+} even by calcination at $500°C$. Therefore, it seems that the Mo^{5+} on $SnO_2 - MoO_3$ can be regarded as a relatively unoxidizable species.

Furthermore, it has been reported by Takita et al. [50] that the solid acidity increases on mixing SnO_2 and MoO_3. This increase in the acidity may be associated with the MoO_3, as mentioned above. The origin of acidity may appear to be by the interaction of water and Mo^{5+}, as indicated by Giordano et al. [20], i.e.,

$$Mo^{5+} + H_2O \longrightarrow (Mo^{5+} - OH)^- + H^+ \tag{3.35}$$

The oxidized Mo^{5+} site probably turns into Mo^{4+} or Mo^{3+} on reduction. It is not easy to decide as to which is the plausible reduced state of molybdenum ion. If the reduced site is the Mo^{4+}, which can be usually observed in reduced molybdenum oxide, and if the oxidizing surface may be represented as in Figure 3.2 [38], the reaction mechanism can be described as follows:

1. Methanol may initially interact with $Mo^{5+} - OH$ to give a surface methoxy group in place of an OH group.

2. Abstraction of the hydrogen to produce formaldehyde.

These two steps are repeated after reoxidation of the surface with oxygen.

It is well known that methanol yields methoxy radicals under electron-bombardment, and the OH group exchanges easily with D_2O to produce CH_3OD in a liquid state. The reaction route for methanol oxidation, the methoxy group attached to the metal cation, has been regarded as one of the most likely species [41,44]. However, it seems that the rate-determining step involves the cleavage of the C-H bond.

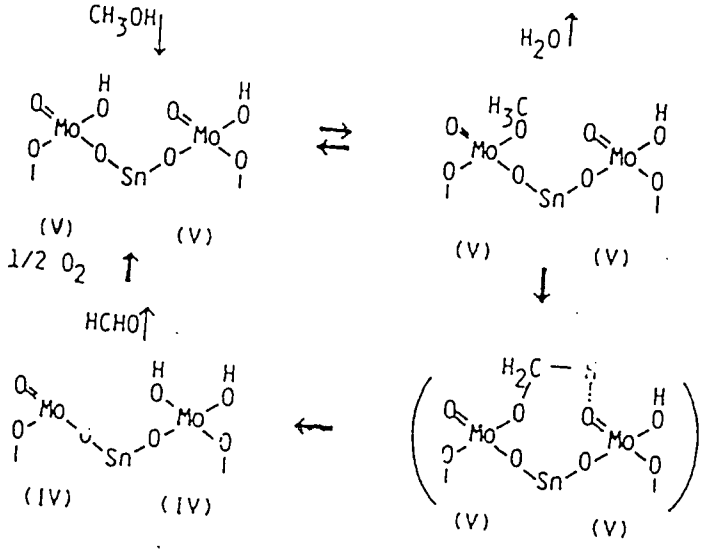

Figure 3.2: Reaction mechanism of methanol oxidation on $SnO_2 - MoO_3$

Chapter 4

Methodology

The strategies followed in designing the experiments are fully explained in this chapter. The description of the experimental scheme for the selection of the best catalyst composition, as well as the methods used to select the rate equation, and the procedure to evaluate the parameter estimate of the kinetics models are also given in detail.

4.1 Design of Experiments

The objectives of this work were to verify the effect of process variables (T, W/F, R) and catalyst composition on the yield of formaldehyde, establishing the reaction networks, and finding the kinetic model or models that fit the experimental data adequately.

However, it is to be noted that the kinetic study had to be carried out with the catalyst that gives the highest yield. Therefore, a set of experiments were designed in such a way as to achieve the best catalyst composition.

The operating conditions considered in this study were chosen in ranges close to the typical ones for the industrial production of formaldehyde, except for the

temperature range which was chosen close to the range suggested by Niwa et al. [39]. These ranges are: temperature between 513 and 593 K, methanol/air molar feed ratio between 0.04 and 0.1g-mol methanol per g-mol air in the feed, space time between 10 and 40 hr g cat/g-mol methanol fed, and total operating pressure of 1 atm. Five different levels of the catalysts were prepared to study the effect of catalyst composition. These levels were 10, 30, 50, 70, and 90 weight percentage of SnO_2 in the $SnO_2 - MoO_3$ catalyst.

4.1.1 Optimal Catalyst Composition

Two-level fractional factorial design [6] for the three operating variables, namely the temperature, the space time and methanol/air feed molar ratio, was used at each level of the catalyst composition to determine the optimal catalyst composition. First the following full second-order model was employed to express the yield :

$$\begin{aligned} E(Y) &= \beta_0 + \beta_1 x_1 + \beta_2 x_2 + ... + \beta_k x_k \\ &\quad + \beta_{11} x_1^2 + \beta_{22} x_2^2 + ... + \beta_{kk} x_k^2 \\ &\quad + \beta_{12} x_1 x_2 + \beta_{13} x_1 x_3 + ... + \beta_{k-1,k} x_{k-1} x_k \end{aligned} \tag{4.1}$$

where $k = 4$, since there are four variables.

Then the model was reduced by excluding the non-significant parameters. The final expression of the model was used to maximize the yield with respect to the catalyst composition at the center point for the remaining operating variables.

Construction of a two-level fractional factorial design for the case of the three operating variables is illustrated in Table 4.1. Values of the operating variables are quoted in coded form, where -1, 1, and 0 are the lower value, the upper value,

and the center point of the operating variables, respectively. The forth variable is quoted in coded form as -1, -0.5, 0, 0.5, and 1, where these codes represent the different level of catalyst composition defined previously.

Model Building

In model building, the most independent variable is not measured directly but is calculated from other quantities. In this case here, the yield can be expressed as the product of selectivity and fractional conversion and is defined by Y. The temperature is defined as:

$$X_1 = \frac{T - 543}{30} \tag{4.2}$$

The space time is defined as:

$$X_2 = \frac{W/F - 25}{15} \tag{4.3}$$

The methanol/air molar feed ratio is defined as:

$$X_3 = \frac{R - 0.06}{0.02} \tag{4.4}$$

The catalyst composition is defined as:

$$X_4 = \frac{X - 50}{40} \tag{4.5}$$

where X is the weight percentage of SnO_2 in the $SnO_2 - MoO_3$ catalyst. Then the full model can be expressed as:

$$\begin{aligned} E(Y) \;=\; & a_0 + a_1 X_1 + a_2 X_2 + a_3 X_3 + a_4 X_4 \qquad (4.6) \\ & + a_{12} X_1 X_2 + a_{13} X_1 X_3 + a_{14} X_1 X_4 + a_{23} X_2 X_3 + a_{34} X_3 X_4 \\ & + a_{24} X_2 X_4 + a_{11} X_1^2 + a_{22} X_2^2 + a_{33} X_3^2 + a_{44} X_4^2 \end{aligned}$$

(4.7)

Table 4.1: Two-level fractional factorial design for the three operating variables at each level of catalyst composition.

X_1	X_2	X_3	X_4
-1	-1	1	-1
1	-1	-1	-1
-1	1	-1	-1
1	1	1	-1
0	0	0	-1
0	0	0	-1
0	0	0	-1
-1	-1	1	-0.5
1	-1	-1	-0.5
-1	1	-1	-0.5
1	1	1	-0.5
0	0	0	-0.5
0	0	0	-0.5
0	0	0	-0.5
-1	-1	1	0.0
1	-1	-1	0.0
-1	1	-1	0.0
1	1	1	0.0
0	0	0	0.0
0	0	0	0.0
0	0	0	0.0
-1	-1	1	0.5
1	-1	-1	0.5
-1	1	-1	0.5
1	1	1	0.5
0	0	0	0.5
0	0	0	0.5
0	0	0	0.5
-1	-1	1	1
1	-1	-1	1
-1	1	-1	1
1	1	1	1
0	0	0	1
0	0	0	1
0	0	0	1

4.1.2 Kinetic Experiments

After determining the optimum catalyst composition, a full scale design was considered for the kinetic study. Each set of experiments consisted of sixteen runs. In each set the space time was kept constant while the temperature was varied at four different values. Methanol/air molar feed ratio was also changed at four different values for each temperature.

The samples considered for analyzing were collected at steady state. All these experiments may provide complete information on how one variable interacted with the other two.

4.1.3 Selection of Rate Equation

There are several approaches to find the rate expression that fits the data best. The relationship between conversion, flow rate and reaction rate in a steady flow system, is given by the equation:

$$\frac{W}{F} = \int_0^x \frac{dx}{r} \tag{4.8}$$

where x is the fractional conversion of the reactant material and r is rate of the reaction.

This general rate equation of a catalytic flow system is based on unit mass of the catalyst. In order to obtain a rate equation that can accurately predict the reaction behavior, the mechanism that controls the reaction must be obtained. The mechanism of a reaction can be detected by the initial rate method described by Yang and Hougen [56]. The initial rate is obtained by plotting the fractional conversion versus the space time and determining the slope of the curve as the space time approaches zero. One can predict the mechanism from the shape of

the curve obtained by plotting the initial rates versus the partial pressure of the reactants' molar ratio.

Besides the initial rate procedure, there are several methods that use the finite values of conversion in order to establish the true rate equation which represents the data. The method of linearization of the rate equation was used to solve for the rate constants using linear regression method.

4.1.4 Mathematical Modelling

Analysis of the experimental results can only be accomplished through mathematical modelling of kinetics. The integrated form of the rate equations in Table 2.1 can be rearranged into a new form as shown in Table 4.2, where $Y = A_0 + A_1 x$ represents a typical straight line, Y being the dependent variable, X the independent variable, A_0 the intercept and A_1 the slope. The values for Y and X are calculated from the experimental data by substituting the values of W/F and the respective partial pressures. The parameter of these equations are estimated by a linear least-square regression technique. The best estimates of these parameters are taken as those that minimize the sum of squares of deviations between observed and predicted values of all the response variables rather than one response variable. By doing so one can expect more precise estimates of the model parameters.

After the conversion of the estimation algorithm the model adequacy is confirmed by several checks:

- Determine whether the estimate parameters are reasonable.
- Check for the discrepancies between observed and predicted values of the

responses.

- Plot the residuals versus the predicted values of the responses. In general, trends in the plots of residuals indicate lack of fit.

- Plot the observed values of the responses versus the predicted values.

These kinds of plots offer easy ways to detect inadequacies.

Table 4.2: Correlated Y and X relations for two-stage Redox Mechanism

No.	Reaction Order m (CH_3OH)	Reaction Order n (O_2)	A_0	A_1	Y	X
1	0.5	0	$\frac{\alpha}{k_2}$	$\frac{-2}{k_2}$	$\frac{W}{F}\frac{1}{x}$	$[\frac{(1-x)^{0.5}-1}{xP_{M_o}^{0.5}}]$
2	0.5	0.5	$\frac{-1}{k_1}$	$\frac{-2\alpha}{k_2}$	$\frac{W}{F}\frac{P_{M_o}^{0.5}}{2[(1-x)^{0.5}-1]}$	$[\frac{(P_{O_2^o}-0.5P_{M_o}x)^{0.5}-(P_{O_2^o})^{0.5}}{P_{M_o}^{0.5}[(1-x)^{0.5}-1]}]$
3	1	0	$\frac{-1}{k_1}$	$\frac{\alpha}{k_2}$	$\frac{W}{F}\frac{P_{M_o}}{ln(1-x)}$	$[\frac{xP_{M_o}}{ln(1-x)}]$
4	1	0.5	$\frac{-1}{k_1}$	$\frac{-4\alpha}{k_2}$	$\frac{W}{F}\frac{P_{M_o}}{ln(1-x)}$	$[\frac{(P_{O_2^o}-0.5P_{M_o}x)^{0.5}-(P_{O_2^o})^{0.5}}{ln(1-x)}]$
5	1	1	$\frac{-1}{k_1}$	$\frac{-2\alpha}{k_2}$	$\frac{W}{F}\frac{P_{M_o}}{ln(1-x)}$	$\frac{1}{ln(1-x)}ln[\frac{P_{O_2^o}-0.5P_{M_o}x}{P_{O_2^o}}]$
6	1.5	0	$\frac{\alpha}{k_2}$	$\frac{1}{k_1}$	$\frac{W}{F}\frac{1}{x}$	$[\frac{1}{P_{M_o}^{1.5}(1-x)^{0.5}}]$
7	1.5	0.5	$\frac{1}{k_1}$	$\frac{-2\alpha}{k_2}$	$\frac{W}{F}\frac{P_{M_o}^{1.5}}{2[(1-x)^{-0.5}-1]}$	$P_{M_o}^{0.5}[\frac{(P_{O_2^o}-0.5P_{M_o}x)^{0.5}-(P_{O_2^o})^{0.5}}{[(1-x)^{-0.5}-1]}]$
8	1.5	1	$\frac{1}{k_1}$	$\frac{-\alpha}{k_2}$	$\frac{W}{F}\frac{P_{M_o}^{1.5}}{2[(1-x)^{-0.5}-1]}$	$\frac{P_{M_o}^{0.5}}{[(1-x)^{-0.5}-1]}[ln\frac{(P_{O_2^o}-0.5P_{M_o}x)}{P_{O_2^o}}]$
9	2	0	$\frac{\alpha}{k_2}$	$\frac{1}{k_1}$	$\frac{W}{F}\frac{1}{x}$	$[\frac{1}{P_{M_o}^2(1-x)}]$
10	2	0.5	$\frac{1}{k_1}$	$\frac{-4\alpha}{k_2}$	$\frac{W}{F}P_{M_o}^2(\frac{1-x}{x})$	$\frac{P_{M_o}(1-x)}{x}[(P_{O_2^o}-0.5P_{M_o}x)^{0.5}-(P_{O_2^o})^{0.5}]$
11	2	1	$\frac{1}{k_1}$	$\frac{-2\alpha}{k_2}$	$\frac{W}{F}P_{M_o}^2(\frac{1-x}{x})$	$\frac{P_{M_o}(1-x)}{x}ln[\frac{(P_{O_2^o}-0.5P_{M_o}x}{P_{O_2^o}}]$

Chapter 5

Properties of Materials

This chapter deals with the various properties of materials used in this research, mainly the reactant material (methanol) and the main product of the reaction carried out in this research (formaldehyde). A general discussion of the physical and chemical properties is given. Health and safety factors, as related to use, handling and storage of materials, are discussed as well.

5.1 Formaldehyde

Formaldehyde, $H_2C = O$, is the first of the series of the aliphatic aldehydes. It was discovered by Butlerov in 1859 and has been manufactured since the beginning of this century. At ordinary temperatures, pure formaldehyde is a colorless gas with a pungent, suffocating odor. It is produced and sold as water solutions that contain variable amounts of methanol or other alcohols. These solutions are complex equilibrium mixtures of methylene glycol, $(CH_2(OH)_2)$, poly(oxymethylene glycols), and hemiformals of these glycols.

5.1.1 Source, Synthesis and Uses

Today, all the world's commercial formaldehyde is manufactured from methanol and air by either an older process using a metal catalyst or a newer one using a metal oxide catalyst. Reactor feed to the former is on the methanol-rich side of a flammable mixture and virtually complete reaction of oxygen is obtained. Conversely, feed to the metal oxide catalyst is lean in methanol and almost complete conversion of methanol is achieved.

As a basic chemical building unit, formaldehyde is an intermediate in a large variety of organic compounds. The largest use of formaldehyde is in the manufacture of amino and phenolic resins. Other important uses include wood-industry products, molding compounds, foundry resins, and adhesives for insulation. It is also used in the synthesis of chelating agents, for example, in the manufacture of ethylenediaminetetraacetic acid (EDTA). Other important uses are in the manufacture of permanent-press finishes of cellulose fabrics and of acetal resins. Other applications of formaldehyde are in the manufacture of a great variety of chemicals, elastomeric sealants, herbicides, fertilizer coatings, and pharmaceuticals. Pyridines and isocyanates consume large amounts of formaldehyde. Methylenediphenyl isocyanate (MDI), used in the production of polyurethane foams, coatings and elastomers, is expected to be one of the fastest growing consumers of formaldehyde.

5.1.2 Physical and Chemical Properties

The physical properties of formaldehyde are given in Table 5.1 [27]. Formaldehyde is noted for its reactivity and its versatility as a chemical intermediate. It is used in

Table 5.1: Physical properties of monomeric formaldehyde.

Property	Value
density,g/cm^3	
at-80°C	0.9151
at-20°C	0.8153
boiling point at 101.3 kPa, °C	-19
melting point,°C	-118
vapor pressure, Antoine constants, Pa	
A	9.28176
B	959.43
C	243.392
heat of vaporization, ΔH_v	
at 19°C, kJ/mol	23.3
heat of formation, ΔH_f^o	
at 25°C, kJ/mol	-115.9
std free energy, ΔG_f^o	
at 25°C, kJ/mol	-109.9
heat capacity, Cp^o, J/(mol.K)	35.4
entropy, S^o, J/(mol.K)	218.8
heat of combustion, kJ/mol	561-571
critical constants	
temperature, °C	137.2-141.2
pressure, MPa	6.784-6.637
flammability in air	
lower/upper limits, mol ignition temperature, °C	430

the form of anhydrous monomer, solutions, polymers, and derivatives. The pure, dry gas is relatively stable at 353-373 K, below this range it starts to slowly polymerize. This action is greatly accelerated if there are traces of polar impurities. At ordinary temperatures, formaldehyde gas is readily soluble in water, alcohols, and other polar solvents. Its heat of solution in water and the lower aliphatic alcohols is approximately 63 kJ/mol. The reaction of unhydrated formaldehyde with water is very fast; the first-order rate constant at 22°C is 9.8 s^{-1} [27].

The decomposition of formaldehyde without a catalyst at temperature be-

low 573 K is a very slow process, and the rate of decomposition increases with temperature; CO and H_2 are the main products of the decomposition.

Formaldehyde reduces to methanol in a hydrogen atmosphere with several metal and metal oxide catalysts. It oxidizes to form either formic acid or CO_2 and H_2O.

In an aldol-type reaction, formaldehyde condenses with itself yielding hydroxy compounds. This reaction occurs mostly under alkaline conditions.

5.1.3 Health and Safety Factors

Solutions of formaldehyde are unstable. Both formic acid (acidity) and paraformaldehyde concentrations increase with time and depend on temperature. Formic acid concentration increases at a rate of 1.5-3 ppm/day at 65°C. Although low storage temperature minimizes acidity, it also affects polymerization, which is inhibited by addition of methanol or of stabilizers. Material of construction preferred for storage vessels is stainless steel.

According to the material safety data sheet provided by the manufacturer, concentrations of 0.5-5.0 ppm may cause eye, nose and throat irritation, and lacrimation; 10-20 ppm may cause difficulty in breathing, burning of the nose and throat, cough and profuse lacrimation; 25-50 ppm may cause tissue damage and serious respiratory tract injury. Prolonged or repeated exposure may result in respiratory impairment and pulmonary sensitization. Long term exposure to formaldehyde has been shown to be associated with an increased risk of cancer of the nose and lung in humans. Data regarding health and safety factors are given in Table 5.2 [27].

Table 5.2: Health and safety factors for formaldehyde concentration.

Factor	Value
expose time	
8-h time-weighed average, ppm	3
ceiling	5
max peak above ceiling, ppm for 30 min	10
minimum level for sensory detection	
air borne, odor detectable at ppm	1
in water, odor detectable at mg/l	20-50
profuse lacrymation, ppm	20
eye irritation, ppm	0.05-0.0

5.2 Methanol

Methanol (methyl alcohol), CH_3OH, is a clear, water-like liquid with a mild odor at ambient temperatures. Methanol has been called wood alcohol (or wood spirit) because it was obtained commercially from the destructive distillation of wood for over a century. However, the wood alcohol contained more contaminants (primarily acetone, acetic acid, an d allyl alcohol) than the chemical-grade methanol available today.

For many years the largest use for methanol has been as a feed stock in the production of formaldehyde, consuming almost half of the methanol produced. However, formaldehyde's importance to methanol will decrease as newer uses increase, such as the production of acetic acid and methyl tert-butyl ether (MTBE). Methanol's direct use as a fuel may be significant in special circumstances.

5.2.1 Source, Synthesis and Uses

Methanol is manufactured from synthesis gas which, in turn is usually produced from methane. All new plants use low pressure technology which is dis-

tinguished from older, high pressure plants by the reactor design and capacity. Above 150 t/day rates, centrifugal compressors generally can be used to compress synthesis gas to methanol-reactor pressure. Basically, two types of reactors are in commercial use: the shell and tube reactor and the quench type. Both reaction loops have similar equipment. The main difference is that shell-and tube-type reactor recovers heat of reaction by generation of steam on the shell side, while quench-type recovers this heat in a separate heat exchanger that preheats boiler feed water. Alcohols other than methanol are produced in small quantities with ethanol the chief impurity. Other by-products produced in small amounts are aldehydes, ketones, ethers and esters. Methanol is purified by distillation. The complexity required depends on the desired methanol purity and the purity of the crude methanol.

Historically, almost half of all methanol produced has been used to produce formaldehyde. In the future formaldehyde will lose some of this position owing to methanol use in the production of faster-growing chemicals such as acetic acid, methyl tert-butyl ether (MTBE), and oxinol (a methanol-tert-butyl alcohol blend for gasoline octane improvement). One area of promise for methanol is its direct use in fuels. Potentially it can be used as a replacement for diesel fuel and gasoline or a gasoline extender. Another potential large market for methanol, is its use in the production of single-cell protein (SCP), which is used as animal feed additives. Methanol is also considered for use in many other areas. These include its use as feed stock to produce olefins, as a reducing-gas source for steel mills, to remove nitrogen from sewage sludge, and it is used also in fuel cells.

5.2.2 Physical and Chemical Properties

The physical properties of methanol are given in Table 5.3 [27].
Methanol undergoes reactions that are similar of alcohols as a chemical class [53]. From an industrial standpoint the reactions of particular importance are dehydrogenation and oxidative dehydrogeneration to formaldehyde over silver or molybdenum-iron oxide catalysts and carbonylation to acetic acid catalyzed by cobalt or rhodium. The acid-catalyzed reaction of isobutylene and methanol form methyl tert-butyl ether. Methyl esters of carboxylic acids can be prepared by acid-catalyzed reactions with isotropic removal of water to force the reaction to completion. The direct reaction of methanol with ammonia gives mono-, di- and trimethylamine. Methyl hydrogen sulfate, methyl nitrite, methyl nitrate, and methyl halides are formed by the reaction of methanol with appropriate inorganic acids.

5.2.3 Health and Safety Factors

Methanol may be stored and handled in clean carbon-steel equipment. In order to minimize vapor emissions, storage tanks should be constructed with an internal floating roof with an inert gas pad. Because of the flammability of the product, tanks are usually enclosed by a dike and protected by a foam-type (either CO_2 or dry chemical) fire extinguishing system. Air pressure should never be used to load or unload methanol. Pumping is preferred but inert gas should be used when pressure loading or unloading is required. The most general health hazard associated with methanol is blindness, usually as a result of ingestion. The ingestion of methanol has resulted in a wide range of responses, probably owing

to the concurrent intake of varying amounts of ethanol. Ethanol is selectively metabolized by the body, allowing detoxification by respiration to occur to some extent. 25-100 ml of methanol can cause death if taken by mouth. The initial symptoms vary: weakness, fatigue, headache, dizziness, nausea, and abdominal pain are typical.

Table 5.3: Physical properties of methanol.

Property	Value
boiling point at 101.3 kPa, °C	64.7
freezing point,^oC	-97.68
entropy, S^o, J/(mol.K)	218.8
critical constants	
temperature, ^oC	239.43
pressure, kPa	8096
volume, mL/mol	118
critical compressibility factor, z	0.224
heat of formation, (liquid)	
at 25^oC, kJ/mol	-239.03
std free energy, (liquid)	
at 25^oC, kJ/mol	-166.81
heat of fusion, J/g	103
heat of vaporization, at boiling point J/g	1129
heat of combustion, at25^oC J/g	22662
flammable limits in air	
lower/upper limits, vol autoignition temperature, ^oC	470
flash point, closed cup, ^oC	12
surface tension, mN/m	22.6
specific heat	
of vapor at 25^oC, J/(g.K)	1.370
of liquid at 25^oC, J/(g.K)	2.533
vapor pressure, at 25^oC, kPa	16.96
solubility in water	miscible
density, at 25^oC g/cm^3	0.78663
viscosity of liquid at 25^oC, mPa.s	0.541
thermal conductivity at 25^oC, W/(m.K)	0.202

Chapter 6

Experimental Aspects

This chapter describes the equipment used in this study, and its operation, as well as the procedure for preparing the catalysts and analyzing various samples. The experimental apparatus used in the kinetic study was similar to the ones used by Dosi [16], Jain [24], Hahn [22], and Diaz [15].

6.1 Kinetic Studies

The kinetic data were collected from an integral-flow, fixed-bed catalytic reactor under steady-state conditions at a pressure of 1 atm, a temperature range between 513 and 593 K, a space time (W/F) between 10 and 40 hr g-cat./g-mol feed and a molar ratio (R) between 0.04 and 0.1 g-mol CH_3OH/g-mol air in the feed. Heat and mass transfer were negligible under the operating conditions (see Appendix E).

6.1.1 Experimental Apparatus

A schematic diagram of the apparatus is shown in Figure 6.1. The experimental setup consisted essentially of a packed bed reactor, a furnace (fluidized sand bath), a hot inlet chamber, a feed and facilities for controlling sampling,

a liquid trap, metering and analysis of the product. The main sections of this apparatus are described in detail in the following sections.

Reactant Feed Section

Two streams of gases were connected to the system. A first stream carrying a mixture of gases (9.76% CO_2, 9.89% CO, 80.35% N_2), was used to prepare gaseous mixture for calibration. A second stream carried air (21.5% O_2, 78.5% N_2). The calibration gas mixture and the compressed air were purchased from Air Products (Brampton, Ont.). Flow rates for the gas streams were measured by rotameters (body) model no. 622 PSV, with flow meter tube size R-15-2-AA from Matheson of Canada Ltd. (Whitby, Ont.). Another air stream was used for fluidizing the sand bed which surrounded the reactor assembly.

Dry air was passed at high velocity through a temperature controlled hot inlet chamber (temperature=473 K). The temperature was controlled by a variable autotransformer of the type 3 PN 1010 from STACO, Inc. and a temperature controller (Honeywell). In this chamber methanol was injected into the feed stream by means of a syringe pump, model 901 from Harvard Apparatus Co. Inc. (Millis, MA) and 10 cm^3 gas tight syringes model 1010-LT from Hamilton Co. (Reno, NV). Methanol was continuously vaporized and carried away in the air stream. Pure methanol was purchased from BDH Ltd. (Toronto, Ont.). The reactant stream coming out of the hot inlet chamber could either be sent directly to the liquid trap for calibration or to the preheater and reactor for an experimental run. Stainless steel tubing carrying the air and methanol mixture to the reactor was heated externally by a heating tape from Canada Wide Scientific Ltd. (Ottawa,

Ont.). The feed stream going to the reactor was preheated in a stainless steel tubing wound around the reactor.

Reactor Section

A schematic of the reactor assembly is shown in Figure 6.2. The reactor was a 316 stainless steel tubing of length 19.05 cm and 1 cm I.D. A porous stainless steel plate was fixed at the bottom of the reactor. At the top of the reactor an iron-constantan thermocouple was connected to a temperature controller (Honeywell). The reactor and preheater were kept immersed in a constant temperature fluidized sand bath.

The container for the fluidized sand bath was a 9 cm OD steel cylinder. Sand size was between 0.37 and 0.25 mm (40/60 mesh). A porous stainless steel plate was welded at the bottom. Compressed air for the fluidization was obtained from the building air supply. A metering valve controlled the air supply to the sand bed. Sufficient air was passed at all times in order to keep the sand fluidized and maintain a uniform temperature around the reactor. Ceram-A-Flexbeaded heating wires were wrapped around the cylinder and connected to one of the autotransformers and in series with a temperature controller (Honeywell). The temperature of the sand bath was adjusted by changing either the input voltage in the autotransformer or more easily, by changing the temperature set in the temperature controller. At steady state the temperature of the sand bed and that of the reactor were within 2 to 3°C, thus insuring isothermal operation.

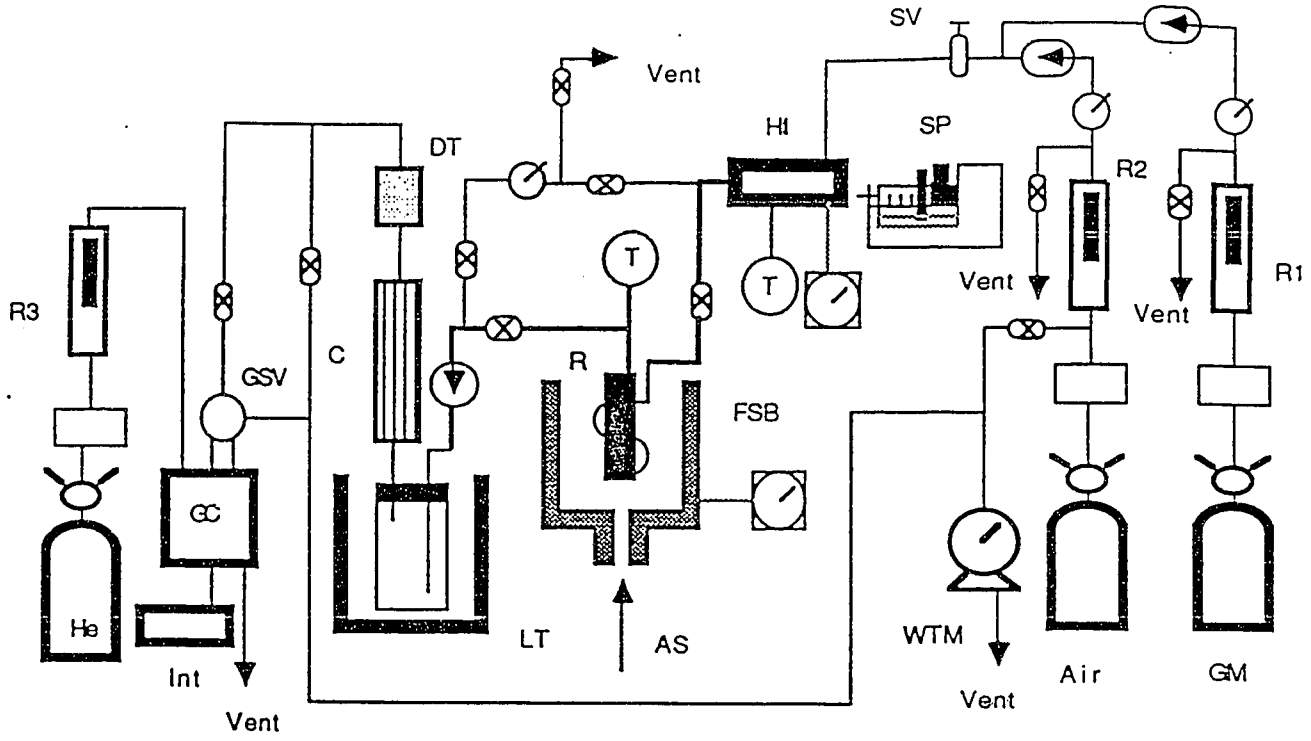

Key

Regulator	
Bellow valve	
Check valve	
Purification	
Thermocouple	
Temperature Controller	
Pressure gauge	

AS	Air Supply
C	Condenser
DT	Drying Tube
FSB	Fluidized Sand Bed
GC	Gas Chromatograph
GM	Gas Mixture (N_2 CO_2, CO)
GSV	Gas Sampling Valve
HI	Hot Inlet
Int	Integrator
LT	Liquid Trap
R1,R2,R3	Rotameters
SP	Syringe Pump
SV	Solenoid Valve
WTM	Wet Test Meter

Figure 6.1: Schematic diagram of the experimental apparatus

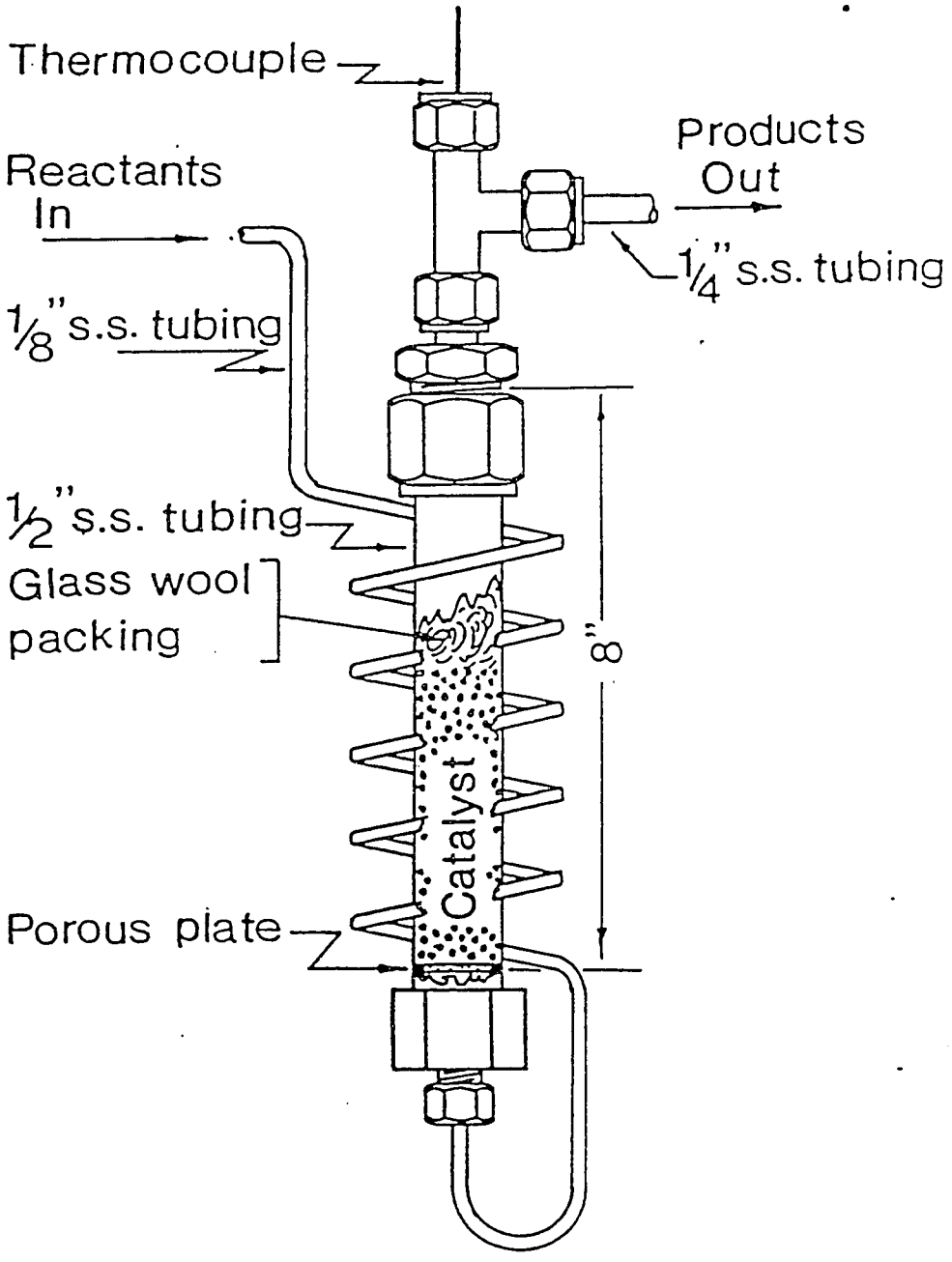

Figure 6.2: Reactor and Pre-heater

Sampling and Analysis Section

Products coming out of the reactor were passed through stainless steel tubing which was heated externally. They were then passed through a liquid trap, from which samples were taken for further analysis. Within the liquid trap, connected on line, there was a sampling bottle containing small amount of water, where products such as $HCHO$, CH_3OH, H_2O were continuously condensed and/or absorbed by H_2O. This bottle was of pyrex with a 29/42 ground joint at the top where a two-hole rubber strapper was fitted. A properly isolated 4L Dewar flask containing ice surrounded the sampling bottle. Gases and uncondensed vapors passed through a 0.635 cm OD stainless steel tubing placed in a 32 cm long and 6.3 cm OD condenser cylinder. Fresh cold water passed through this cylinder to cool the gas products going through the tubing. Any products condensing inside the tube drop back into the liquid trap (a 13 cm long and 5.8 cm OD acrylic tube filled with molecular sieve 13X). All traces of moisture from the gas products were removed in the drying tube and in the condenser.

Gaseous products were then passed through an HP 5700 gas chromatograph equipped with a thermal conductivity detector (TCD), dual columns, and temperature programming capability. Chromatograms, retention times, and peak areas were produced by an integrator (HP-3380A). Liquid samples were analyzed by injecting them into the same gas chromatograph.

6.1.2 Gas Chromatographic Analysis

A 10.97 m long and 0.3175 cm OD (36' × 0.125") Hayesep A stainless steel column was utilized to analyze the gas products containing CO, CO_2, N_2, and

O_2. A 0.5 cm^3 sampling loop was used to inject the gas sample into the column. The following operating conditions were found suitable for the separation: initial column temperature 25°C, initial time 8 min, program rate 32°C/min, final column temperature 100°C, final time 30 min, and carrier gas (helium) flow rate of 30 cc/min at 25°C. For calibration purpose, several different mole ratios of the calibration gas mixture to the compressed air were injected into the column. A plot of the peak area versus the mol % of CO, CO_2, and O_2 was found to be linear in the range of interest. A typical analysis of the gas mixture is given in Figure 6.3.

A 152.4 cm long and 0.3175 cm OD (5' × 0.125") Hayesep T stainless steel column was used for analyzing liquid products containing CH_2O, H_2O, and CH_3OH. The following operating conditions were found suitable for the separation: Injector temperature 150°C, detector temperature 200°C, initial column temperature 100°C, initial time 0 min, program rate 32°C/ min, final column temperature 140°C, final time 8 min, and carrier gas (helium) flow rate 30 cc/min. A liquid sample of 0.2 μL was used for all analyses. A certified formaldehyde solution from Fisher Ltd. was used to prepare the standard solutions for calibration. A plot of the % area versus the concentration of the corresponding compound was found to be linear in the range of interest. A typical analysis of the liquid product is shown in Figure 6.4.

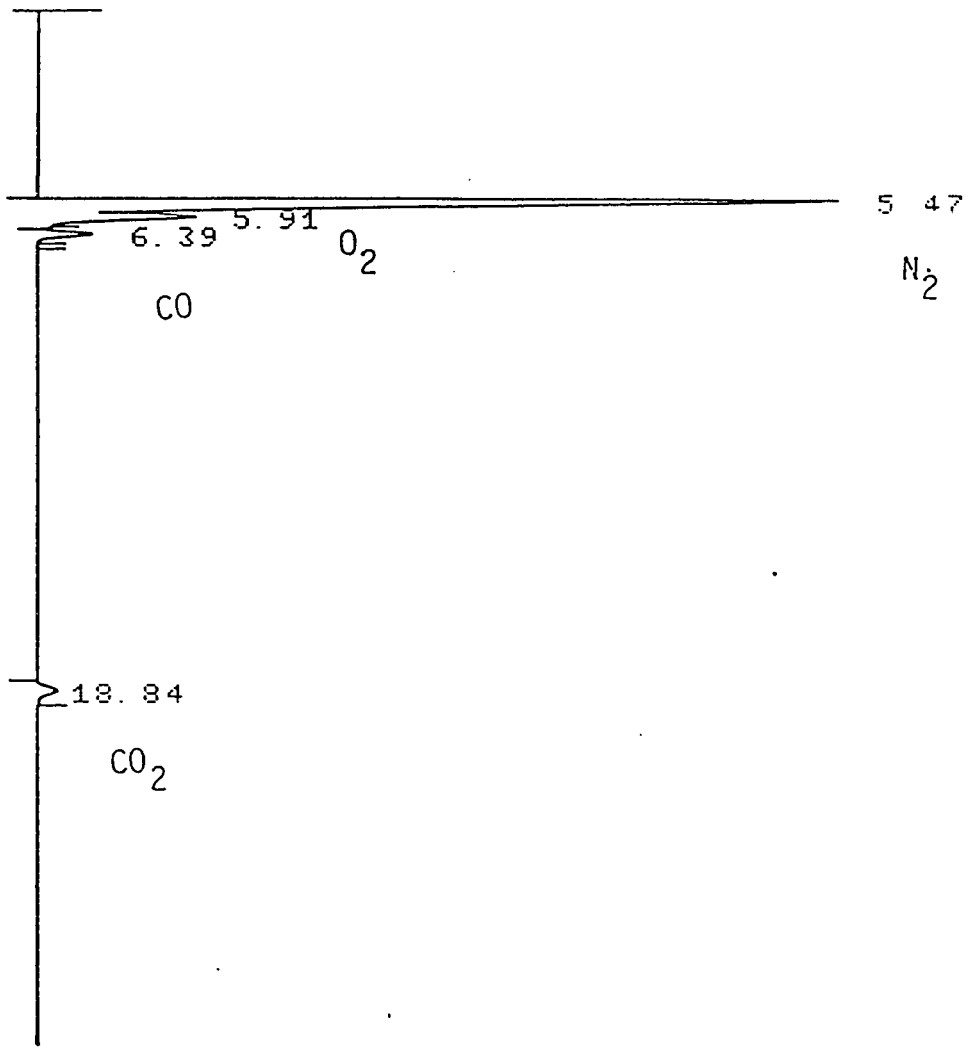

		AREA %	
RT	TYPE	AREA	
5. 47		318159	89 11
5. 91	T	19851	5 56
6. 39	T	10874	3 046
18. 84		8152	2 283

Figure 6.3: A typical GC chromatogram for the gas products

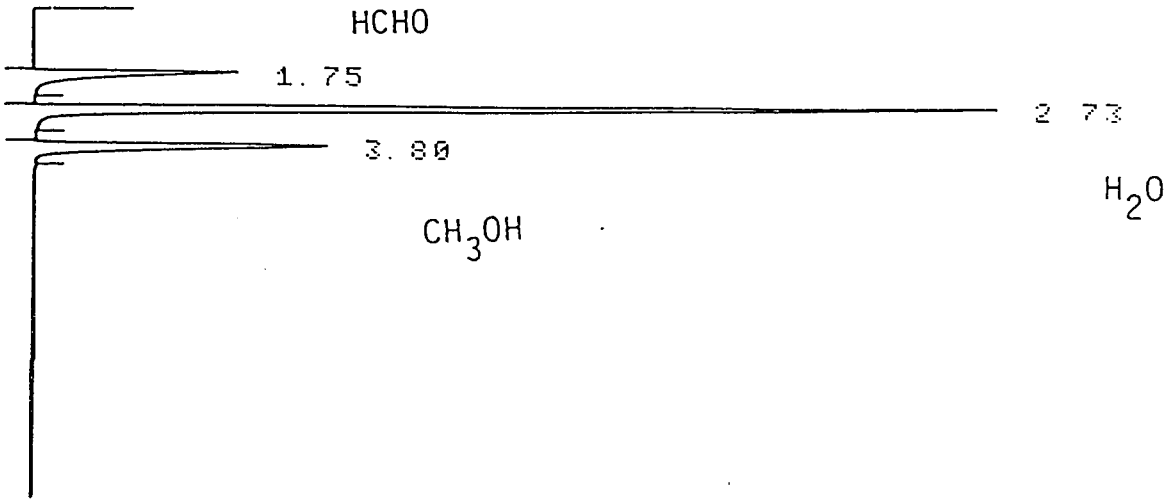

		AREA %	
RT	TYPE	AREA	
1.75		27907	14.76
2.73		119861	63.38
3.80		41338	21.86

Figure 6.4: A typical GC chromatogram for the liquid products

6.1.3 Preparation of Catalyst

Pure molybdenum trioxide catalyst was obtained by the thermal decomposition of ammonium molybdate tetrahydrate. It was heated at 423 K for 6 hours and for 2 hours each at 473 K, 573 K, and 673 K. Finally it was calcined at 773 K for 6 hours and activated at 873 K for 2 more hours.

Pure tin oxide catalyst was prepared by drying tin(IV) hydroxide gel in a 120°C oven for 12 hours, and then calcining at 500°C for 6 hours. The $Sn(OH)_4$ gel was precipitated by adding excess amount of ammonium hydroxide solution to stannic chloride (tin(IV) chloride 5-hydrate, $SnCl_4.5H_2O$).

In order to prepare the proper weight ratio of $MoO_3 : SnO_2$ a known amount of ammonium molybdate was dissolved in water completely to which tin(IV) hydroxide gel was added. The amount of the gel was prepared in such a way as to obtain the desired molybdenum to tin oxides weight ratio. The resulting solution was slowly evaporated to dryness and then calcined at 500°C for 6 hours.

The catalyst thus formed was ground to a particle size of 0.246 to 0.175 mm, 60/80 mesh. To obtain the proper W/F ratio, a weighed amount of catalyst was mixed with pumice stone to a volume of 7 cm^3. Pumice stone, a porous indigenous rock, usually containing 67 to 75% silica and 10 to 20% alumina of glassy texture, was crushed, sieved to 60/80 mesh, and calcined at 500°C for 12 hours.

Ammonium molybdate tetrahydrate ($N_6H_{24}Mo_7O_{24}.4H_2O$) and stannic chloride (tin(IV) chloride 5-hydrate, $SnCl_4.5H_2O$) were bought from BDH Ltd. (Toronto, Ont).

An Accusorb 2100E Physical Adsorption Analyzer from Micromeritics Instruments Corp. of Georgia, U.S.A., was used to determine the specific surface area

using the Langmuir equation or the Bet method [1].

Chapter 7

Results and Discussion

The effects of several variables, namely SnO_2/MoO_3 ratio, reaction temperature, partial pressure of methanol, and space time, on conversion, selectivity, and yield of the oxidation of methanol to formaldehyde were studied. Experimental data were obtained under steady state isothermal conditions at nearly atmospheric pressure and between 513-593 K, using an integral fixed-bed reactor. The conversion of methanol (C) is defined as moles of methanol reacted per mole of methanol fed. The yield of formaldehyde (Y) is defined as moles of formaldehyde formed per mole of methanol fed. The selectivity of the catalyst (S) is defined as the ratio of number of moles of formaldehyde formed to that of the total products (formaldehyde, carbon dioxide and carbon monoxide) formed per unit time. The ratio of moles of methanol to moles of air in the feed multiplied by 100 is defined as ($\overline{R}$). The feed rate was kept constant except set (P), which shows the effect of feed velocity on conversion. The methanol concentration in the feed was changed by altering the flow rate of air. The space velocity (W/F) was varied by changing the weight of the catalyst charged in the reactor.

Preliminary experimental data obtained had indicated that the experimental

apparatus was operating properly. This was verified by running few experiments under similar operating conditions as previous researchers had with a known catalyst. In addition, the analysis of the products from these experiments had shown that the results were reproducible. This was confirmed by running the experiment at standard conditions or by repeating some of the experimental runs.

7.1 Results with Inert Medium

The advantages of diluting the catalyst with an inert medium in the catalyst bed were to enhance the isothermal condition [10] and to standarize the reactor bed size to 7 cm^3.

In order to verify how the inert medium affected the reaction, a set of experimental runs, termed set M, was carried out.

Set M kept the operating conditions of the center point, i.e. $\overline{R} = 6$. Temperature was varied between 623 and 698 K at intervals of 25 K. Results for these runs are shown in Table 7.1 and Figure 7.1. It can be noticed that methanol conversion due to thermal or support effects was very small, less than 10% at 698 K. Since the range of operating temperatures used in the kinetic study were between 513 and 593 K, the conversion of methanol on pumice stone was less than 1%. It was considered to be negligible.

7.2 Results with Molybdenum Trioxide

In order to test the performance of the experimental apparatus a set of runs, termed set A, was carried out using MoO_3 as catalyst. For this set of runs the intent was to verify the proper behavior of a known catalyst system, by studying

the effect of temperature on conversion, selectivity and yield of methanol oxidation while keeping the remaining operating conditions constant.

The temperature was varied between 598 and 698 K. Other operating conditions were set at the center point of the fractional factorial design, i.e. W/F=25 hr g-cat/g-mol methanol fed and $\overline{R} = 6$. Results for these runs are shown in Table 7.2 and Figure 7.2. The reaction with a MoO_3 catalyst followed the expected behavior [2,33,34,35,16,39,57,15] and proved to be very selective to formaldehyde production.

It can be noticed also that the conversion slightly increased with temperature and reached a maximum of about 50% which made this catalyst alone of very little use for a chemical industry.

7.3 Results with Tin Oxide

A set of experimental runs, termed set G, was carried out in order to study the effect of tin oxide catalyst on the conversion, selectivity and yield of methanol oxidation to formaldehyde. The operating conditions were the same as those for set A except that the temperature range was lower, between 523 and 623 K. Results for these runs are shown in Table 7.3 and Figure 7.3.

It is obvious from Figures 7.2 and 7.3 that the activity of SnO_2 catalyst is higher than the activity of MoO_3 catalyst even at lower temperatures. It gave high conversion of methanol. However, its selectivity to formaldehyde was very small and even negligible at high levels of conversion. This indicates that methanol was oxidized completely to carbon oxides on SnO_2 catalyst. These results agree with those found by Buiten [9] for the oxidation of propylene on SnO_2 catalyst.

Table 7.1: Effect of temperature on conversion, selectivity and yield of methanol oxidation with inert medium

Run	Temperature (K)	Conversion (%)	Selectivity (%)	Yield (%)
M01	623	1.3	3.0	0.3
M02	648	3.0	2.0	0.6
M03	673	4.5	1.5	0.7
M04	698	6.0	1.2	0.7

Table 7.2: Effect of temperature on conversion, selectivity and yield of methanol oxidation with MoO_3 as a catalyst

Run	Temperature (K)	Conversion (%)	Selectivity (%)	Yield (%)
A01	598	0.7	1.0	1.0
A02	623	1.1	1.0	1.0
A03	648	30.0	0.95	28.5
A04	673	35.0	0.93	32.5
A05	698	42.0	0.90	38.0

Table 7.3: Effect of temperature on conversion, selectivity and yield of methanol oxidation with SnO_2 as a catalyst

Run	Temperature (K)	Conversion (%)	Selectivity (%)	Yield (%)
G01	523	5.0	0.44	0.022
G02	548	20.0	0.35	0.071
G03	573	78.6	0.098	0.077
G04	598	90.0	0.0	0.0

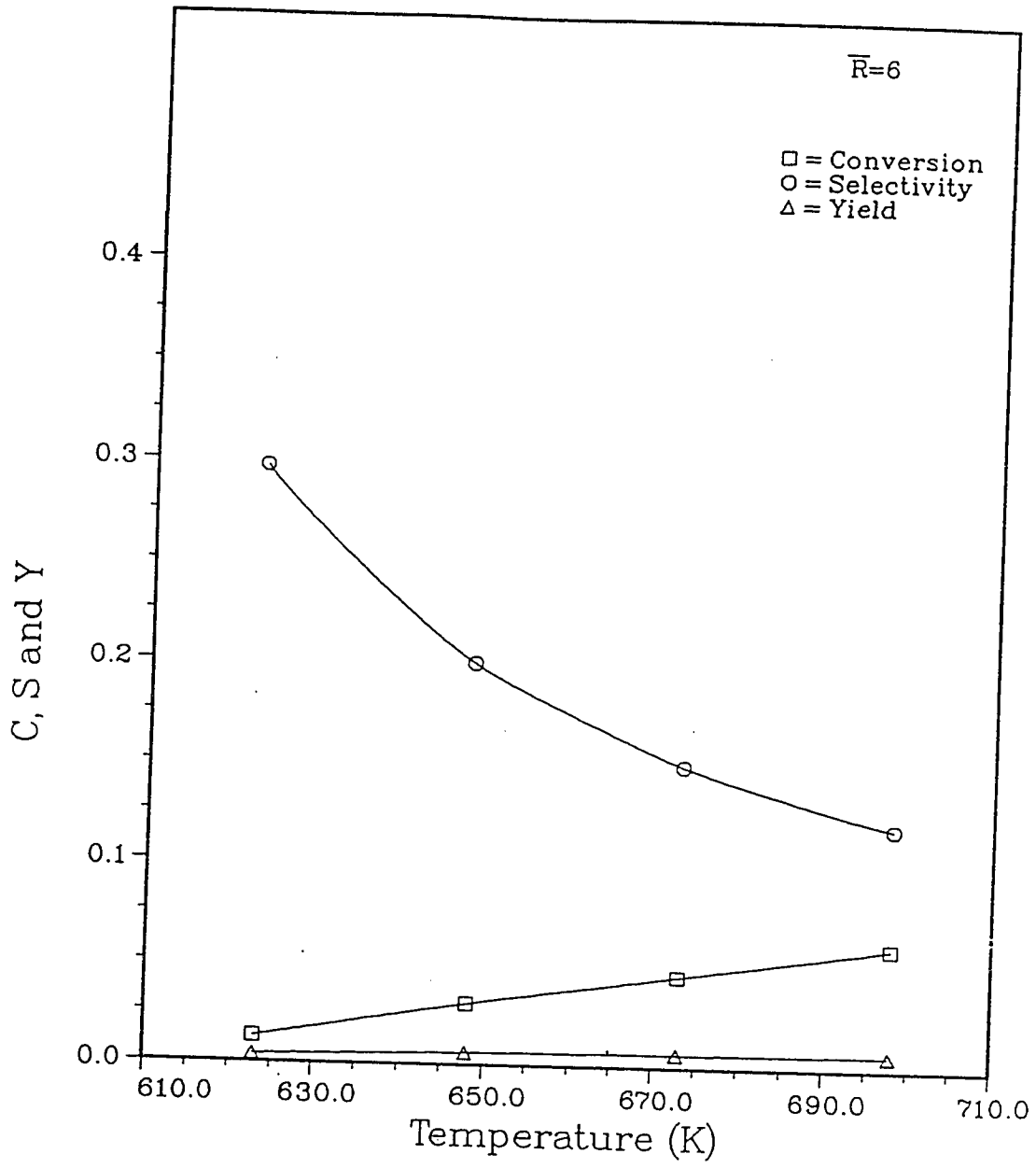

Figure 7.1: Effect of temperature on conversion, selectivity, and yield with pumice stone.

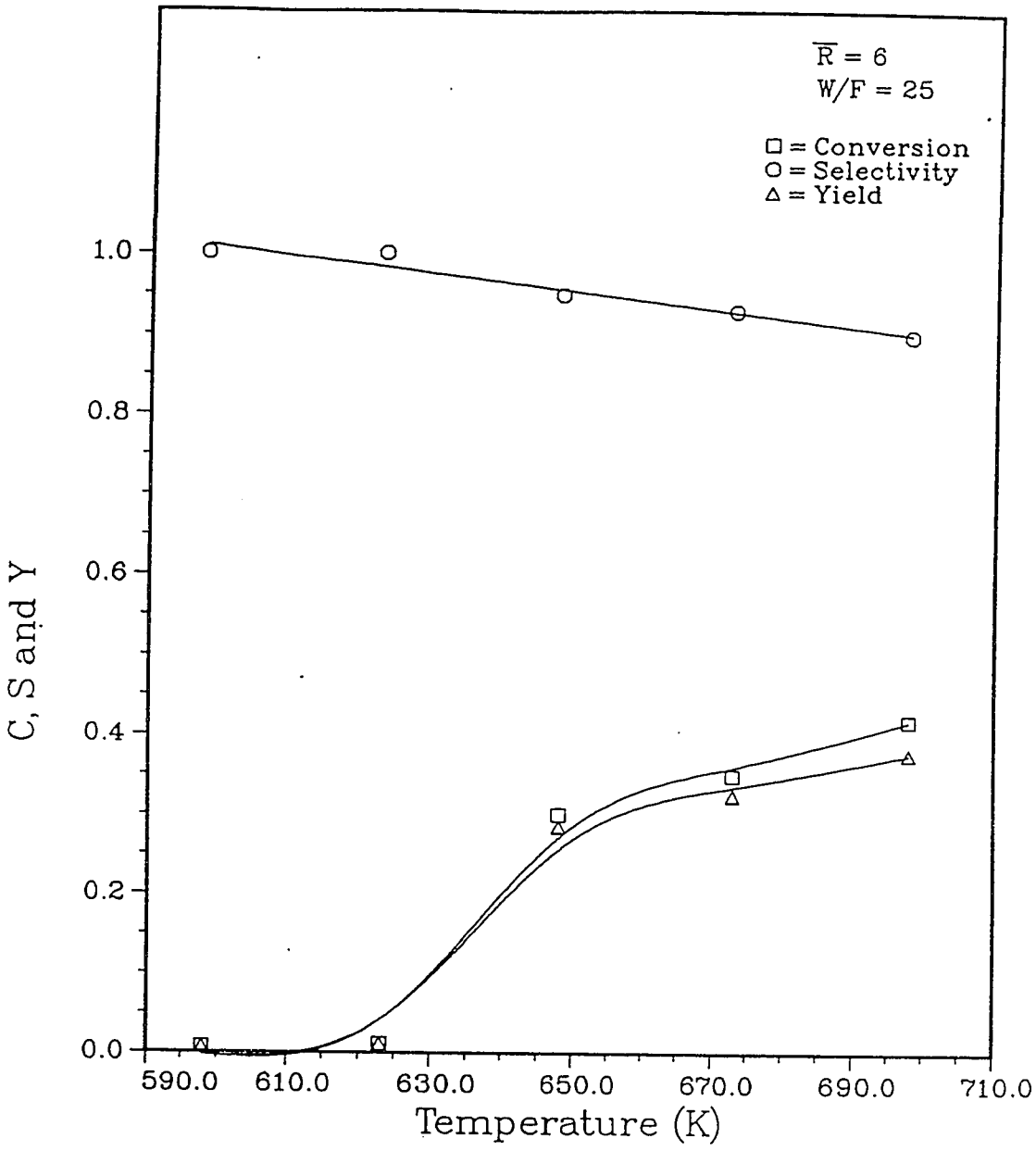

Figure 7.2: Effect of temperature on conversion, selectivity, and yield with MoO_3 as catalyst.

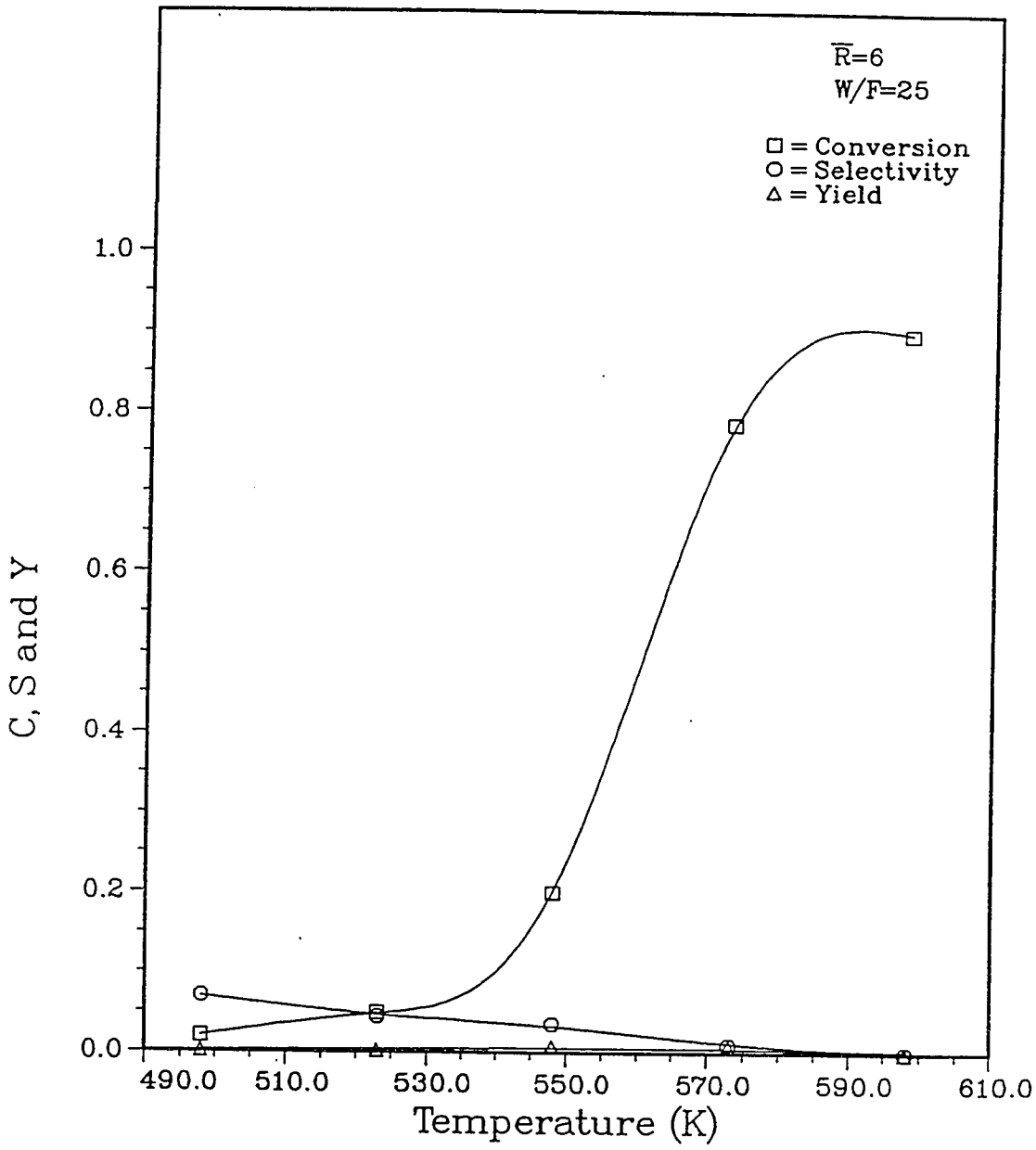

Figure 7.3: Effect of temperature on conversion, selectivity, and yield with SnO_2 as catalyst.

It was found that half or more of the reacted propylene was completely broken down to CO and CO_2.

7.4 Results with Mo-Sn Oxide Mixtures

There is abundant literature regarding the use of MoO_3 as catalyst for the oxidation of methanol to formaldehyde. Several mixtures of MoO_3 with other oxides have been investigated [22,16,24,15]. However, little information is available regarding tin oxide catalyst for this reaction. Hence, the primary goal of this study was to produce high yield Sn-Mo oxides catalyst for the production of formaldehyde under the specified operating conditions.

In order to find an optimum catalyst composition, one that gave the highest yield, five new catalysts were prepared by mixing different amounts of ammonium molybdate and tin hydroxide gel in such a way as to give the desired weight ratio of SnO_2/MoO_3. This high yield catalyst was characterized later in a kinetic study. Table 7.4 shows the catalysts used, their composition and their tag for proper identification. It is to be noticed that there was a change in the color with a change in the composition of the catalysts. As the amount of MoO_3 increased the catalysts color became lighter.

A statistical model was built in order to determine the optimal catalyst composition. In this model the random variable, Y, is the product of conversion times selectivity. The independent variables X_1, X_2, X_3, X_4 represent the temperature, the space time, the reactants' molar ratio, and the catalysts' composition, respectively. The data used for model building are represented in Table 7.5.

The complete form of the model that represented these data is:

Table 7.4: Catalysts' composition.

Catalyst	Tag set (#)	MoO_3 (wt%)	SnO_2 (wt%)	Color
I	A	100.0	0.0	blue
II	B	90.0	10.0	cream-green
III	C	70.0	30.0	green-yellow
IV	D	50.0	50.0	dark green
V	E	30.0	70.0	yellow-green
VI	F	10.0	90.0	yellow
VII	G	0.0	100.0	cream-blue

$$\begin{aligned} E(Y) &= a_0 + a_1X_1 + a_2X_2 + a_3X_3 + a_4X_4 \\ &+ a_{12}X_1X_2 + a_{13}X_1X_3 + a_{14}X_1X_4 \\ &+ a_{23}X_2X_3 + a_{24}X_2X_4 + a_{34}X_3X_4 \\ &+ a_{11}X_1^2 + a_{22}X_2^2 + a_{33}X_3^2 + a_{44}X_4^2 \end{aligned} \tag{7.1}$$

The linear regression of the data after excluding the non-significant parameters gave the following model:

$$\begin{aligned} E(Y) &= 45.88 + 7.58X_1 + 6.94X_2 + 0.4380X_3 - 12.22X_4 \\ &- 17.19X_1X_4 - 11.25X_2X_4 - 0.4434X_3X_4 - 35.12X_{44}^2 \end{aligned} \tag{7.2}$$

Equation 7.2 indicates that the yields would increase with an increase in temperature and catalyst to feed flow rate ratio (W/F). The yield would also increase with the decrease of tin oxide content in MoO_3/SnO_2 catalysts. Another information that can be deduced from the above model is that temperature and space time have the greatest impact on the methanol oxidation to formaldehyde, while the effect of methanol/air molar feed ratio is almost negligible. As a result the interaction between the temperature and the tin oxide content was significant, and so

was the interaction between the space time and the tin oxide content, while the other interactions and squared terms were not significant. Therefore they were excluded from the model.

The above model was maximized with respect to the catalyst composition at the center point for the remaining operating conditions. The maximum value of E(Y) was obtained at the center point of the catalyst composition. The effect of catalyst composition at the center point of the operating variables is represented graphically in Figure 7.4. It is obvious that the conversion of methanol increased significantly as tin oxide content in the catalysts mixture was increased. This behavior was as expected since tin oxide catalyst is generally more active than molybdenum oxide catalyst. However, the selectivity of the catalyst decreased sharply when the SnO_2 weight % increased more than 50%. It can be concluded that the maximum yield was obtained when the catalyst composition was 50% SnO_2 – 50%MoO_3.

The results of this work agreed with those obtained by Buiten [9] for the oxidation of propylene by means of $SnO_2 - MoO_3$ catalysts. SnO_2 showed some catalytic activity; half or more of the reacted propylene was completely broken down to CO and CO_2. MoO_3 was found to be a much less active oxide. However, SnO_2 covered with a monolayer of molybdenum oxide was 5 to 10 times more active in the oxidation of propylene than SnO_2 alone, and gave completely different product distribution. It was concluded that although MoO_3 did not form a bulk compound with SnO_2, it could be bound to the SnO_2 surface, which then exhibited a peculiar catalytic activity. These results were confirmed later by Niwa et al. [39,38] for the oxidation of methanol over $SnO_2 - MoO_3$ catalysts. They concluded

that methanol is selectively oxidized to formaldehyde over MoO_3 catalysts at temperatures above 350°C, but was oxidized to carbon oxides only on SnO_2. For the mixed $SnO_2 - MoO_3$ catalyst, formaldehyde was formed selectively even at 180°C. Thus it can be postulated that the high oxidation activity arises from the presence of tin oxide itself and the high formaldehyde selectivity from the presence of molybdenum oxide.

Coupling the results obtained at the center point of the operating conditions with those obtained from the fractional factorial design and model building scheme, a composition of 50% SnO_2 and 50% MoO_3 weight percent was chosen to be an optimum composition of the catalyst which was used for further detailed kinetic study of the reaction.

The surface area of this catalyst (0.246 to 0.175 mm particle size) as determined experimentally was 51.2 m^2/g.

Table 7.5: Two-level fractional factorial design for the three operating variables at each level of catalyst composition.

Run number	Temperature (K)	W/F hr g-cat/g-mol	R g-mol CH_3OH/g-mol air	SnO_2 wt %	E(Y) %
B01	513	10	0.08	10	1.10
B02	573	10	0.04	10	16.24
B03	513	40	0.04	10	28.53
B04	573	40	0.08	10	67.65
B05	543	25	0.06	10	25.78
B06	543	25	0.06	10	25.12
B07	543	25	0.06	10	26.55
C01	513	10	0.08	30	4.56
C02	573	10	0.04	30	60.61
C03	513	40	0.04	30	28.33
C04	573	40	0.08	30	68.91
C05	543	25	0.06	30	39.84
C06	543	25	0.06	30	42.65
C07	543	25	0.06	30	35.05
D01	513	10	0.08	50	11.29
D02	573	10	0.04	50	63.65
D03	513	40	0.04	50	34.29
D04	573	40	0.08	50	83.58
D05	543	25	0.06	50	69.88
D06	543	25	0.06	50	67.43
D07	543	25	0.06	50	66.88
E01	513	10	0.08	70	28.84
E02	573	10	0.04	70	5.81
E03	513	40	0.04	70	40.01
E04	573	40	0.08	70	0.0
E05	543	25	0.06	70	26.7
E06	543	25	0.06	70	25.0
E07	543	25	0.06	70	26.02
F01	513	10	0.08	90	29.06
F02	573	10	0.04	90	0.0
F03	513	40	0.04	90	8.76
F04	573	40	0.08	90	0.0
F05	543	25	0.06	90	1.02
F06	543	25	0.06	90	1.11
F07	543	25	0.06	90	1.04

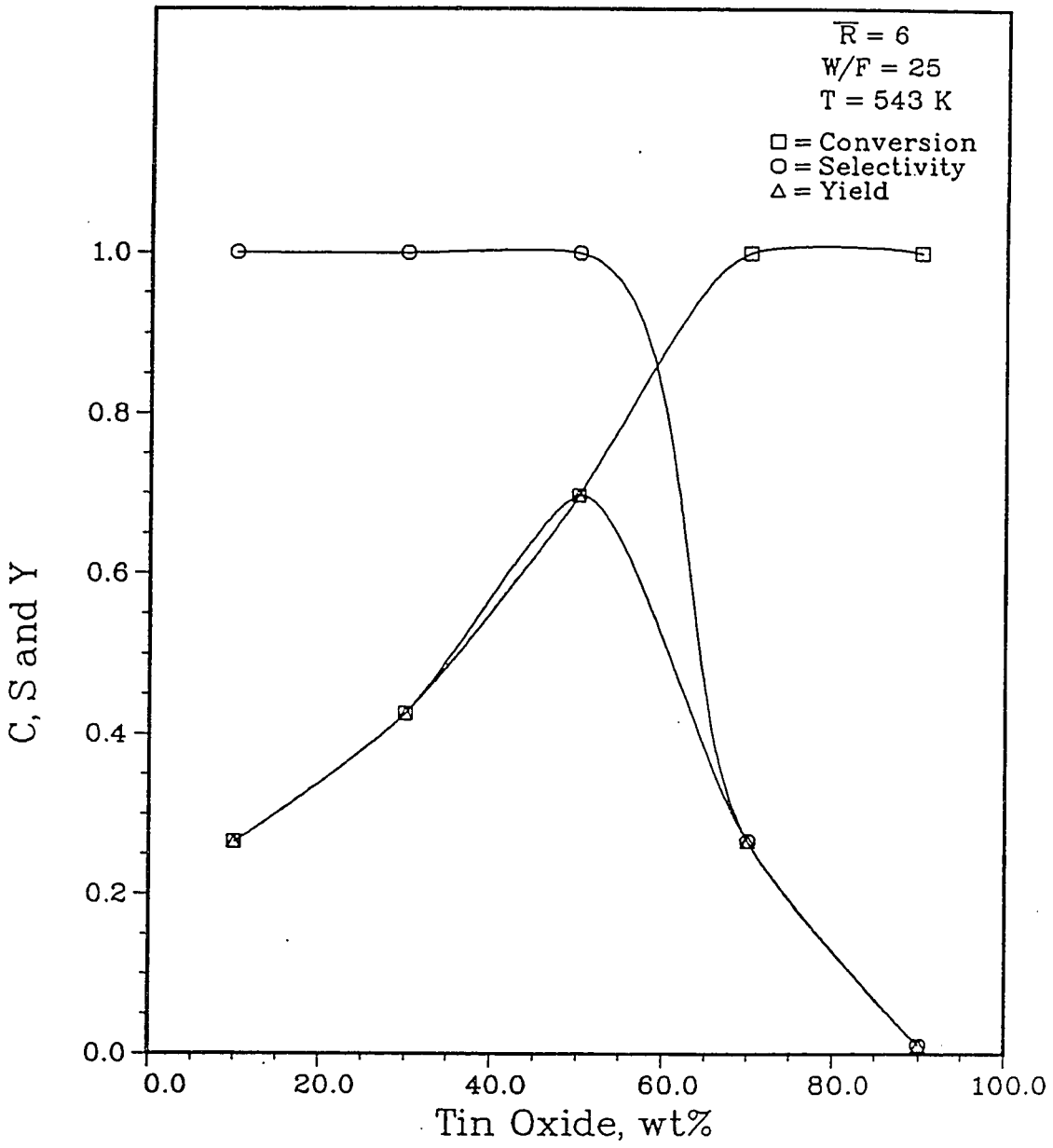

Figure 7.4: Effect of catalyst composition on conversion, selectivity, and yield of the oxidation of methanol to formaldehyde.

7.5 Kinetic Analysis of Data

7.5.1 Factors Affecting Rate Mechanism

The rate equation is generally derived in terms of temperature, pressure, and composition of the reactants. The other factors which might affect kinetics are considered below:

- Catalyst Activity - The activity of the catalysts remained fairly constant for all the runs for the kinetic study. This was confirmed by carrying out replicate runs at the center point conditions after making each set of runs.

- Homogeneous Reactions and Reactions in the Absence of Catalyst - As indicated in section 6.1, the amount of product produced in the absence of catalyst at the operating conditions for the kinetic analysis was negligible.

- Side Reactions - The main by-products of methanol oxidation over Mo-Sn oxide catalysts were carbon oxides. Carbon monoxide is believed to be caused by the thermal decomposition of formaldehyde [39]. Carbon dioxide is formed by the oxidation of carbon monoxide. As observed in most of the experimental data, especially those obtained for the kinetic analysis, the amount of carbon oxides formed was quite small compared to the total products. Experimental runs, where carbon oxides formed more than 5% of the total product, were very few. These runs were not considered for kinetic analysis. No traces of formic acid, dimethyl ether, dimethoxy methane or methyl formate were found in the analysis of the products.

- Pressure Drop Through Catalyst Bed - There was no pressure drop across the reactor. This was confirmed by measuring the pressure at the inlet and at the outlet of the reactor. It was generally the same as the atmospheric pressure for almost all the runs. The total pressure in the catalyst bed was thus taken as 1 atm for ease of calculation.

- Plug Flow - In the present study, the velocity profile in the reactor was assumed to be flat. The flat pattern in the tube is affected by a number of factors. The two most important ones are axial dispersion and channeling. The effects of axial dispersion was considered to be negligible for $L/d_p > 350$, where L was the length of the bed and d_p the diameter of the catalyst particle. Channeling can be avoided by having a large d_t/d_p ratio, larger than 20 according to some authors [46]. The ratio of d_t/d_p in the present case was 44. Hence, the assumption of plug flow could not result in any significant error.

- Diffusion - Diffusion can be of two kinds:

  (a) Molecular Diffusion: This kind of diffusion is significant only when the mean free path of diffusing molecules is small with respect to the pore radius. In such cases, the partial pressure of the different reactants control the diffusion process. It is insignificant unless the pressure is very high or the pore radii is very large. Since the present work was conducted at nearly atmospheric pressure, molecular diffusion was expected to be negligible. A set of runs, termed set P, was taken at the same operating conditions and with different feed velocity of methanol to check the effect of molecular diffusion.

It can be seen from Figure 7.5 that there was no effect of the feed velocity on conversion. Hence, it can be assumed that molecular diffusion did not control the reaction.

(b) Knudsen Diffusion: When pore size of catalyst (or porous medium) is small, collision between molecules and walls controls the diffusion process. In the present study the catalyst particles used had an average particle diameter of 0.21 mm. For such small catalyst particles, Knudsen diffusion did not affect the results significantly.

A set of runs, termed set Q, was carried out at the center point operating conditions but changing particle diameter to find out if Knudsen diffusion affected the results. Results are shown in Figure 7.6. It is obvious that conversion was nearly the same. In case Knudsen diffusion was affecting the results significantly, changing catalyst diameter would have resulted in significant change in the rate of reaction. Therefore, for such small particles the effectiveness factor can be considered one [18,47,11].

- Resistance to External Heat and Mass Transfer - In order to simplify the correlation for experimental data, it is necessary to minimize these resistances so that they become negligible. The values of partial pressure and temperature in the bulk stream and at the gas-solid interface may differ significantly in certain systems. The effect of heat and mass transfer is explained in detail in section 3.5. A sample calculation based on the method of Yoshida et al. [58], that estimates the temperature and pressure drops from the bulk phase to the catalyst surface, is given in Appendix E. The maximum temperature drop of 0.1 K and the maximum pressure drop of less than 100 Pa suggested

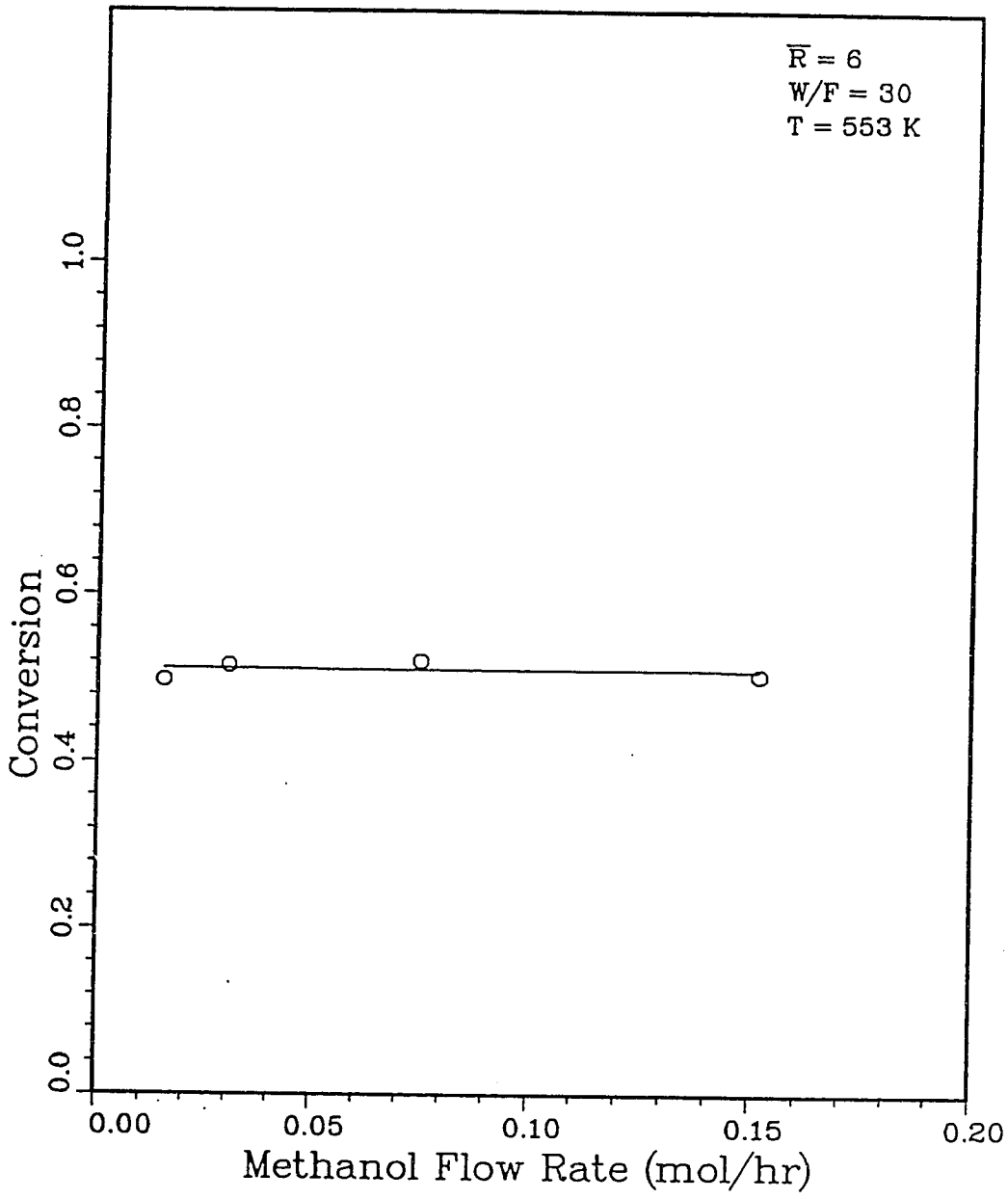

Figure 7.5: Effect of feed velocity on the conversion of methanol

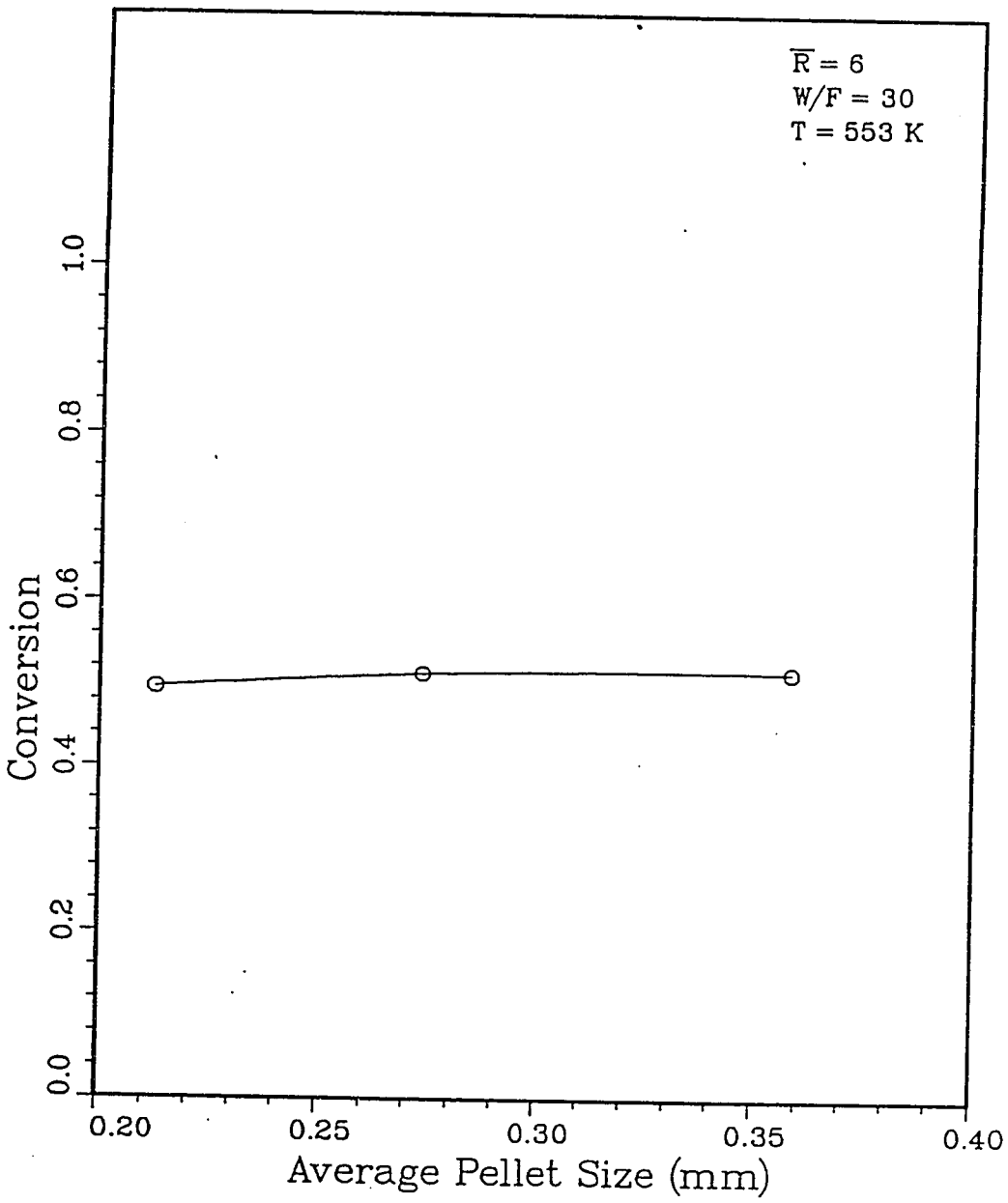

Figure 7.6: Effect of catalyst particle size on the conversion of methanol

that the heat and mass transfer effects were negligible.

7.5.2 Effect of Process Variables

The effect of temperature (T), space velocity (W/F), and methanol to air molar feed ratio ($\overline{R}$) on conversion of methanol (C), yield of formaldehyde (Y), and selectivity of the catalyst (S) were investigated.

Effect of Temperature

The effect of temperature on conversion, yield and selectivity was investigated in the temperature range between 513 and 593 K. An increase in the temperature resulted in an increase in the overall conversion of methanol. This increase is more accentuated at higher space times. However, at temperature equal 573 K there were some cases where selectivity to formaldehyde decreased due to further oxidation of methanol to carbon oxides. In some cases conversion reached 100% and selectivity remained nearly at 100%. Figures 7.7-7.9 clearly show these effects.

Effect of W/F

The effect of W/F on conversion selectivity and yield was studied at temperatures between 513 and 573 K, methanol to air molar feed ratio between 4 and 10. For all methanol concentrations an increase in W/F caused a dramatic increase in the conversion without affecting the selectivity significantly. This conforms the fact that an increase in W/F ratio with constant feed, gas flow rate and methanol results in increased contact time. Similar results have been reported in the literature for other metal oxide catalysts. Figures 7.9-7.11 show the importance of an adequate contact time to attain high yields.

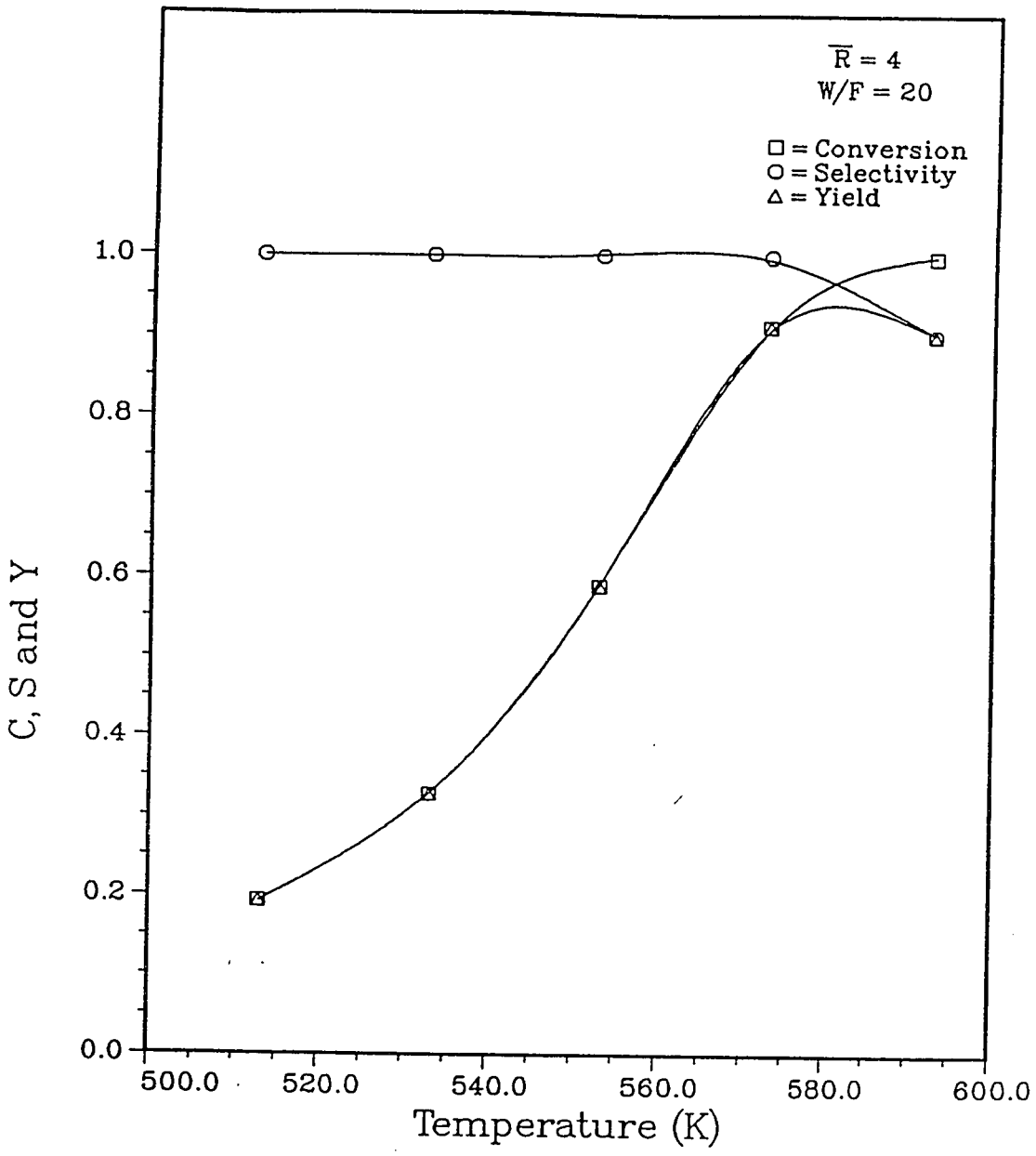

Figure 7.7: Effect of temperature on conversion, selectivity, and yield of the oxidation of methanol to formaldehyde at W/F of 20 and $\overline{R}$ of 4

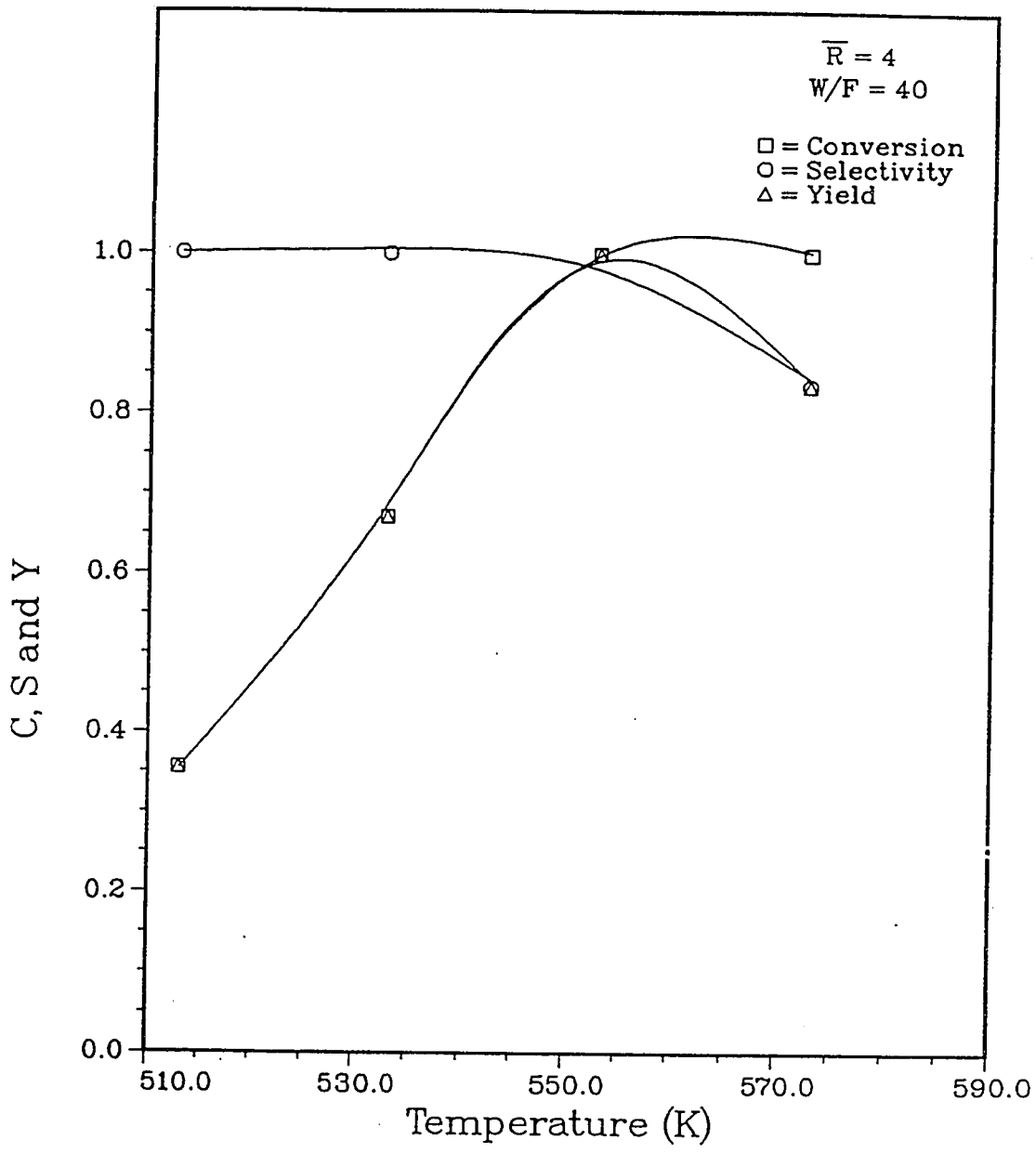

Figure 7.8: Effect of temperature on conversion, selectivity, and yield of the oxidation of methanol to formaldehyde at W/F of 40 and $\overline{R}$ of 4

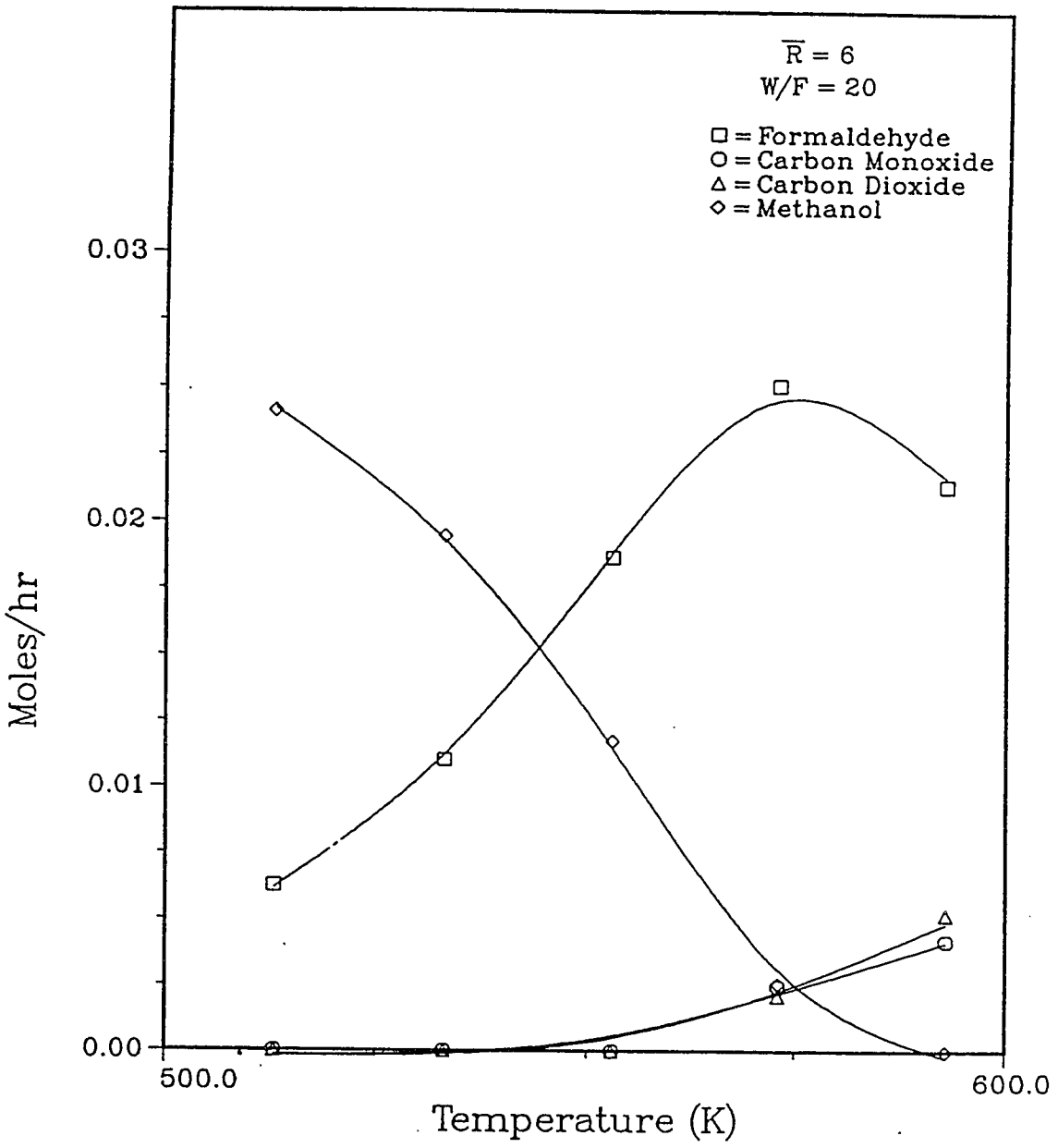

Figure 7.9: Effect of temperature on products distribution of the oxidation of methanol at W/F=20 and $\overline{R}$=6

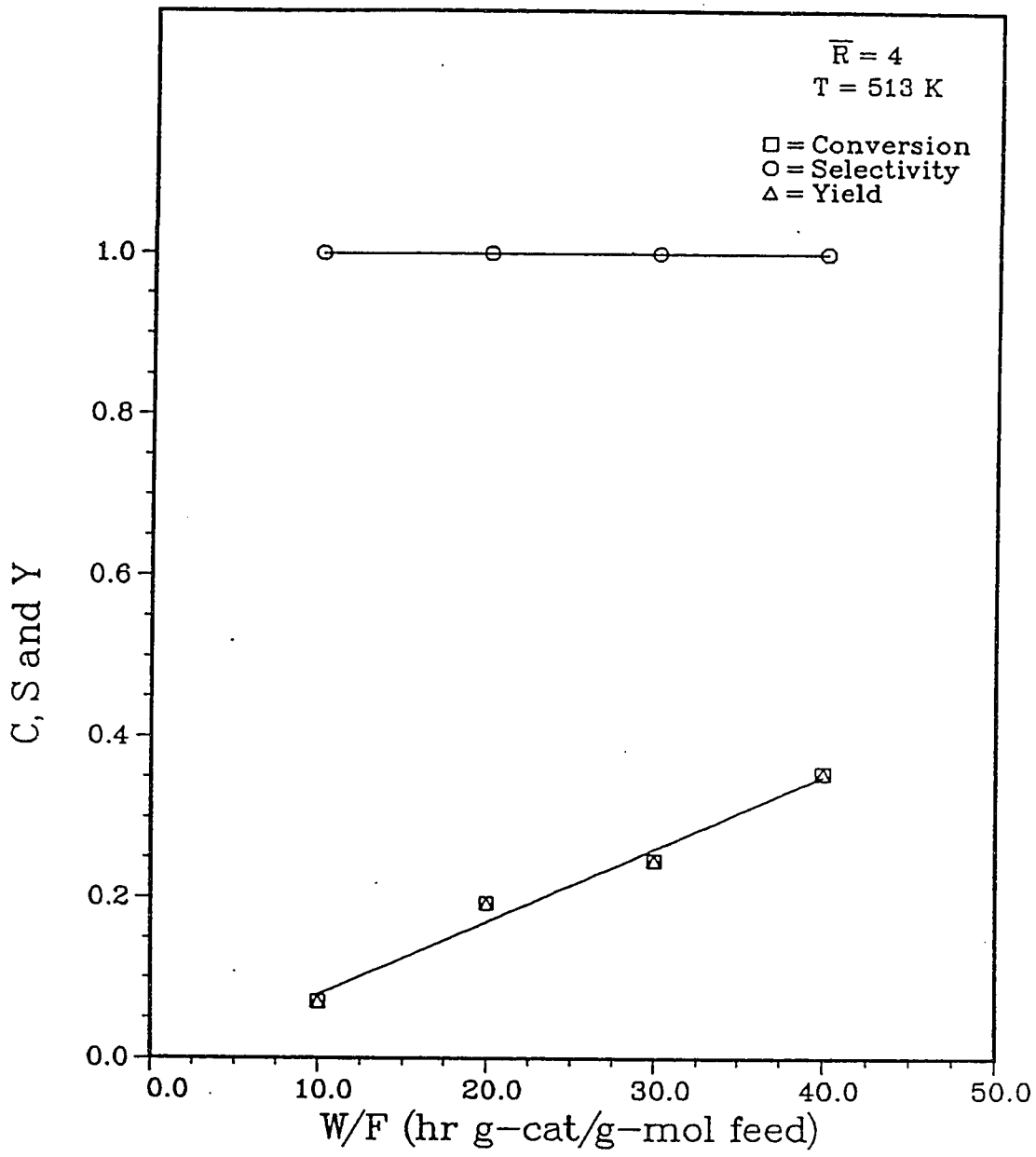

Figure 7.10: Effect of space time on conversion, selectivity, and yield of the oxidation of methanol to formaldehyde at T of 513 K and $\overline{R}$ of 4

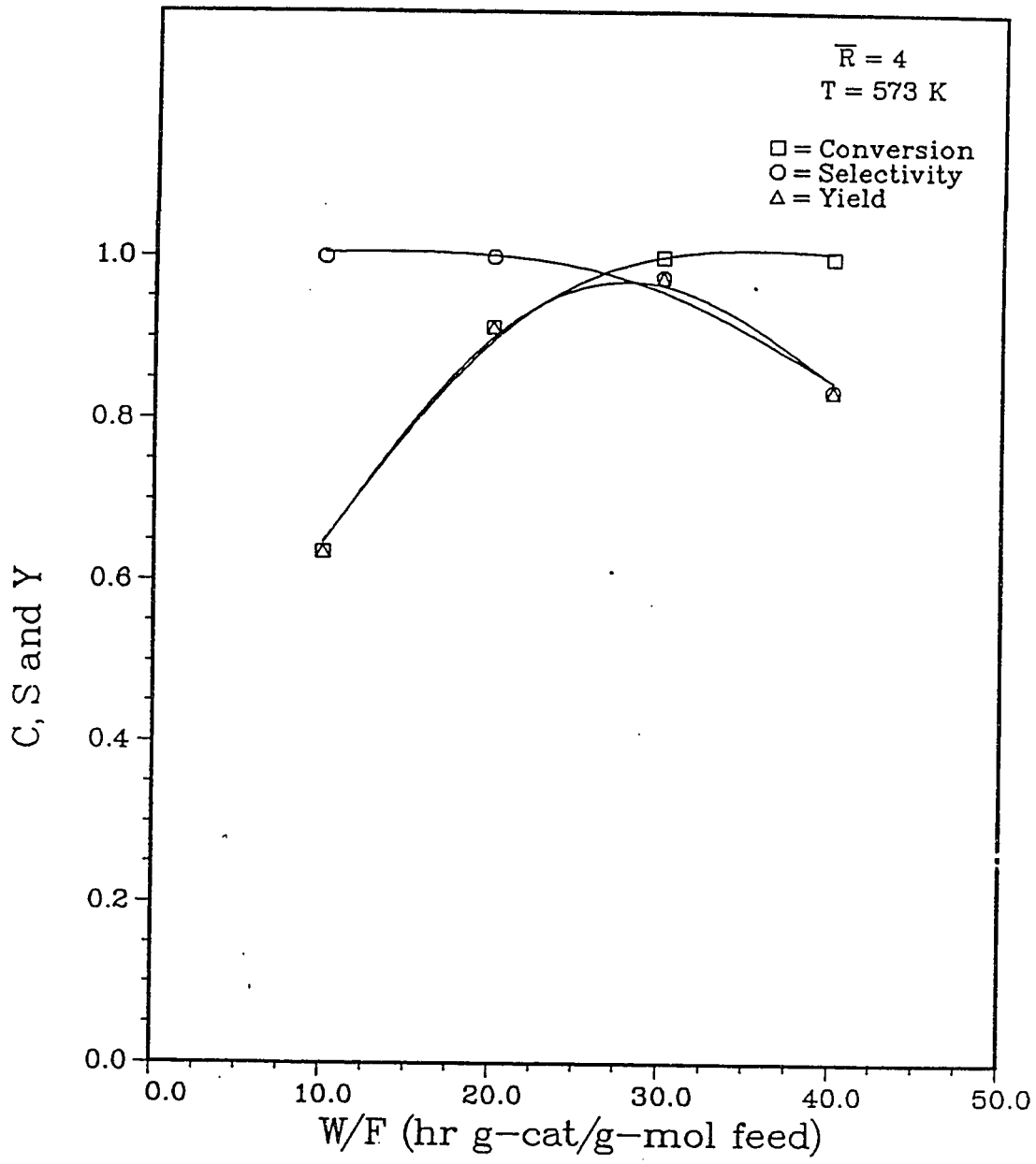

Figure 7.11: Effect of space time on conversion, selectivity, and yield of the oxidation of methanol to formaldehyde at T of 573 and $\overline{R}$ of 4

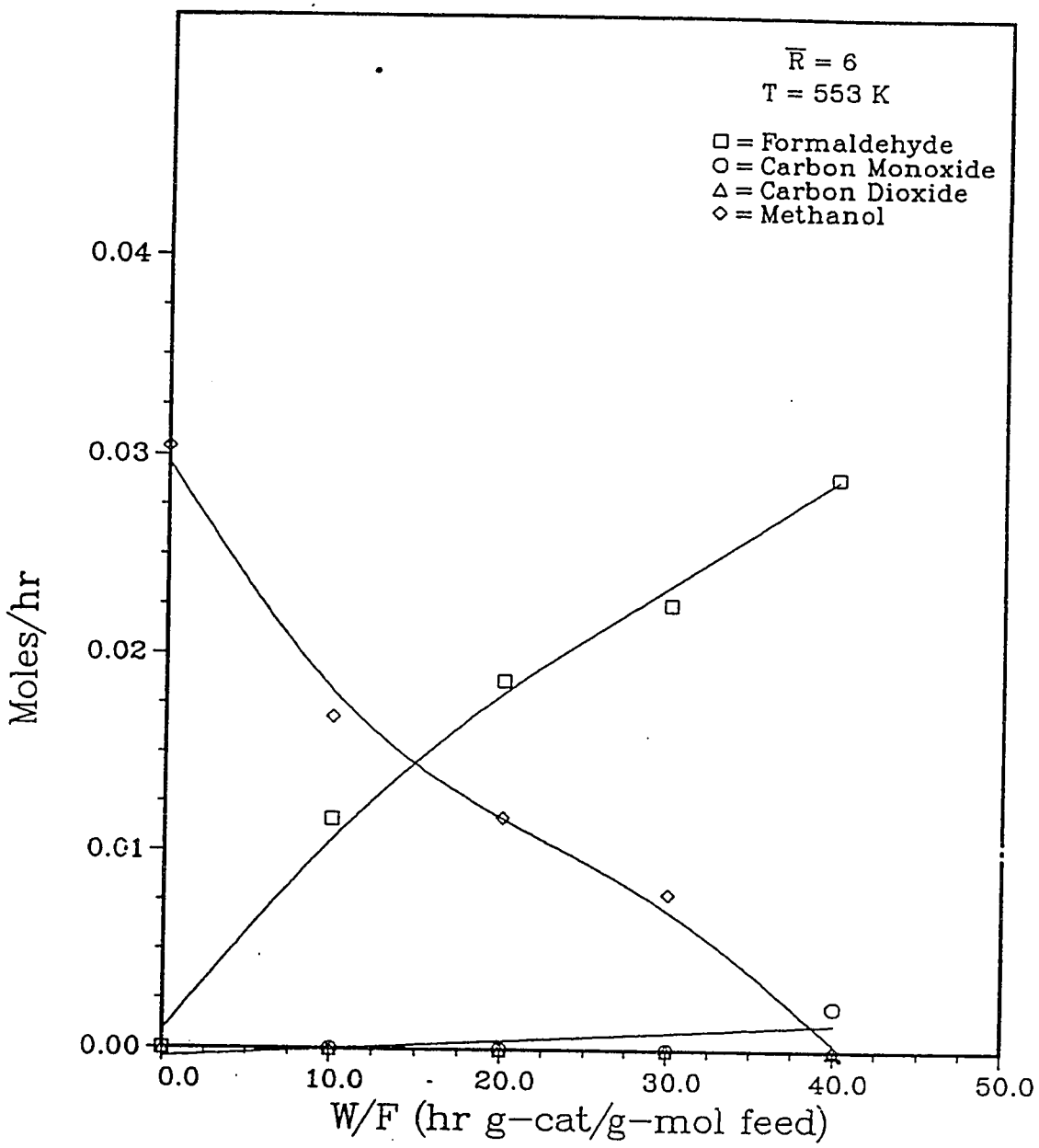

Figure 7.12: Effect of space time on products distribution of the oxidation of methanol at T=553 and $\overline{R}$=6

Effect of Methanol-Air Flow Rates

The effect of methanol to air molar flow ratio in the feed, $\overline{R}$, on conversion, selectivity and yield was studied at temperatures between 513 and 573 K, for space times between 10 and 40 hr g-cat/g-mol methanol. For most cases little increase in conversion was found with an increase in methanol concentration. However, at higher conversions the selectivity decreased with an increase in methanol concentration in the feed. This is clearly observed in Figures 7.12 and 7.13.

The effects of different operating variables have been found to be the same as those found by Dosi [16], Jain [24] and Diaz [15].

As a result of this study it was found that the best operating conditions at which the yield was nearly 100%, considering the detecting capabilities of our instruments, are a reaction temperature of 553 K, a W/F ratio of 40 and $\overline{R}$ of 4.

7.5.3 Initial Rates

As indicated in section 4.1.3 it is necessary to determine the initial rate in order to obtain the rate equation that can accurately predict the reaction behavior.

The value of the equilibrium constant K_p for methanol oxidation is of the order of 10^{12} at 250°C and 10^{18} at 450°C, while the value of free energy change ΔG for the reactions varies from -22.7 Kcal/mole at 527°C to -26.2 Kcal/mole at 25°C. Hence this reaction can be considered highly irreversible.

The results of section 7.5.1 have shown that the effects of heat and mass transfer, diffusion, fouling and deactivation were negligible. It is desirable to minimize the resistances offered by each of these physical steps in order to simplify the interpretation of the experimental data, and thus to deal only with the chemical

aspects of the reaction.

For catalyzed reactions chemical steps involve activated adsorption of reactants, surface reactions on active sites, and activated desorption of products. Yang and Hougen [56] described a technique to determine the rate-controlling chemical step. They developed the initial rate method that is helpful in reducing the numbers of possible rate- controlling steps by eliminating some of them. Initial rate was obtained by plotting the fractional conversion of methanol versus space time and determining the slope of the curve as the space time approached zero. Figures 7.14-7.16 show this phenomenon. According to Yang and Hougen [56] the effect of feed composition in a bimolecular reaction upon the rate of disappearance of the limiting reactant falls into six types of rate curves, assuming only one rate-controlling step. The plots of initial rates, r_o, versus the moles percentage of methanol in the feed are given in Figures 7.17-7.19. A comparison of the curves in these figures with the type of curves used by Yang and Hougen [56] for identifying various mechanisms, suggested that the controlling step during the reaction was either adsorption of reactants or a surface reaction between the reactants. Also it was concluded that the desorption of products was not a rate-controlling step.

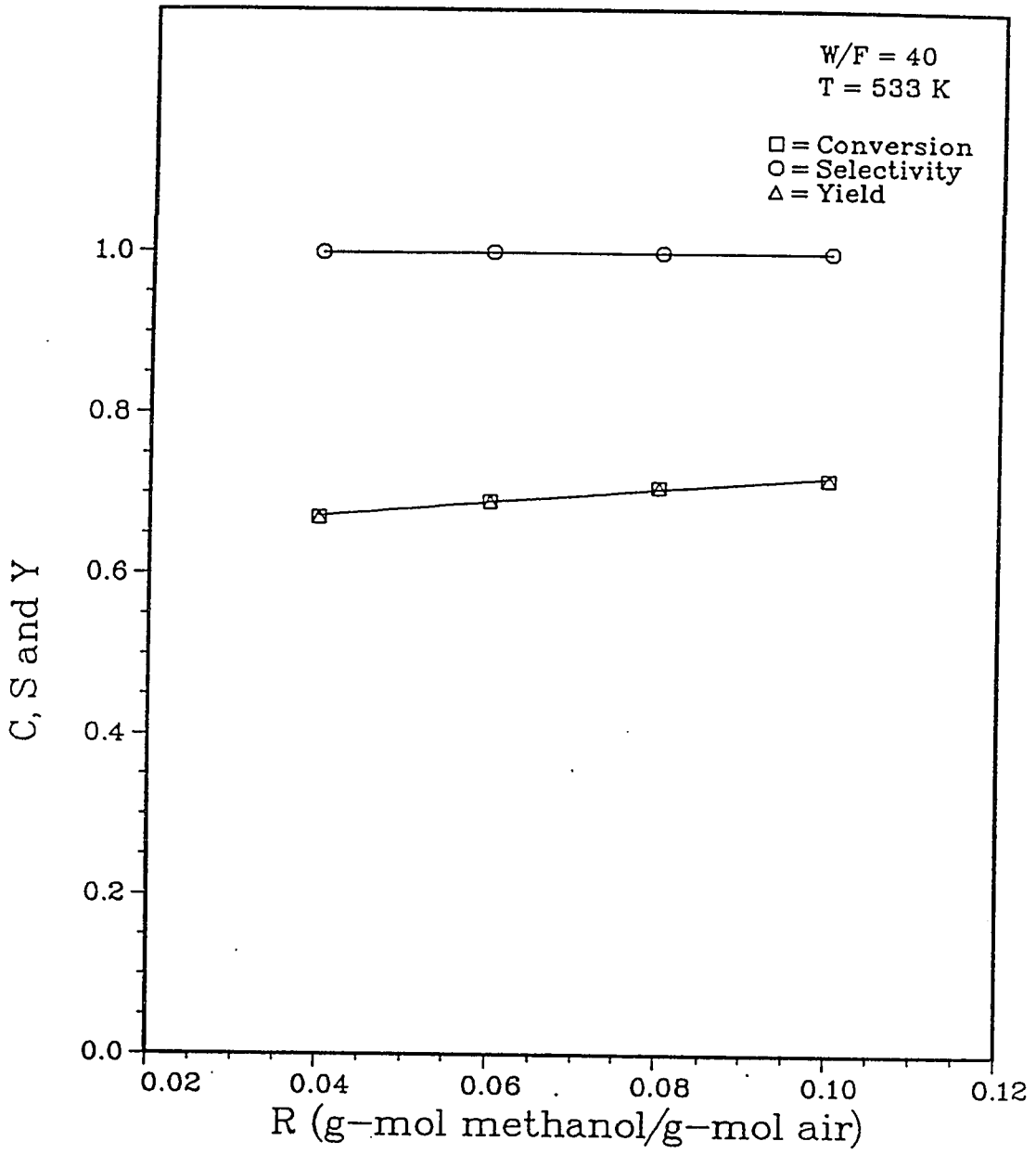

Figure 7.13: Effect of methanol-air flow rate ratio on conversion, selectivity and yield of the oxidation of methanol to formaldehyde at T of 513 K and W/F of 20

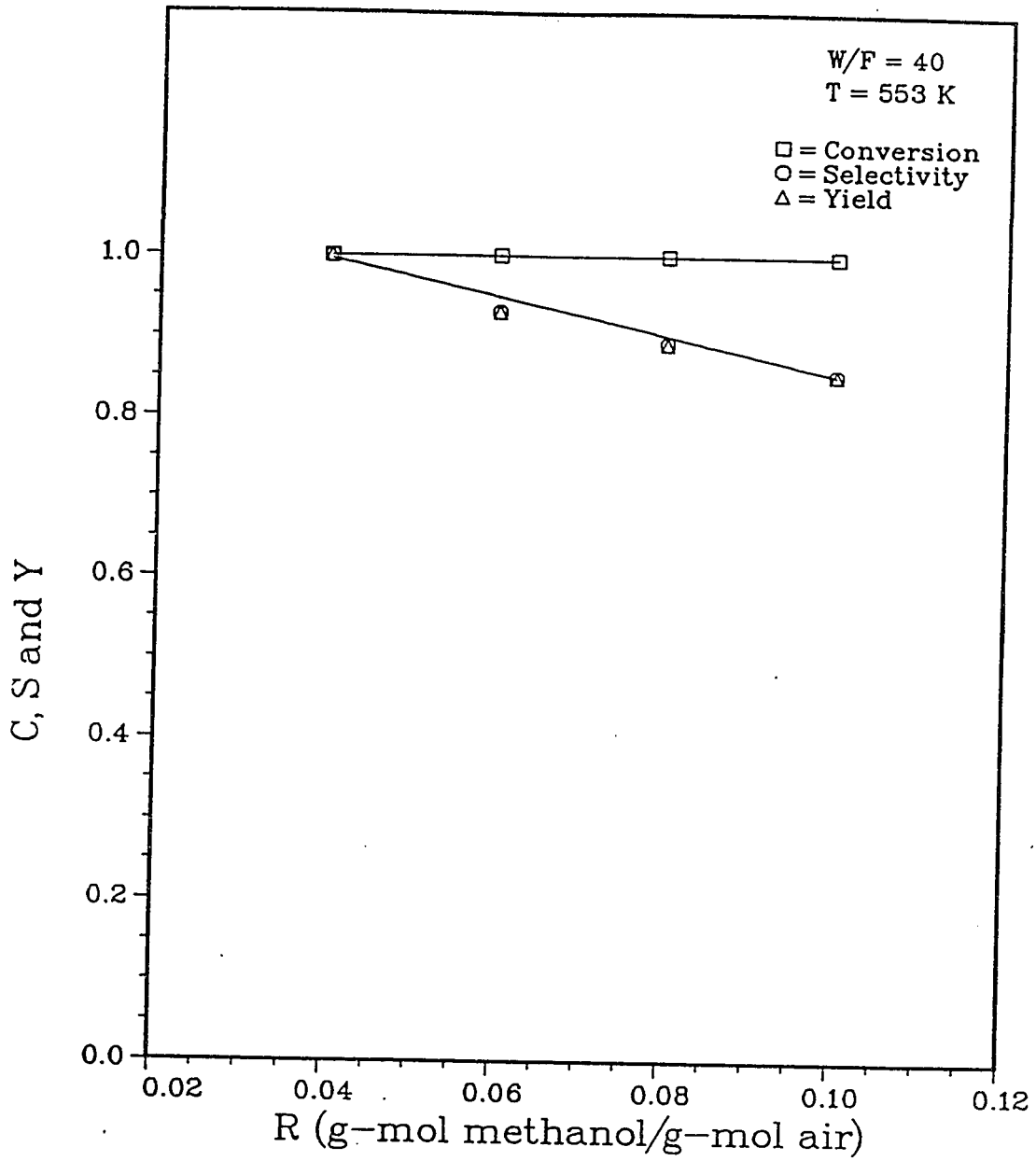

Figure 7.14: Effect of methanol-air flow rate ratio on conversion, selectivity and yield of the oxidation of methanol to formaldehyde at T of 573 and W/F of 40

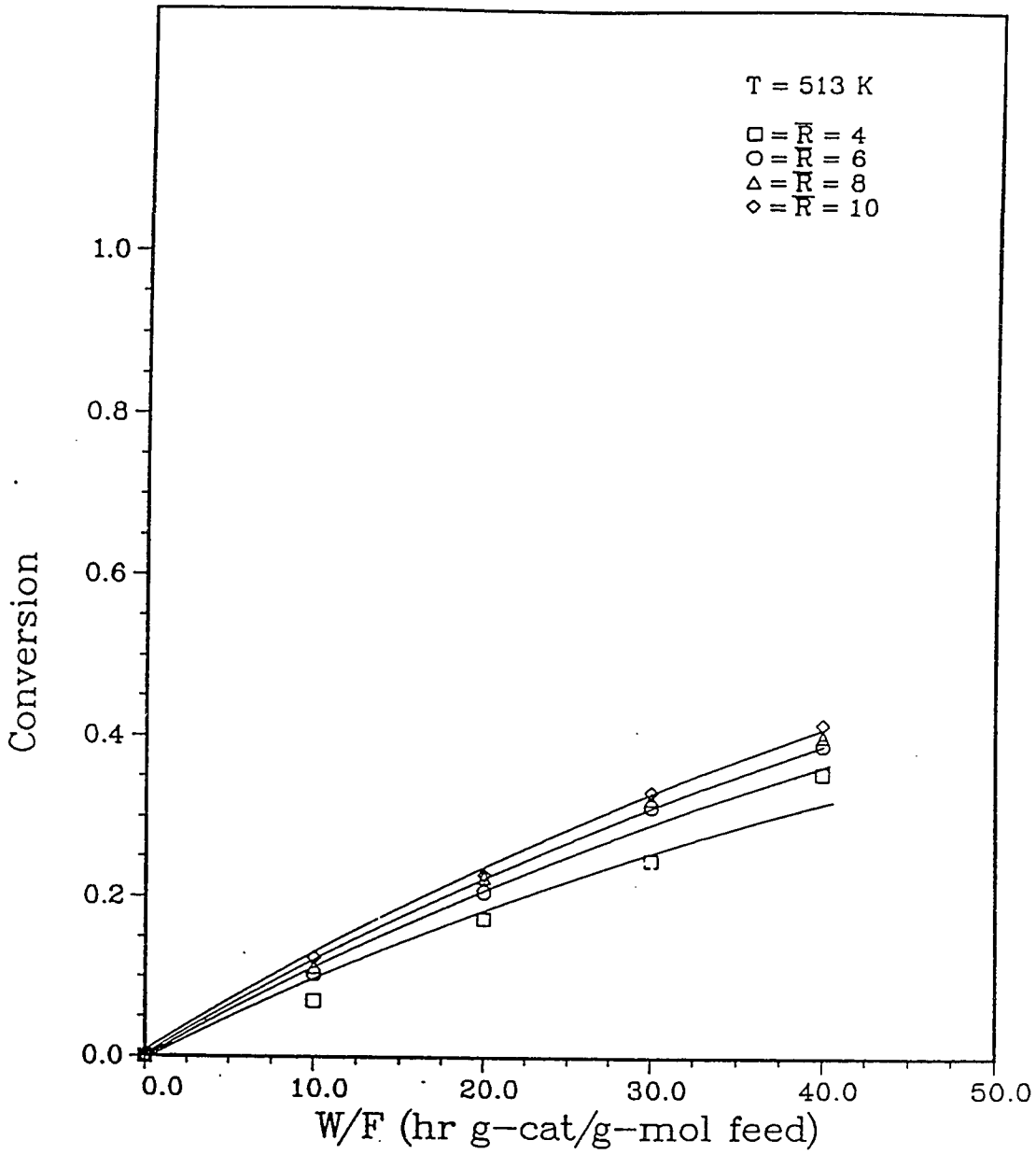

Figure 7.15: Effect of W/F on the conversion of methanol at T=513 K

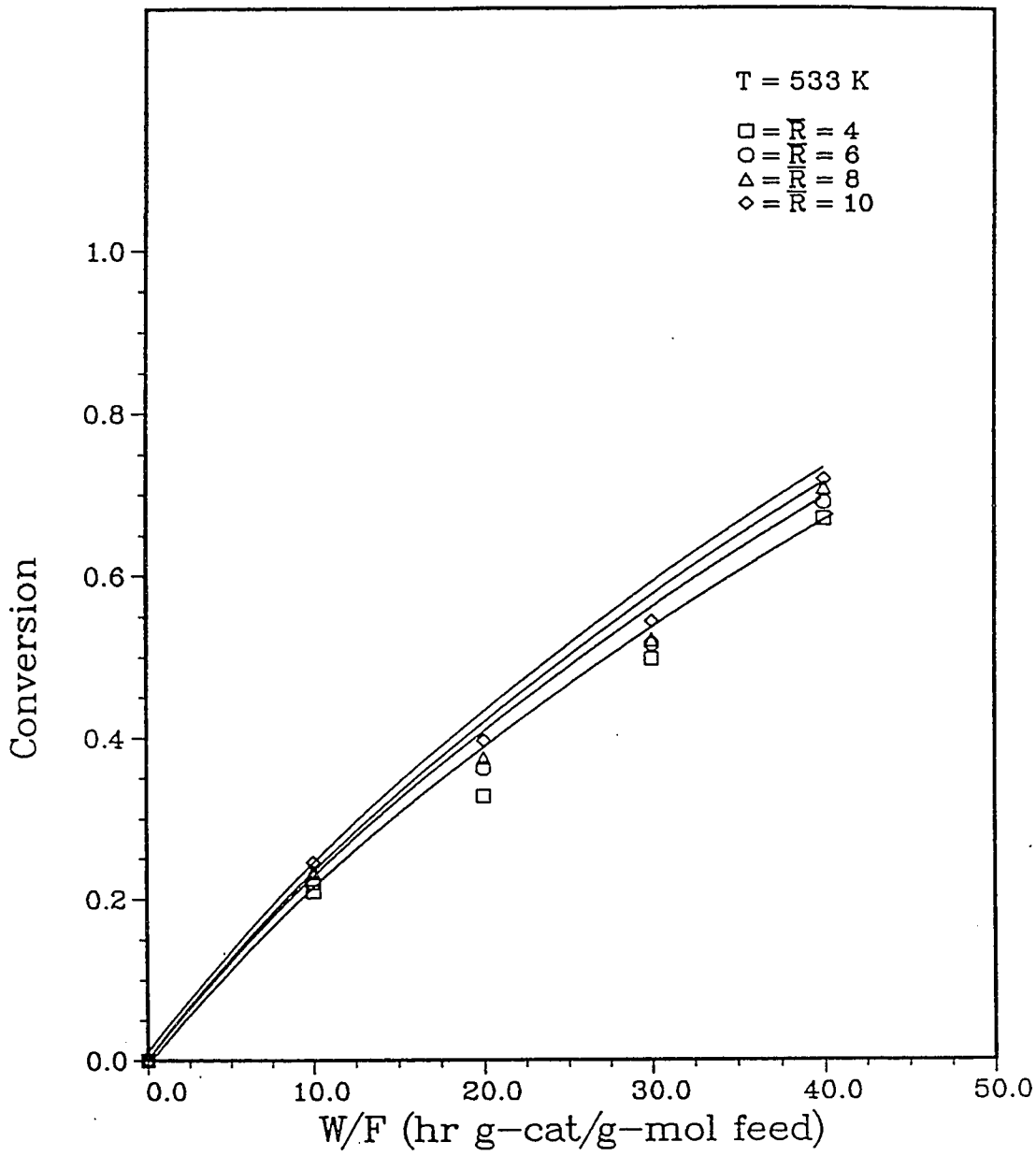

Figure 7.16: Effect of W/F on the conversion of methanol at T=533 K

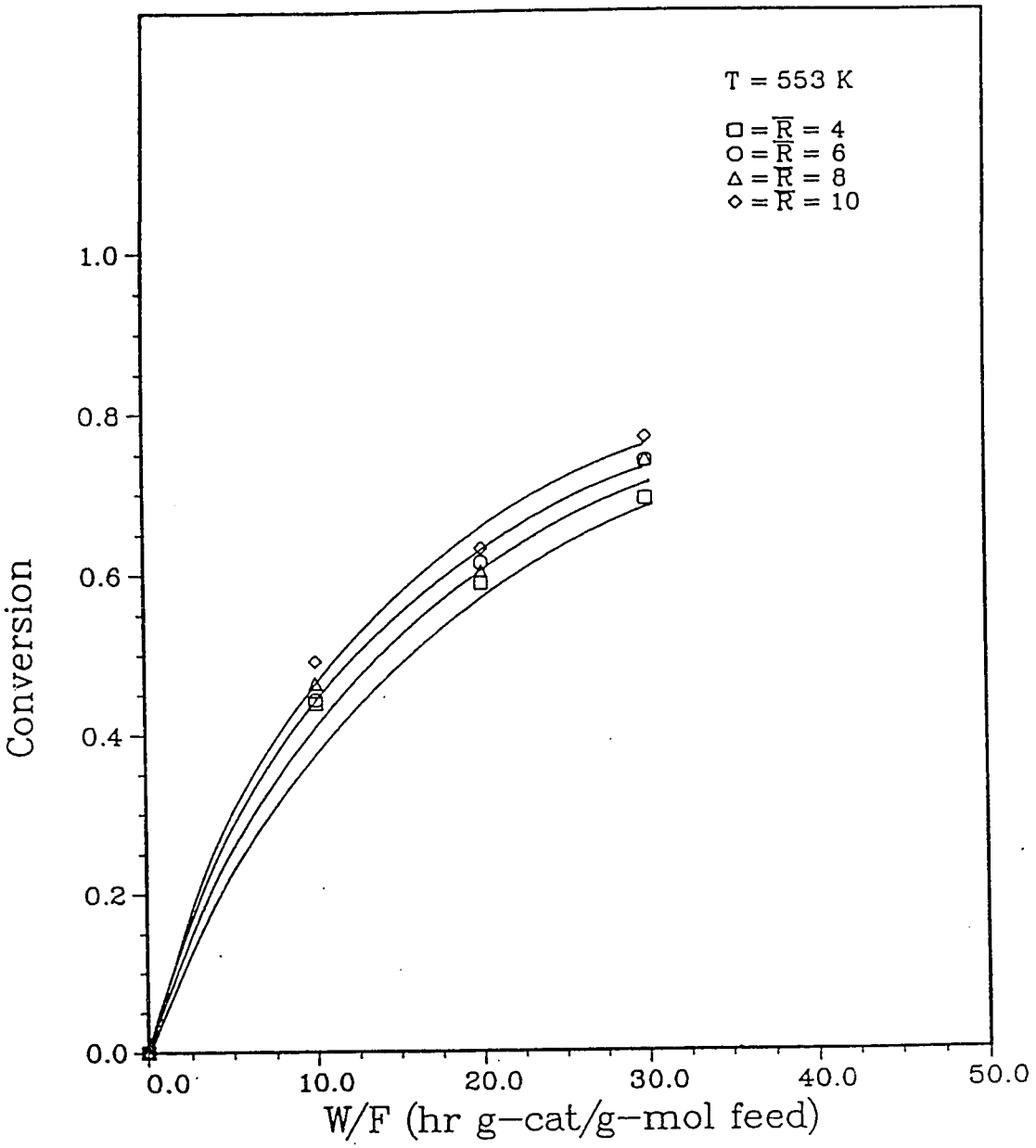

Figure 7.17: Effect of W/F on the conversion of methanol at T=553 K

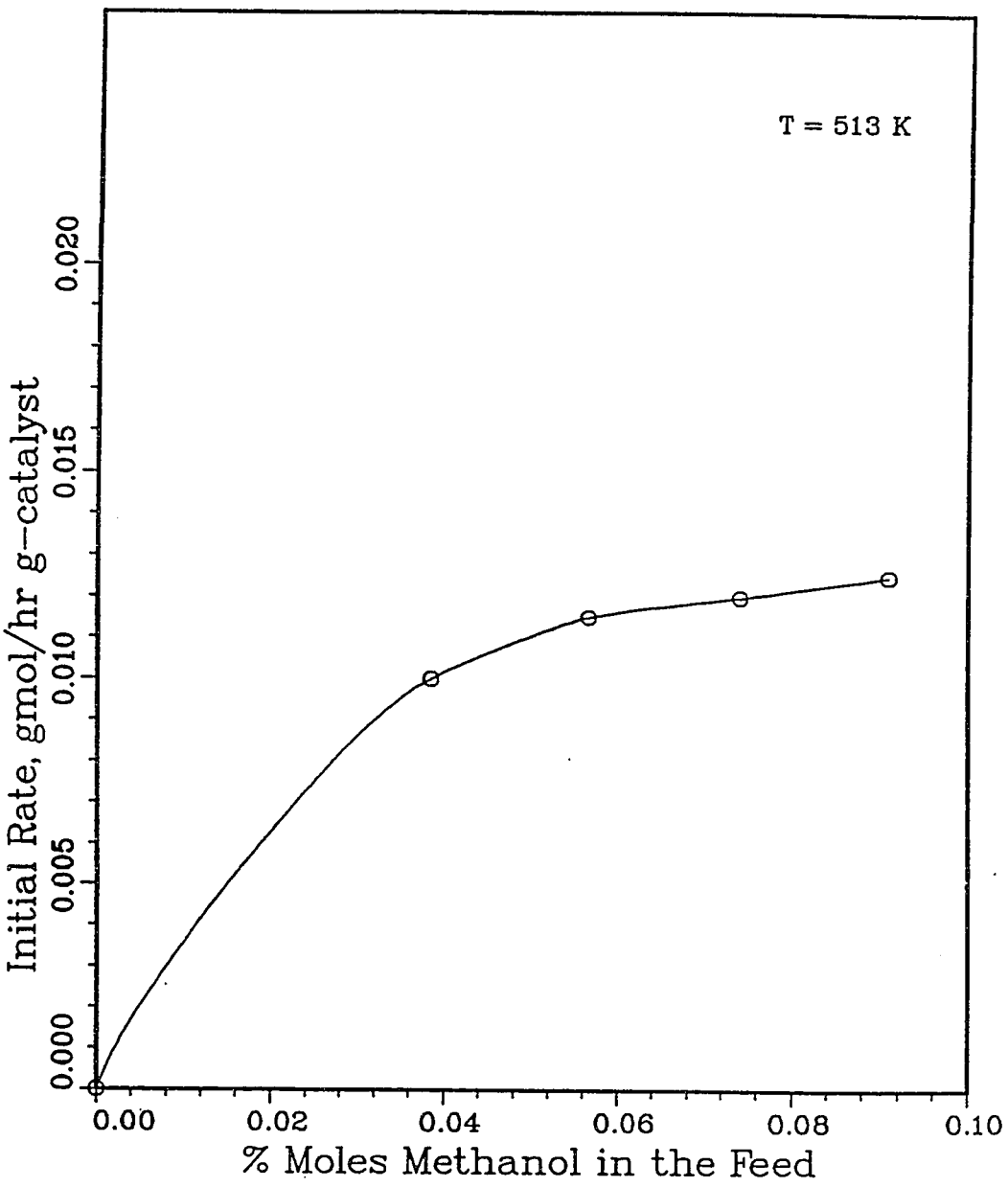

Figure 7.18: Initial rates vs. moles % methanol in the feed at T=513 K

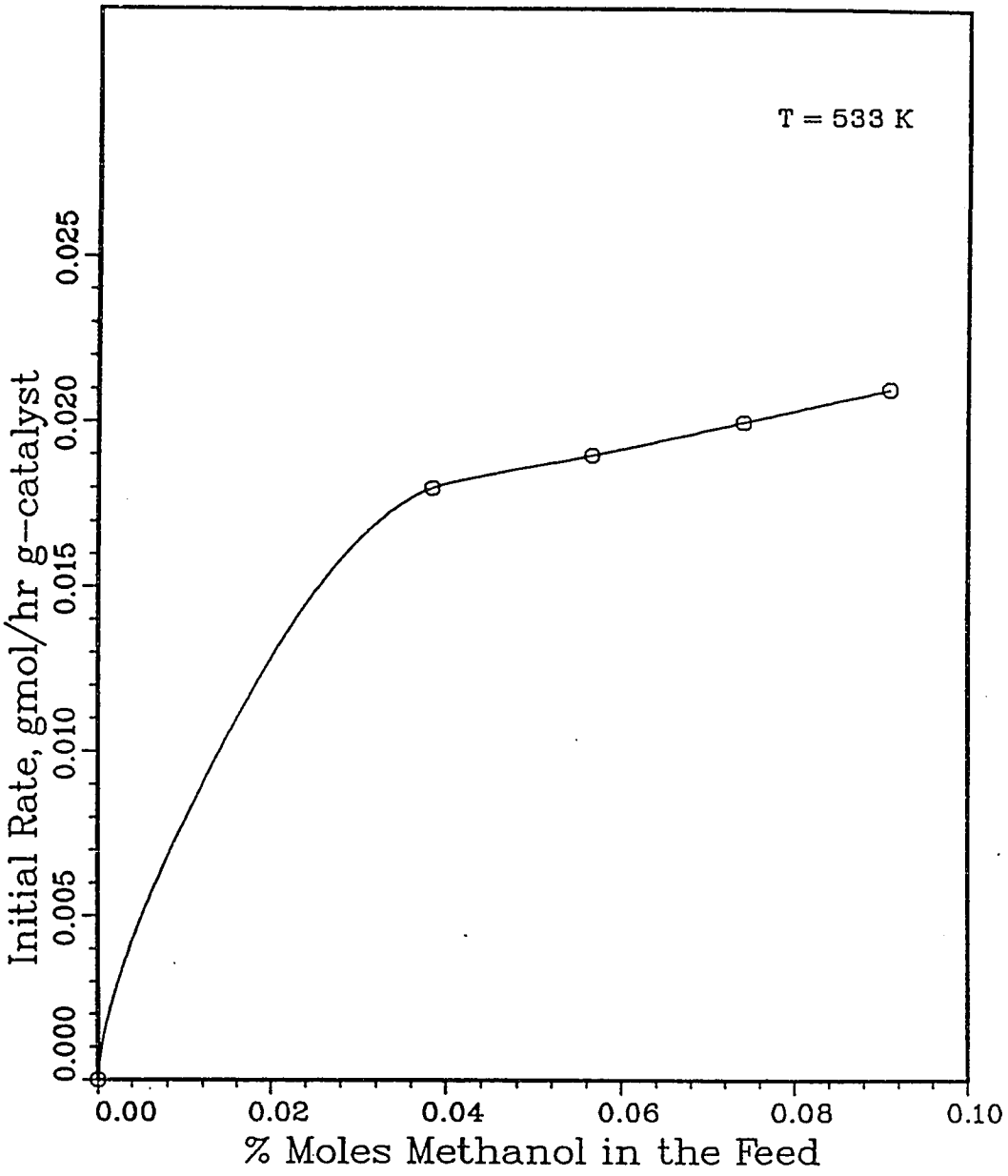

Figure 7.19: Initial rates vs. moles % methanol in the feed at T=533 K

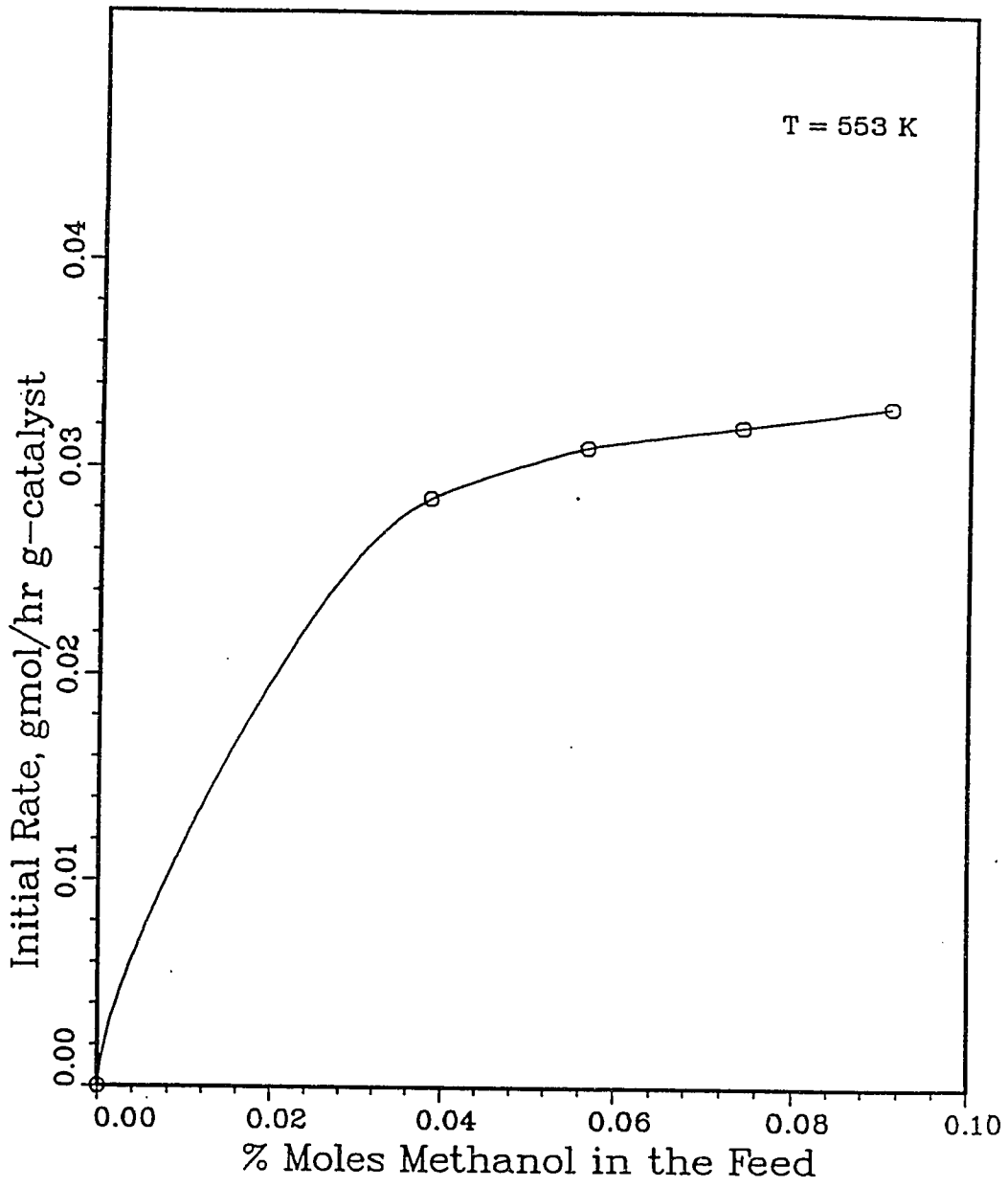

Figure 7.20: Initial rates vs. moles % methanol in the feed at T=553 K

7.6 Kinetic Modelling

The mechanism and the general kinetics of the oxidation of methanol over tin-molybdenum oxides have been found to be similar to those obtained by Jiru et al. [25], Mars and Krevelen [36], Machiels et al. [32] and Yang and Lunsford [57].

Mars and Krevelen suggested that the oxidation reactions involve a two-stage redox mechanism. According to this mechanism the overall reaction of the oxidation of methanol to formaldehyde is represented by the following two steady-state steps

$$CH_3OH + S_{ox} \xrightarrow{k_1} HCHO_{(g)} + H_2O + S_{red} \tag{7.3}$$

$$O_{2(g)} + S_{red} \xrightarrow{k_2} S_{ox} \tag{7.4}$$

The appropriate modified Langmuir-Hinshelwood rate expression for the above reaction is

$$r_M = r_1 = \frac{k_1 P_M^m}{1 + \frac{\alpha k_1 P_M^m}{k_2 P_{O_2}^n}} \tag{7.5}$$

where r_M is the rate of oxidation of methanol to formaldehyde, m and n are the reaction order constants with respect to methanol and oxygen and α is the number of oxygen molecules required to oxidize one molecule of methanol to formaldehyde. The partial pressure of methanol is ($P_M = P_{M_o}(1-x)$) and the partial pressure of oxygen ($P_{O_2} = P_{O_2^o} - 0.5P_{M_o}x$), where x is the conversion of methanol. The above equation thus can be rewritten as:

$$r_M = \frac{k_1(P_{M_o}(1-x))^m}{1 + \frac{\alpha k_1 (P_{M_o}(1-x))^m}{k_2(P_{O_2^o} - 0.5P_{M_o}x)^n}} \tag{7.6}$$

Recalling the plug-flow reactor material balance,

$$\frac{W}{F_{M_o}} = \int_{x_o}^{x} \frac{dx}{r_M} \tag{7.7}$$

and substituting the value of r_M from Equation 7.6 gives

$$\frac{W}{F_{M_o}} = \frac{1}{k_1 P_{M_o}^m} \int_{x_o}^{x} \frac{dx}{(1-x)^m} + \frac{\alpha}{k_2} \int_{x_o}^{x} \frac{dx}{(P_{O_2^o} - 0.5 P_{M_o} x)^n} \tag{7.8}$$

where F_{M_o} is the molar flow rate of methanol in the feed. It has been used for simplicity as F in this work.

Equation 7.8 was integrated for different values of m and n between 0 and 2. The integrated form of the rate equation was rearranged as shown in Table 4.2 where $\alpha = 0.5$ and

$$Y = A_o + A_1 X \tag{7.9}$$

The values for Y and X were calculated from the experimental data by substituting the vales of W/F, and the respective partial pressures. A_o and A_1 were determined using a linear regression analysis method. These values were used to calculate the rate constants k_1 and k_2.

7.7 Results of Kinetic Modelling

For the two-stage redox mechanism, different values of m and n between 0 and 2 were examined over the whole experimental data. Proper fit was found from 513-573 K for m=2 and n=1. No other values of m and n were found to fit the data best. The parameters were not estimated at temperatures above 573 K due to the complete conversion of methanol. The maximum absolute relative error was found to be 10%, which indicates that this model fits methanol oxidation most satisfactorily (see Appendix D).

The orders of the reaction with respect to methanol and oxygen were found to be higher than those found by Hahn [22], Dosi [16], Jain [24] and Diaz [15] (see

Table 7.6). This indicates that the rate of this particular reaction with $SnO_2 - MoO_3$ catalyst is higher than the rates with other oxide catalysts. The values of the rate constants, k_1 and k_2, predicted by this model (Table 7.7) were used to calculate the average activation energy.

It can be noticed from Table 7.6 that the values of k_1 and k_2 increased significantly with an increase in temperature. This proved that the rate of this particular reaction over Sn-Mo oxide catalyst increased sharply with an increase in temperature. This is due to the increase in catalyst activity due to temperature. The Arrhenius plot of Ln k_1 and Ln k_2 *vs* $\frac{1}{T}$ gave straight lines, as shown

Table 7.6: The order of the reaction with different catalysts

Catalyst	m	n	reference
$MoO_3 - MnO_2$	1	0.5	Hahn [22]
$MoO_3 - V_2O_5$	1	0.5	Dosi [16]
$MoO_3 - WO_3$	1	0.5	Jain [24]
$MoO_3 - Sb_2O_4$	1.5	1	Diaz [15]
$MoO_3 - SnO_2$	2	1	this work

Table 7.7: Variation of the rate constants k_1 and k_2 with respect to temperature.

Temperature (K)	k_1 g-mol/sec g-cat $atm.^2$	k_2 g-mol/sec g-cat $atm.$
513	0.54×10^{-2}	0.19×10^{-5}
533	1.95×10^{-2}	0.36×10^{-5}
553	5.26×10^{-2}	0.70×10^{-5}
573	14.30×10^{-2}	1.24×10^{-5}

in Figures 7.20 and 7.21, respectively. The respective equations relating k_1 and k_2 with temperature were:

$$\text{Ln } k_1 = 25.86 - \frac{15.923 \times 10^3}{T} \tag{7.10}$$

$$\text{Ln } k_2 = 4.83 - \frac{9.243 \times 10^3}{T} \tag{7.11}$$

The activation energies obtained from Equations 7.16 and 7.17 are 31.7 and 18.1 kcal/g-mol, respectively. These values indicate that the first step in the reaction offers much higher resistance compared to the second step.

The overall activation energy of the oxidation of methanol to formaldehyde was calculated on the basis of the temperature dependence of the rate (Figure 7.23). It was found to be equal to 17.5 kcal/g-mol. This value is within the range (16-20 kcal/g-mol) reported by Golodets [21] for the oxidation of methanol over different oxide catalysts, and very close to the values obtained by Bliznakov et al. [8] for the oxidation of methanol to formaldehyde over modified vanadia catalyst.

The reaction mechanism postulated in this research was similar to the one suggested by Mars and Krevelen [36] for the oxidation of several hydrocarbons over V_2O_5. In their case they suggested that the lattice oxygen ions in the catalyst particles interact with methanol during the oxidation reaction. Therefore, it is reasonable to assume that the reaction takes place by one of the following two mechanisms:

1. Methanol reacts with lattice oxygen of catalyst giving a reduced catalyst. The reduced catalyst then reacts with molecular oxygen in the gaseous phase.

2. Adsorbed oxygen on the catalyst surface reacts with methanol in the gaseous phase and the rate of removal of adsorbed oxygen from the catalyst surface is equal to the rate of adsorption of oxygen on the catalyst surface.

Both mechanisms discussed above, the first in which lattice oxygen atom reacts, and the other in which adsorbed oxygen molecules or atoms are removed, lead ultimately to the same rate expression.

Jiru et al. [25] studied the kinetics of methanol oxidation over iron-molybdenum oxide catalyst at 270°C using a micro catalytic pulse technique. The two-stage oxidation mechanism was confirmed by determining the rate of interaction between methanol and the catalyst without the participation of oxygen in the gaseous phase and the rate of interaction between oxygen and partially reduced catalyst without the participation of methanol in the gaseous phase. This mechanism foresees the same type of oxidation-reduction mechanism as the one postulated by Mars and Krevelen. It envisages the participation of the lattice oxygen of the oxide catalyst in the oxidation processes.

It is difficult to prove the participation of lattice oxygen in the catalytic oxidation process in the manner described by Jiru using pulse technique. The possibilities exists that the lattice oxygen participates in the reaction. However, in this type of experiments, oxygen could have been adsorbed by the oxide catalyst, and when methanol was injected into the reactor by the pulse technique, it reacted with the adsorbed oxygen.

Machiels et al. [32] have proposed a mechanism for the methanol oxidation process over molybdenum containing catalyst, which involves the following steps:

1. Dissociative adsorption of CH_3OH ($CH_3O^- + H^+$) to form surface methoxide ions.

2. The abstraction of a methyl hydrogen by a surface oxygen.

3. This is followed by a rapid intramolecular rearrangement and the desorption of formaldehyde as well as the other products.

The slowest step was the breaking of a C-H bond to form adsorbed formaldehyde. This mechanism has also been widely accepted by Yang and Lunsford [57].

The color of a catalyst is one of its characteristic properties, and a change in color may signify a change in the structure. In our experiments, the catalyst samples turned black after several days of operation. This change in color of the catalyst indicated that probably lattice oxygen is being removed from catalyst particles.

As a consequence of the Mars and Krevelen [36] mechanism, catalytic properties have been shown to depend on the nature and mobility of surface oxygen species, on electron transfer capability which facilitates the redox process during the catalytic reaction and also on geometric considerations, particularly the distance between active cations.

It appears from the present study that all these factors are favorable in the case of $SnO_2 - MoO_3$ catalyst resulting in higher activity and selectivity for the reaction of methanol to formaldehyde. These catalysts, as well as the reaction, are very important from a commercial point of view. Sn-Mo oxide catalyst gave a very high yield to formaldehyde and proved to be a promising catalyst for industrial use. The present work provides a background for further surface and structure studies of the $SnO_2 - MoO_3$ catalyst.

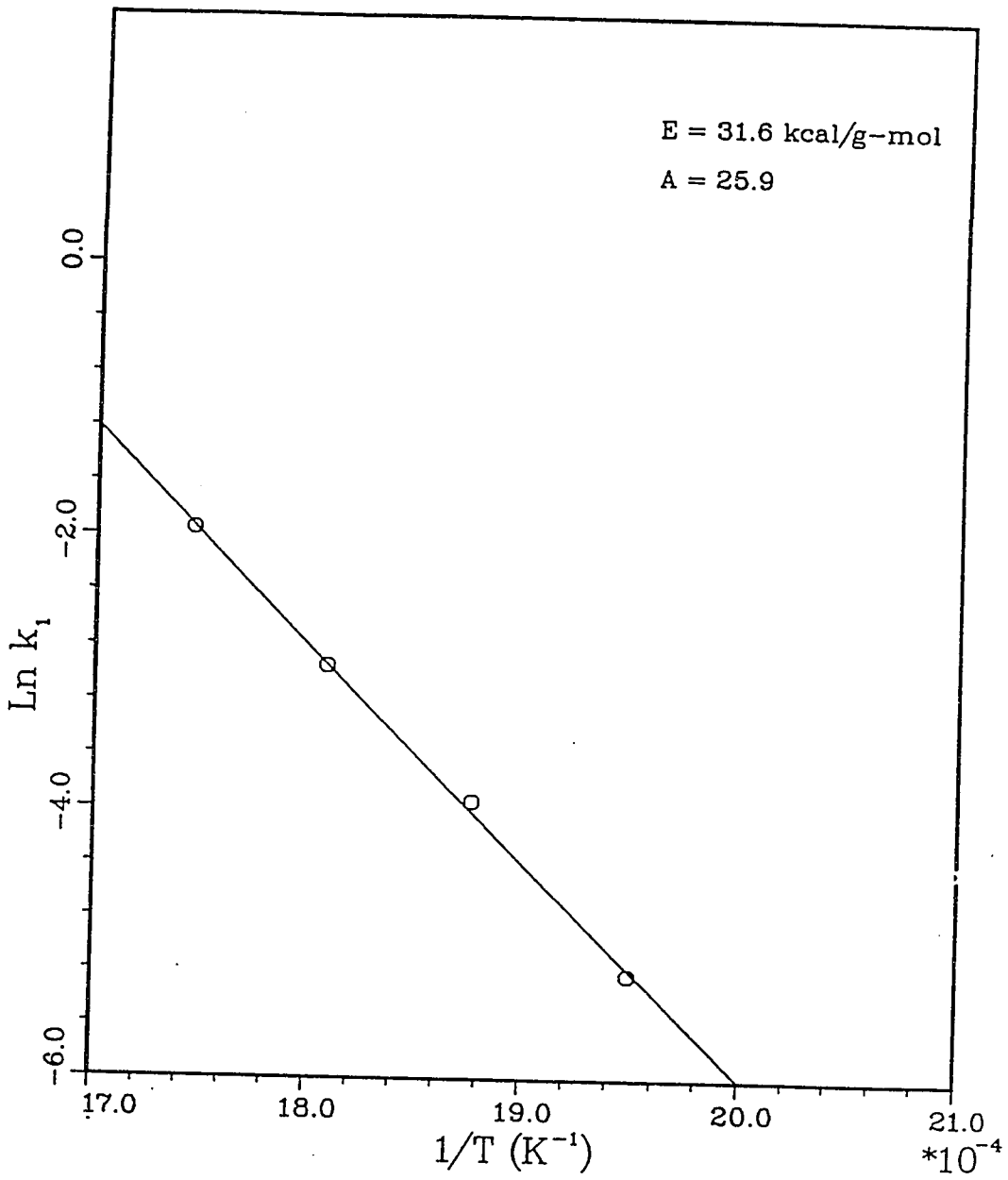

Figure 7.21: Arrhenius plot of Ln k_1 *vs* $1/T$

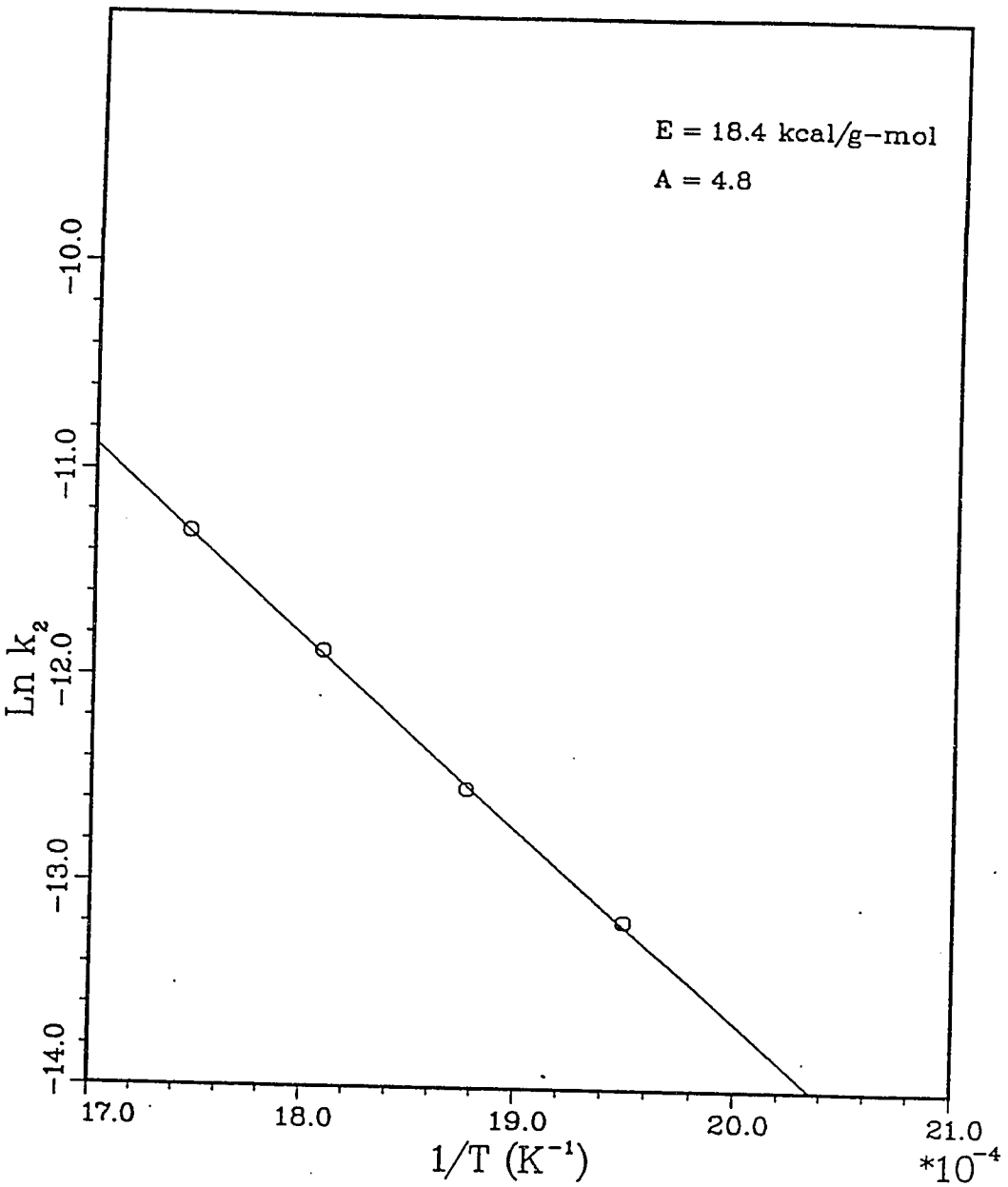

Figure 7.22: Arrhenius plot of Ln k_2 *vs* $1/T$

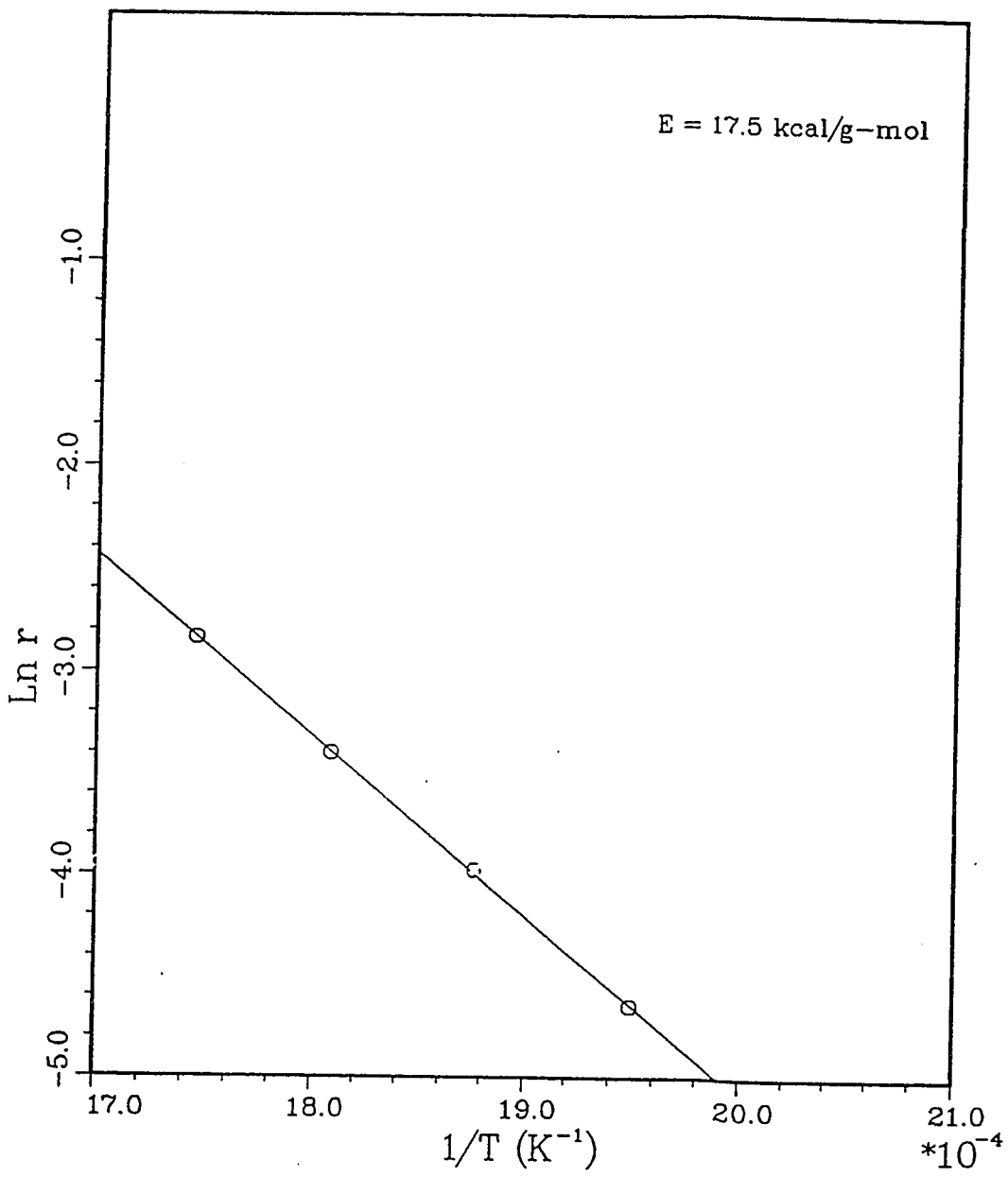

Figure 7.23: Arrhenius plot of Ln r vs 1/T

Chapter 8

Conclusions & Recommendations

In this study, the oxidation of methanol to formaldehyde was investigated. Reaction networks were studied. Several models were examined to fit the data.

8.1 Conclusions

The main conclusions drawn from this research project are:

- The optimum catalyst composition was found to be 50% MoO_3 and 50% SnO_2. This catalyst was chosen for further detailed kinetic study of the reaction.
- The reactor performance was not affected by axial dispersion or channeling.
- The reaction rate was not affected by molecular and Knudsen diffusion.
- The effects of heat and mass transfer from the catalyst pellet to the bulk phase is very small and it can be considered negligible.
- The conversion of methanol increased with temperature. This increase was more accentuated at high space time. On the other hand the selectivity of the catalyst decreased at temperatures above 553 K.

- An increase in W/F ratio with constant feed gas flow rate and methanol concentration, resulted in an increase of the conversion of methanol.
- Generally, the increase in conversion with an increase in the concentration of methanol in the feed was small.
- Following the method of Yang and Hougen [56], it was found that the desorption of the products was not a rate-determining step.
- The best operating conditions that gave almost 100% yield were a temperature of 553 K, a space time of 40 and a methanol/air ratio of 0.04.
- A two-stage redox mechanism fitted the data best. The order of the reaction was found to be 2 with respect to methanol concentration and 1 with respect to oxygen concentration.
- For the two-stage redox mechanism the values of the activation energies obtained were 31.7 and 18.1 kcal/g-mol. These values indicate that the oxidation of methanol proceeds via the oxidation step in the oxidation reduction mechanism.
- The overall activation energy of the oxidation of methanol to formaldehyde over Sn-Mo oxide catalysts obtained was 17.5 kcal/g-mol.

8.2 Recommendations

The following suggestions are recommended for further research:

- More data point should be taken at closer temperature ranges so as to reassess the rate constants and the order of the reaction for the reaction mech-

anism.

- Kinetic studies at lower methanol/air molar feed ratios (less than 4%) should be undertaken.
- Further application of statistical models for kinetic studies should be undertaken.
- Chemisorption studies should be undertaken to analyse the role of lattice oxygen in the Mo-Sn structure.
- ESR spectra should be studied to determine the effect of the amount of each oxide on the overall activity.

Bibliography

[1] *Surface Area and Porosity Seminar.* Micromeritics Instrument Corp., Norcross, GA, U.S.A., 1989.

[2] H. Adkins and W. Peterson. The Oxidation of Methanol with Air over Iron, Molybdenum, and Iron-Molybdenum Oxides. *Journal of The American Chemical Society*, 53(4):1518, 1931.

[3] C. D. Ajaka. *Hydrodenitrogenation of Pyridine and Quinoline.* PhD thesis, University of Ottawa, Ottawa, Ontario, 1991.

[4] M. Araki, I. Nishimura, T. Hayakawa, K. Takihira, and J. Ishikawa. Catalytic Synthesis of Higher Ketones from 2- Propanol. *Shokubai*, 14:47, 1972.

[5] R. Aris. *The Mathematical Theory of Diffusion and Reaction in Permeable Catalysts.* Calendon Press, Oxford, 1975.

[6] D. Bacon. *Strategies for Engineering Process Analysis.* Assembled by D. D. McLean, University of Ottawa, Ottawa, Ontario, 1988.

[7] F. Basolo and R. G. Pearson. *Mechanisms of Inorganic Reaction.* John Wiley & Sons, Inc., New York, 1958.

[8] G. Bliznakov, D. Klissurski, and Y. Pesheva. Selective Oxidation of Methanol to Formaldehyde on Modified Vanadia Catalysts. *Revue Roumaine de Chemie*, 32(9-10):985, 1987.

[9] J. Buiten. Oxidation of Propylene by Means of $SnO_2 - MoO_3$ Catalysts. *Journal of Catalysis*, 10:188, 1968.

[10] Hill G. Charles, Jr. *An Introduction to Chemical Engineering Kinetics & Reactor Design.* John Wiley & Sons, Inc., New York, 1977.

[11] N. Chen. *Process Reactor Design.* Allyn and Bacon Inc., Newton MA, U.S., 1983.

[12] C. H. Chilton and A. P. Colburn. Mass Transfer (Adsorption) Coefficients. *Ind. Eng. Chem.*, 26(11):1183. 1934.

[13] J. S. Chung, R. M. Miranda, and C. O. Bennett. Mechanism of Partial Oxidation of Methanol over MoO_3. *Journal of Catalysis*, 114:398, 1988.

[14] A. Clark. *The Theory of Adsorption and Catalysis.* Academic Press, New York, 1970.

[15] R. A. Diaz Real. *Partial Oxidation of Methanol to Formaldehyde over Sb-Mo Oxides Catalysts.* PhD thesis, University of Ottawa, Ottawa, Ontario, 1990.

[16] M. Dosi. *Oxidation of Methanol over Molybdenum Vanadium Oxide Catalysts.* Master's thesis, University of Ottawa, Ottawa, Ontario, 1971.

[17] A. Estevez, A. Fernandez, and M. Marquez. Oxidation of Methanol to Formaldehyde on Iron-Molybdenum Oxide Catalysts with and without

Chromium as a Promoter. *React. Kinet. Catal. Lett.*, 38(1):193, 1989.

[18] H. Fogler. *Elements of Chemical Reaction Engineering.* Prentice-Hall, Inc., New Jersey, 1986.

[19] D. Gasser and A. Baiker. Methanol Oxidation on Vanadium Oxide Catalyst Prepared in Situ Activation of Amorphous Vanadium Pentoxide Precursor. *Journal of Catalysis*, 113(2):325, 1988.

[20] N. Giordano, M. Meazza, A. Calellan, J. Bart, and V. Ragaini. Structure and Catalytic Activity of $MoO_3 - SiO_2$ Systems. *Journal of Catalysis*, 50:342, 1977.

[21] G. I. Golodets. *Studies in Surface Sience and Catalysis. Heterogeneous Catalytic Reactions Involving Molecular Oxygen.* Elsevier, 1983. vol. 15.

[22] K. Hahn. *Catalytic Oxidation of Methanol.* PhD thesis, University of Ottawa, Ottawa, Ontario, 1968.

[23] B. Hoflund. A Review of Tin Oxide-based Catalytic Systems Preparation, Characterization and Catalytic Behavior. *NASA Conference Publication*, 2456:179, 1987.

[24] S. Jain. *Oxidation of Methanol over Molybdenum Oxide- Tungston Oxide Catalysts.* Master's thesis, University of Ottawa, Ottawa, Ontario, 1976.

[25] P. Jiru, B. Wichterlova, and J. Tichy. Mechanism of Oxidation of Methyl Alcohol to Formaldehyde on Oxide Catalysts. *In Proceedins of the 3rd International Congress of Catalysis*, 199, 1964.

[26] E. Jones and G. Fowlie. Thermodynamics of Formaldehyde Manufacture from Methanol. *Journal of Applied Chemistry*, 3:206, 1953.

[27] Editor Kirk-Othmer. *Encyclopedia of Chemical Technology*. John Wiley & Sons, Inc., New York, 1980. 3rd ed.

[28] D. Klissurski, Y. Pesheva, N. Abadjieva, I. Mitov, D. Filkova, and L. Petrov. Multi-Component Oxide Catalyst for the Oxidation of Methanol to Formaldehyde. *Applied Catalysis*, 77(1):55, 1991.

[29] K. Laider. *Chemical Kinetics*. McGraw Hill Book Co., New York, 1965.

[30] J. M. Lipsch and G. C. Schuit. The $CoO - MoO_3 - Al_2O_3$ Catalyst. II. The Structure of the Catalyst. *Journal of Catalysis*, 15:179, 1969.

[31] C. Louis, J. Tatibouet, and M. Che. Catalytic Properties of Silica-Supported Molybdenum Oxidation:The Influence of Molybdenum Dispersion. *Journal of Catalysis*, 109:354, 1988.

[32] C. J. Machiels, U. Choudhry, W. T. A. Harrison, and A. W. Sleight. Solid State Chemistry in Catalysis. *ACS Symp. Series*, (279):103, 1985.

[33] R. S. Mann and K. Hahn. Kinetics of Vapor-Phase Oxidation of Methyl Alcohol over Manganese Dioxide-Molybdenum Trioxide Catalyst. *Journal of Catalysis*, 15(4):329, 1969.

[34] R. S. Mann and K. Hahn. Oxidation of Methanol over Manganese Dioxide-Molybdenum Trioxide Catalyst. *Ind. Eng. Chem. Process Des.*, 9(1):43, 1970.

[35] R. S. Mann, S. Jain, and M. Dosi. Catalytic Oxidation of Methanol over Molybdenum Oxide Tungsten Oxide. *Journal of Applied Chemistry and Biotechnology*, 27(2), 1977.

[36] P. Mars and D. van Krevelen. Oxidation Carried out by Means of Vanadium Oxide Catalyst. *Special Supplement to Chemical Engineering Science*, 41, 1954.

[37] A. Meyer and A. Renken. Sodium Compound as Catalysts for Methanol Dehydrogenation to Water Free Formaldehyde. *Chemical Engineering and Technology*, 13(3):145, 1990.

[38] M.Niwa, M.Mizutani, M. Takahashi, and Y.Murakami. Mechanism of Methanol Oxidation over Oxide Catalysts Containing MoO_3. *Journal of Catalysis*, 70:14, 1981.

[39] M.Niwa, M.Mizutani, and Y.Murakami. Oxidation of Methanol over $SnO_2 - MoO_3$ Catalysts. *Nippon Kagaku Kai-shi*, 6:757, 1977.

[40] S. Neophytides and C. Vayen. Chemical Cogeneration in Solid Electrolyte Cell . The Oxidation of CH_3OH to H_2CO. *Journal of Electrochemical Society*, 137(3):423, 1990.

[41] J. Novakova, P. Jiru, and V. Zavadil. Oxidation of Methanol and Formaldehyde on Fe_2O_3 in Comparison with MoO_3 and a Mixed Mo^{6+} FeO^{3+} Catalyst. *Journal of Catalysis*, 21:143, 1971.

[42] T. Ono, T. Yamanaka, Y. Kubokawa, and M. Komiyama. Structure and Catalytic Activity of Sb Oxide Highly Dispersed on SnO_2 for Propene Oxidation.

Journal of Catalysis, 109:423, 1988.

[43] U. Ozkan, R. Kueller, and E. Moctezuma. Methanol Oxidation over Non-precious Transition Metal Oxide Catalysts. *Ind. Eng. Chem. Res.*, 29:1136, 1990.

[44] N. Pernicone, F. Lazzerim, and G. Liberti. On the Mechanism of CH_3OH Oxidation to CH_2O over $MoO_3-Fe_2(MoO_4)_3$ Catalyst. *Journal of Catalysis*, 14:293, 1969.

[45] B. Reddy, K.Narsimha. C. Sivaraj, and P. Rao. Titration of Partial Oxidation of Methanol over V_2O_5/SnO_2 and MoO_3/SnO_2 Catalysts by a Low-Temperature Oxygen Chemisorption Technique. *Applied Catalysis*, 55:L1, 1989.

[46] C. N. Satterfield. *Hetrogeneous Catalysis in Practice.* McGraw Hill Book Co., New York, 1980. 3rd ed.

[47] J. M. Smith. *Chemical Engineering Kinetics.* McGraw Hill Book Co., New York, 1980. 3rd ed.

[48] S. M. Sohrabi and B. M. Farhad. Model for the Rate of Catalytic Oxidation of Methanol in a Fixed Bed Reactor. *Chemical Engineering and Technology*, 14(2):96, 1991.

[49] J. Y. Song and S. T. Hwang. Formaldehyde Production from Methanol using Porous Vycor Glass Membrane Reactor. *Journal of Membrane Science*, 57(1):95, 1991.

[50] Y. Takita, A. Ozaki, and Y. Moroka. Catalytic Oxidation of Olefins over Oxide Catalysts Containing Molybdenum. *Journal of Catalysis*, 27:185, 1972.

[51] S. Tan, A. Ozaki, and Y. Moroka. Catalytic Oxidation of Olefins over Oxide Catalysts Containing Molybdenum. *Journal of Catalysis*, 17:132, 1970.

[52] E. W. Thiele. Relation between Catalytic Activity and Size of Particle. *Ind. Eng. Chem.*, 31:916, 1939.

[53] P. Vollhardt. *Organic Chemistry*. W. H. Freeman & Co., New York, 1987.

[54] J. F. Walker. *Formaldehyde*. Robert E. Krieger Pub. Co., New York, 1975. 3rd edition.

[55] A. Wheeler. Reaction Rates and Selectivity in Catalyst Pores. *Advances in Catalysis*, 3:249, 1951.

[56] K. H. Yang and O. A. Hougen. Determination of Mechanism of Catalyzed Gaseous Reaction. *Chemical Engineering Progress*, 46(3):146, 1950.

[57] T. Yang and J. Lunsford. Partial Oxidation of Methanol to Formaldehyde over Molybdenum Oxide on Silica. *Journal of Catalysis*, 103:55, 1987.

[58] F. Yoshida, D. Ramaswami, and O. Hougen. Temperature and Partial Pressures at the Surface of Catalyst Particles. *AICHE J.*, 8(1):5, 1962.

Appendix A

Calibration Curves

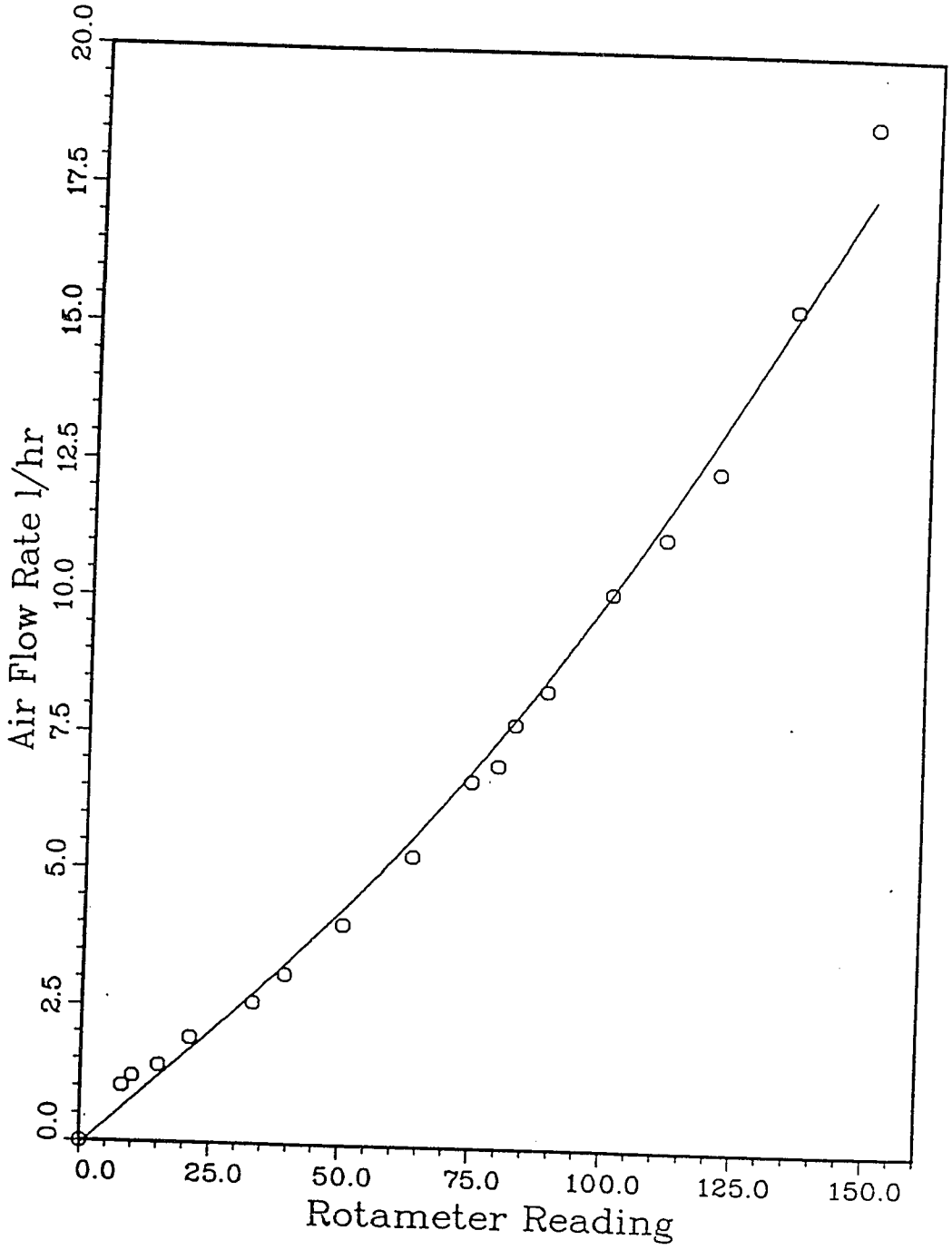

Figure A.1: Air rotameter calibration

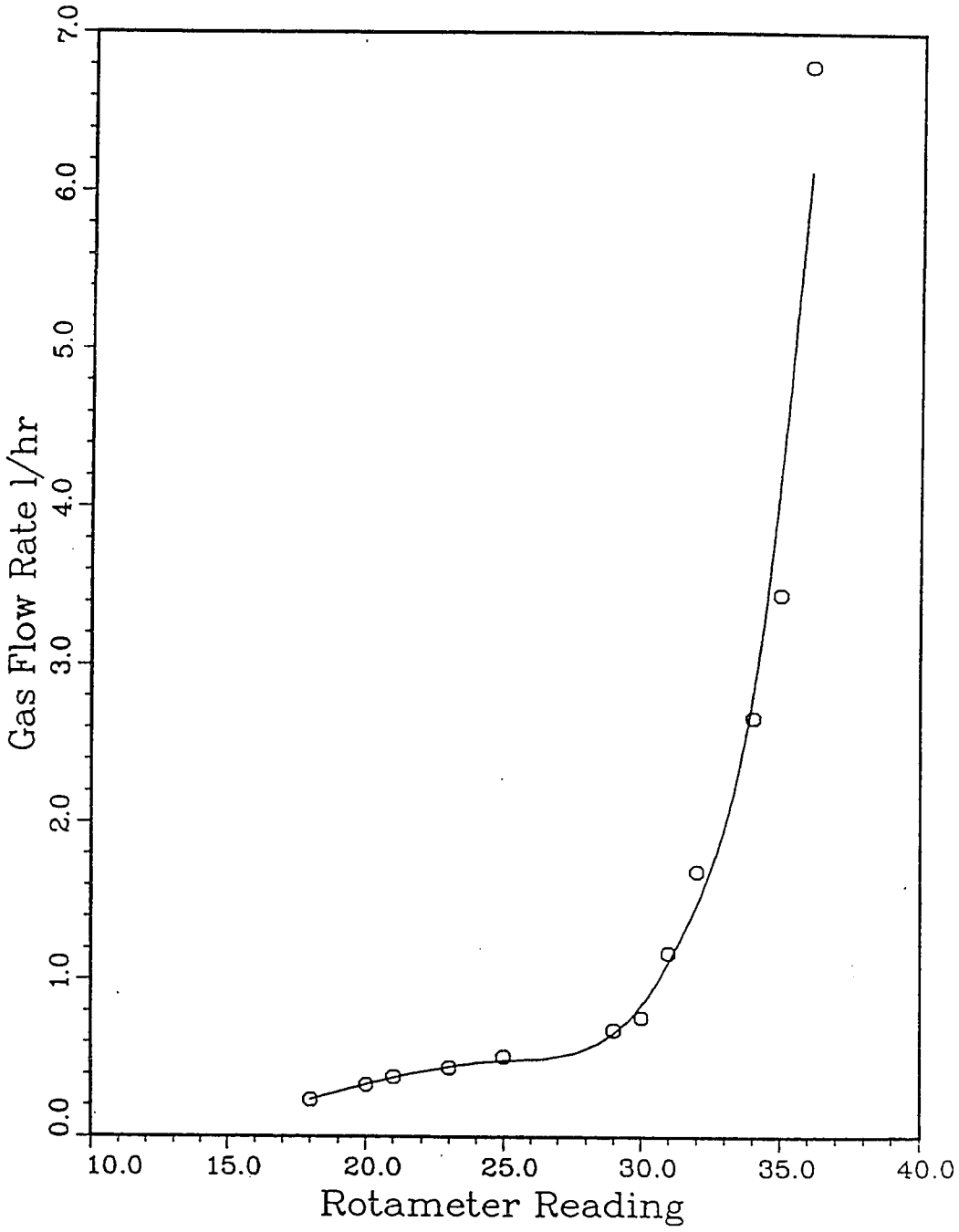

Figure A.2: Gas rotameter calibration

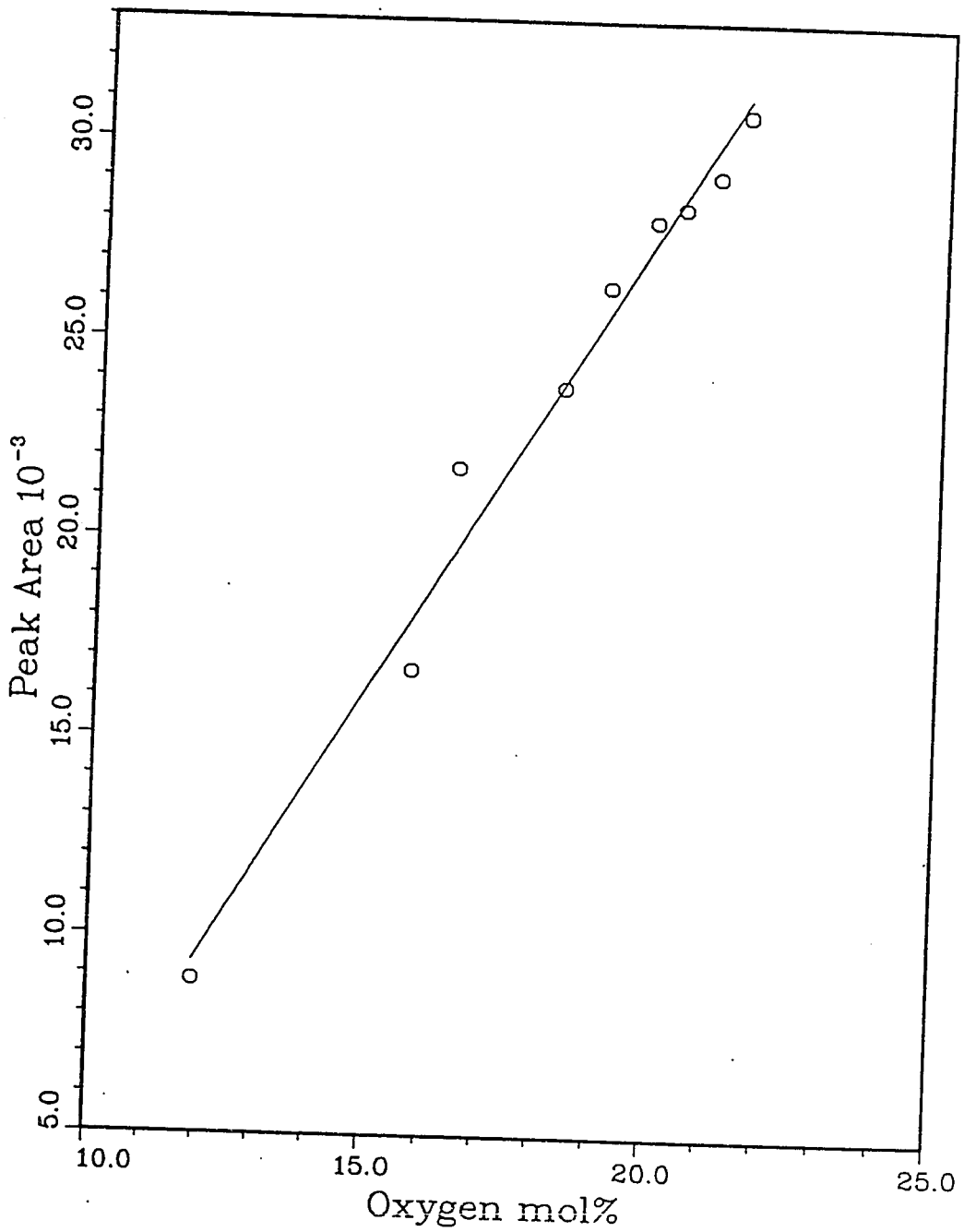

Figure A.3: Oxygen gas chromatograph calibration

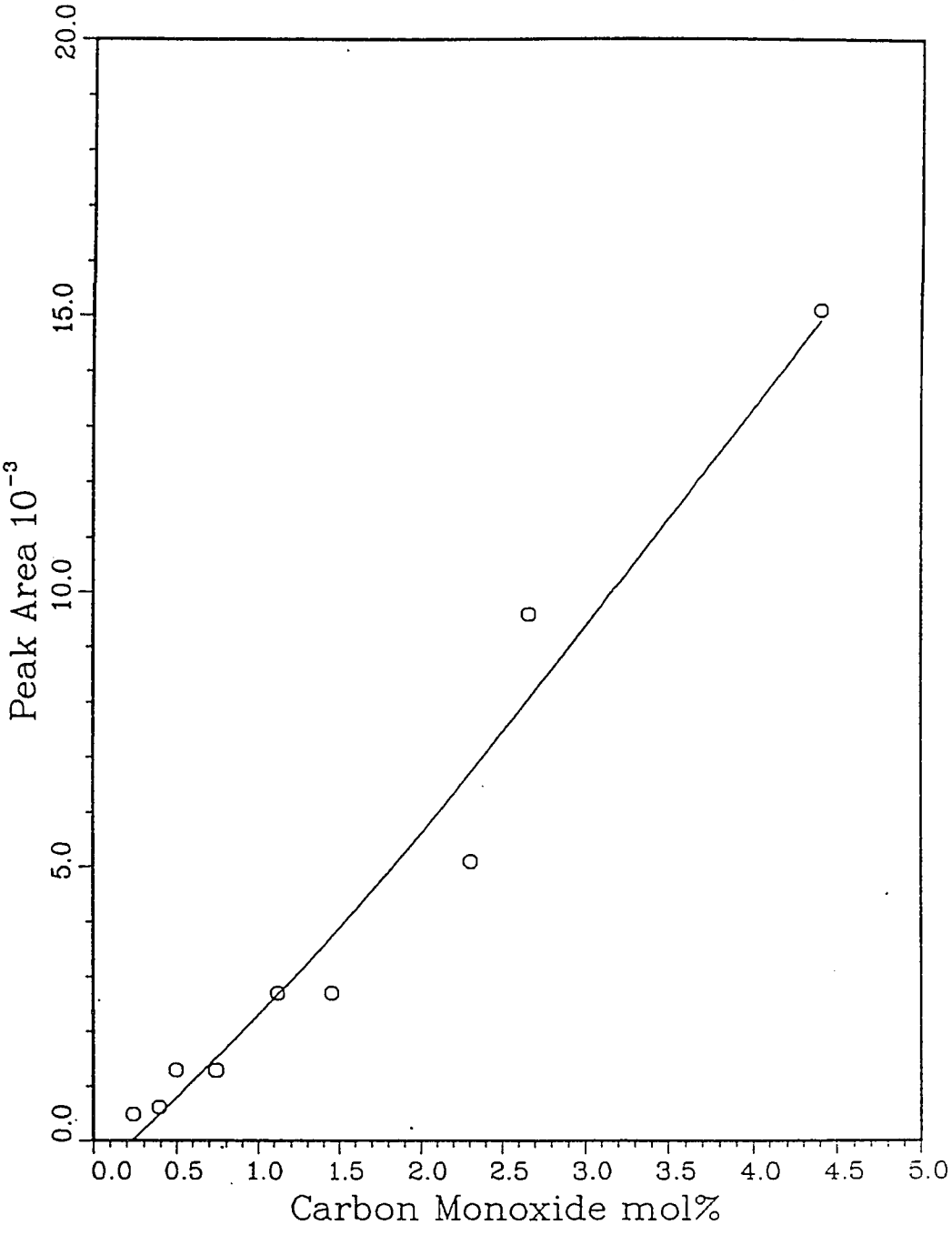

Figure A.4: Carbon monoxide gas chromatograph calibration

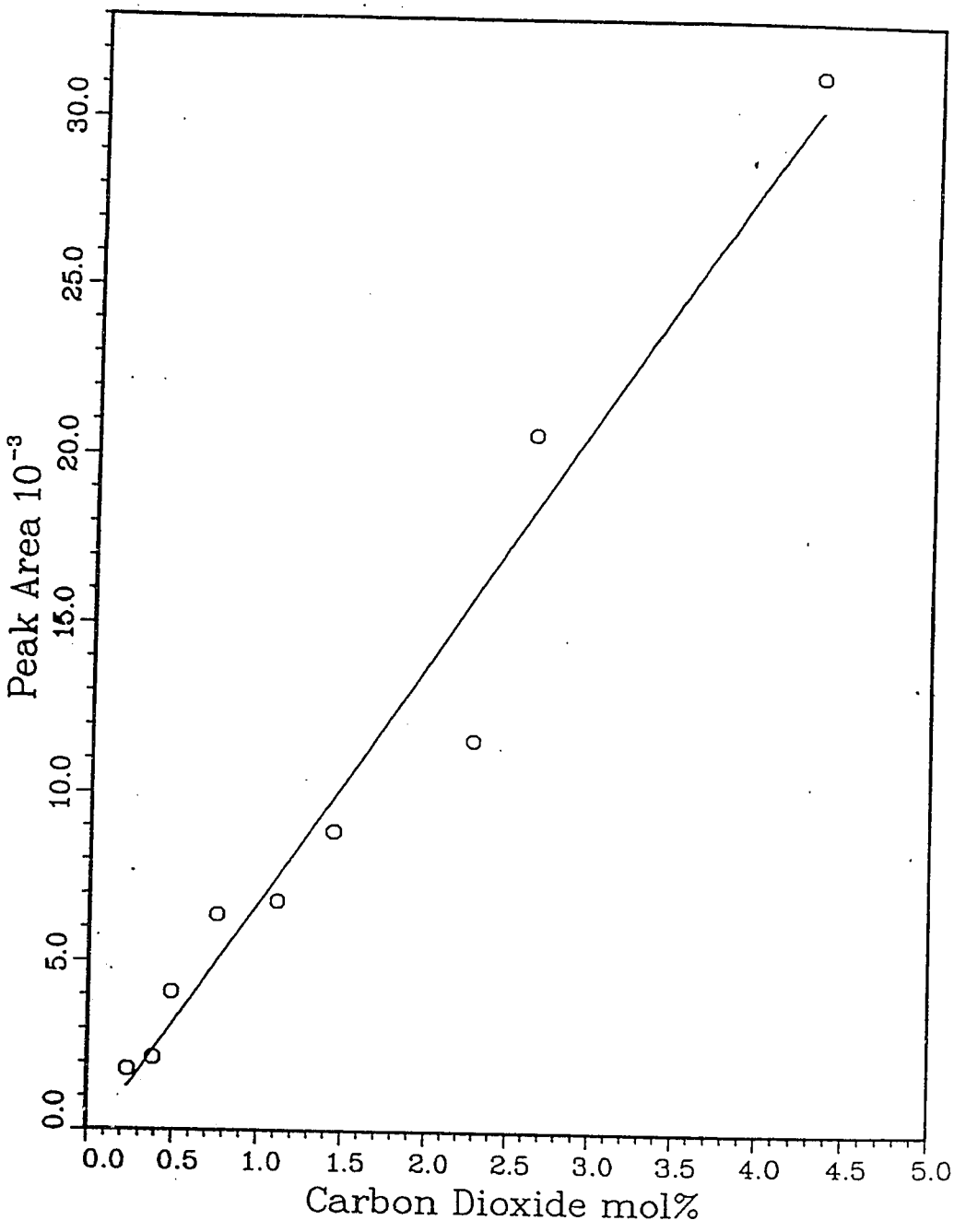

Figure A.5: Carbon dioxide gas chromatograph calibration

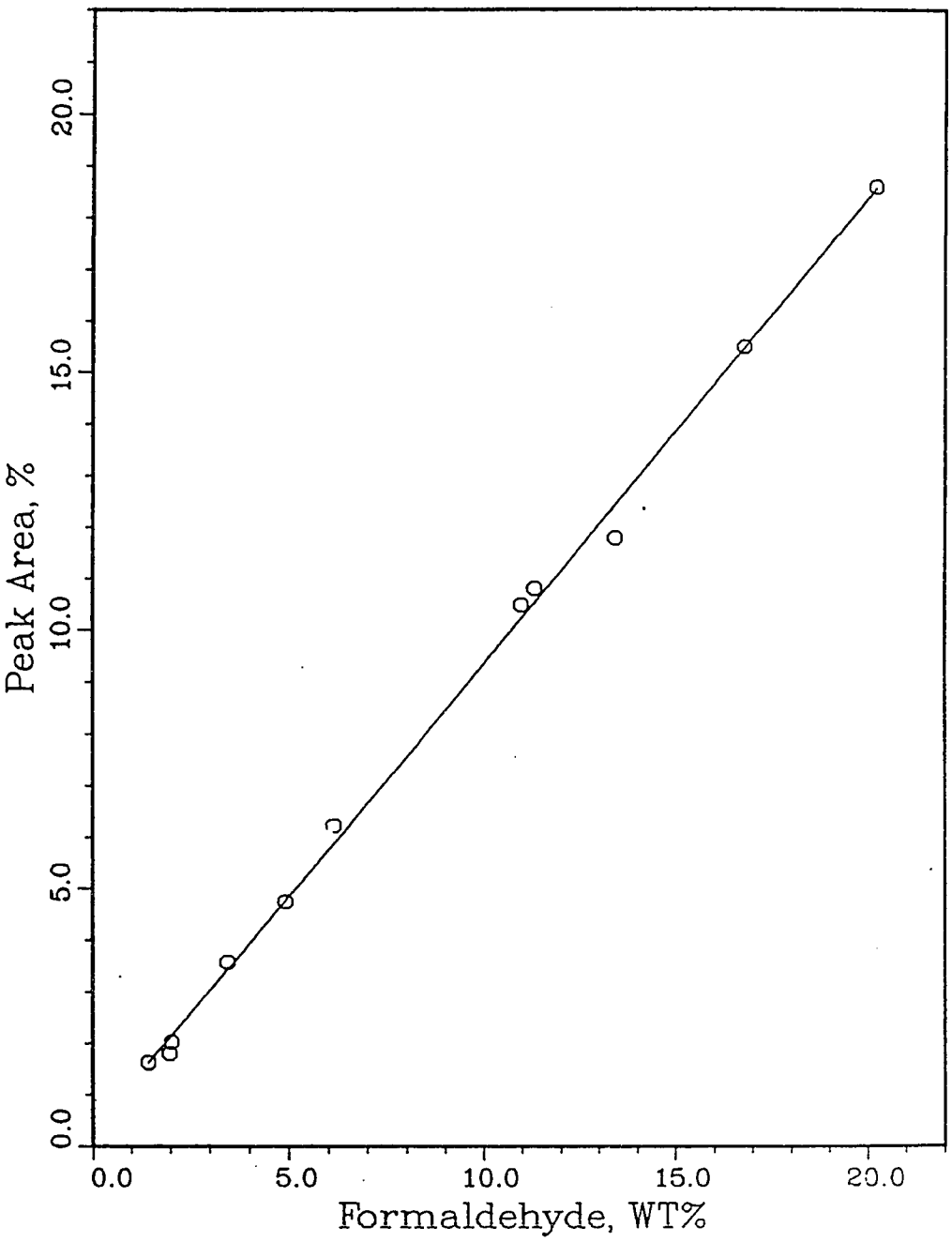

Figure A.6: Formaldehyde gas chromatograph calibration

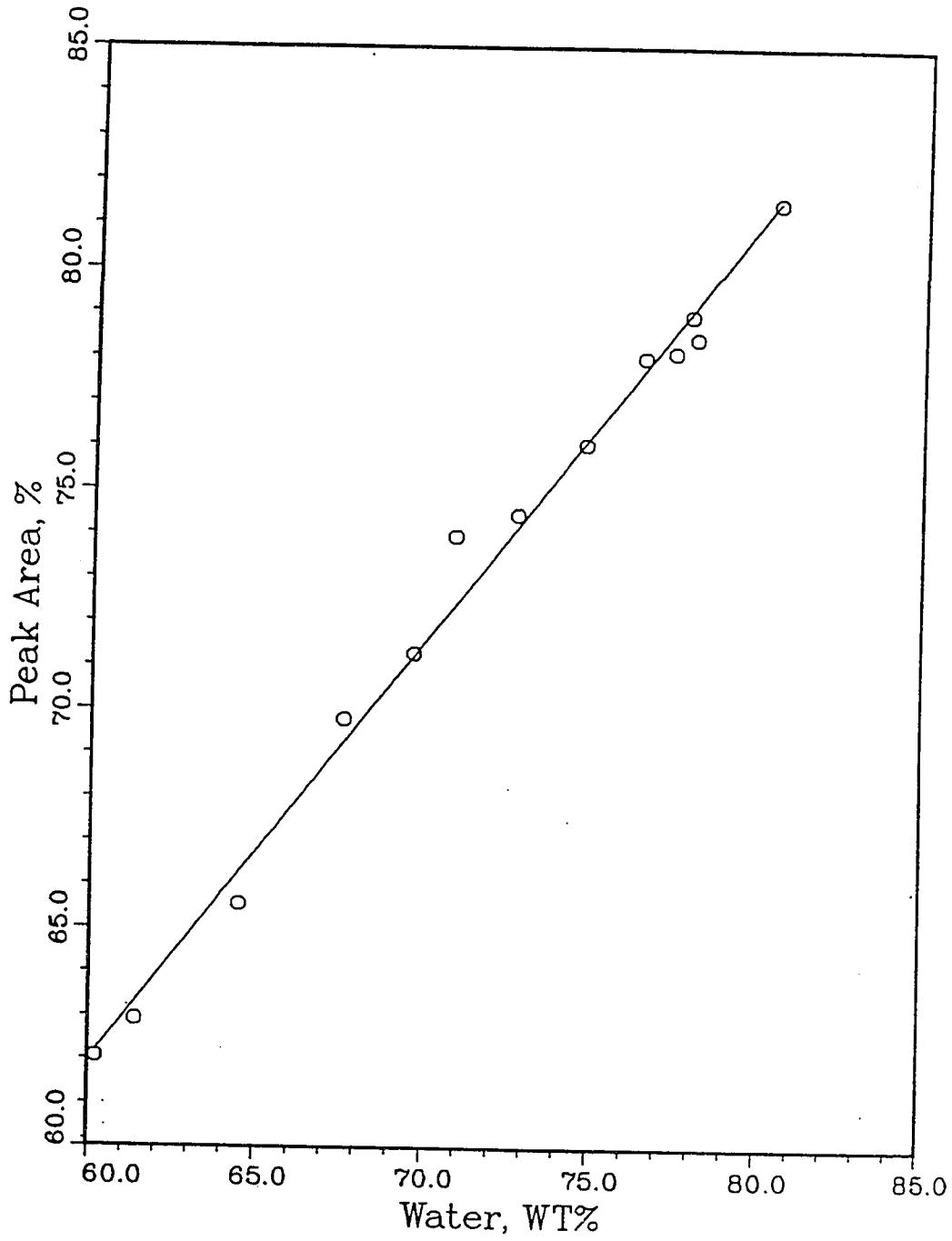

Figure A.7: Water gas chromatograph calibration

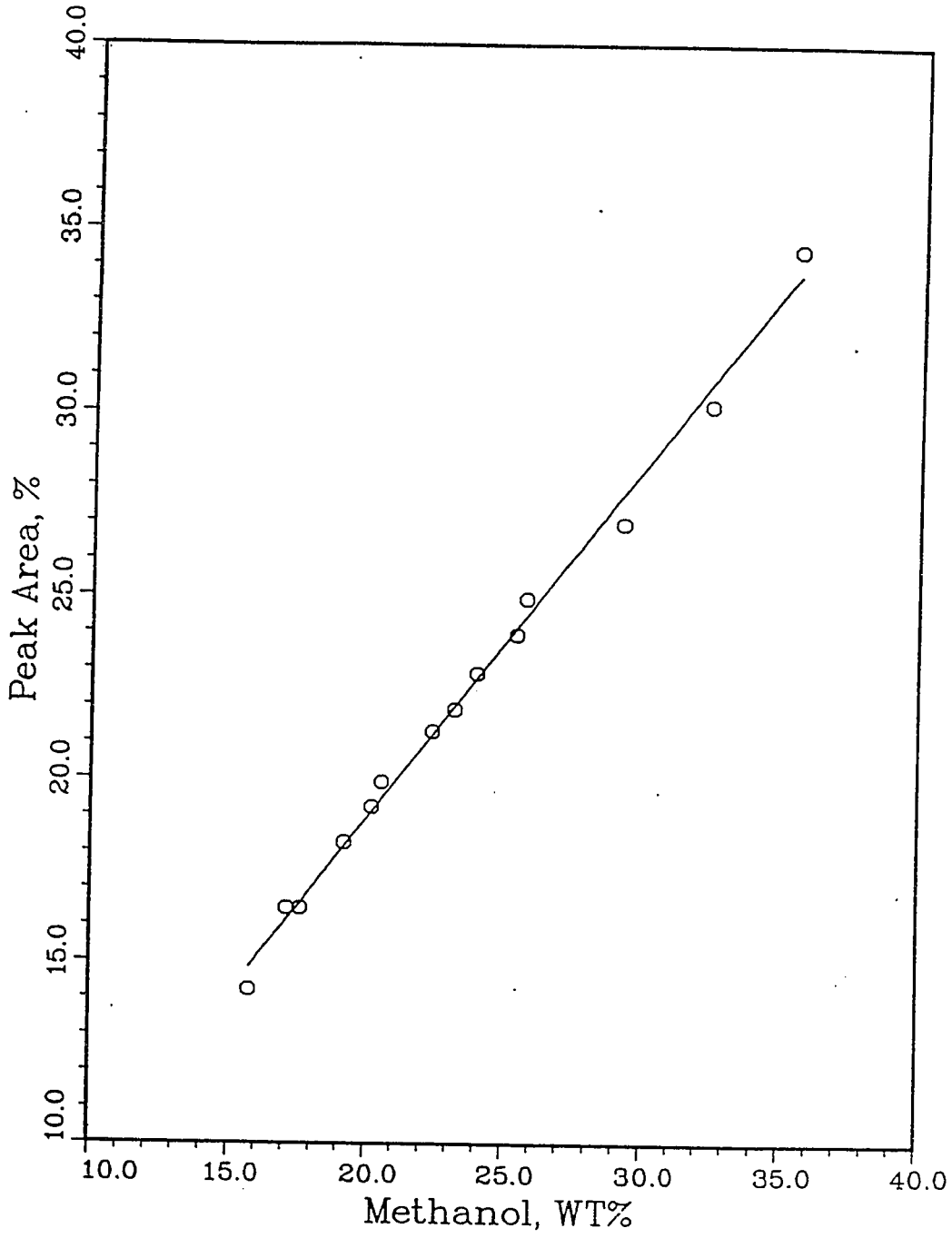

Figure A.8: Methanol gas chromatograph calibration

Appendix B

Mass Balance

The quantitative analysis was achieved by injecting the organic liquid product using a 1.0 μl syringe into the gas chromatograph. The detector of the GC was a thermal conductivity detector (TCD). The percentage areas produced by the chromatograms were converted to concentrations percentage using the calibration curves. Calibrations curves were produced by injecting standard solutions of the expected products. The % peak area and the concentration of each of the products was found to be linear in the region of interest. On the other hand gas products were analyzed by using the on-line analysis. A 0.5 cm^3 sampling loop was used to inject the gas sample into the column.

The mass balance was performed based on carbon-containing products. A sample calculation is given in this Appendix.

B.1 Sample Calculation

This calculation is based on the experimental data of run number K33. From the liquid analysis the mole ratios are:

$$\frac{W}{F} = 0.8430$$

$$\frac{M}{W} = 0.3240$$

where F/W and M/W are the ratios of the number of moles of formaldehyde and methanol to the number of moles of water in the liquid product, respectively.

The total number of moles of liquid product T is:

$$T = F + M + W \tag{B.1}$$

$$1 - \frac{W}{T} = \frac{F}{T} + \frac{M}{T} \tag{B.2}$$

therefore:

$$\begin{aligned} \frac{W}{T} &= \frac{1}{1 + \frac{F}{W} + \frac{M}{W}} \\ &= 0.4615 \end{aligned} \tag{B.3}$$

$$\begin{aligned} \frac{F}{T} &= \frac{F}{W} \times \frac{W}{T} \\ &= 0.3890 \end{aligned}$$

$$\begin{aligned} \frac{M}{T} &= \frac{M}{W} \times \frac{W}{T} \\ &= 0.1495 \end{aligned}$$

From the gas analysis, the mole ratios are:

$$\frac{CO}{N_2} = 4.861 \times 10^{-3}$$

$$\frac{CO_2}{N_2} = 2.523 \times 10^{-3}$$

$$\frac{O_2}{N_2} = 0.2092$$

As nitrogen remains unreacted:

moles of N_2 in the feed = moles of N_2 in the product

moles of N_2 in the feed = 0.2893 moles/hr

Therefore;

$$\begin{aligned} F_{CO_2} &= \text{moles of } CO_2 \text{ in product} \\ &= 2.523 \times 10^{-3} \times 0.2893 \\ &= 7.3 \times 10^{-4} \text{ moles/hr} \end{aligned}$$

$$\begin{aligned} F_{CO} &= \text{moles of } CO_2 \text{ in product} \\ &= 4.861 \times 10^{-3} \times 0.2893 \\ &= 1.41 \times 10^{-3} \text{ moles/hr} \end{aligned}$$

$$\begin{aligned} F_{O_2} &= \text{moles of } CO_2 \text{ in product} \\ &= 0.2092 \times 0.2893 \\ &= 0.0592 \text{ moles/hr} \end{aligned}$$

Material Balance

M_o = moles of methanol in the feed

$$M_o = M + F + F_{CO_2} + F_{CO} \tag{B.4}$$

From stoichiometric relationships:

$$W = F + 2(F_{CO_2} + F_{CO}) \tag{B.5}$$

placing the value of W from relation B.5 into B.1

$$T = M_o + F + F_{CO_2} + F_{CO}$$

$$\frac{F}{T} = \frac{F}{M_o + F + F_{CO_2} + F_{CO}}$$
$$F = \frac{F}{T} \times (M_o + F + F_{CO_2} + F_{CO})$$

rearranging:

$$F = \frac{\frac{F}{T} \times (M_o + F_{CO_2} + F_{CO})}{1 - \frac{F}{T}}$$
$$= 0.0207 \text{ moles/hr}$$
$$T = 0.0532 \text{ moles/hr}$$
$$M = 7.9534 \times 10^{-3} \text{ moles/hr}$$

Carbon Balance Check

$$\text{In feed} = 0.0304 \text{ moles/hr}$$
$$\text{In products} = 0.0207 + 0.0079 + 0.00141 + 0.00073$$
$$= 0.0307 \text{ moles}/hr$$

Error in Material Balance:

$$\frac{0.0304 - 0.0307}{0.0304} \times 100\% = -0.9868\%$$

$$\begin{aligned} \text{Conversion} &= 1 - \frac{0.0079}{0.0307} \\ &= 0.74267 = 74.3\% \end{aligned}$$

$$\begin{aligned} \text{Selectivity} &= \frac{F}{F + F_{CO_2} + F_{CO}} \\ &= 0.90630 = 90.6\% \end{aligned}$$

$$\begin{aligned} \text{Yield} &= \text{Selectivity} \times \text{Conversion} \\ &= 0.67308 = 67.3\% \end{aligned}$$

Appendix C

Experimental Runs

In this Appendix the experimental runs of the kinetic study are presented. The following tables are taken from the output of the computer program that performs the mass balance.

C.1 Two-Level Fractional Factorial Design Runs

T = temperature (K)

W/F = space time (hr g-cat/g-mol)

R = methanol/air feed ratio

C = conversion of methanol

S = selectivity of the catalyst

Y = the yield of formaldehyde

RUN	T	W/F	R	C	S	Y
B01	513	10	0.08	0.01097	1.00000	0.01097
B02	573	10	0.04	0.16237	1.00000	0.16237
B03	513	40	0.04	0.28532	1.00000	0.28532
B04	573	40	0.08	0.67460	1.00000	0.67460
B05	543	25	0.06	0.25778	1.00000	0.25778
B06	543	25	0.06	0.25121	1.00000	0.25121
B07	543	25	0.06	0.26551	1.00000	0.26551
C01	513	10	0.08	0.04504	1.00000	0.04504
C02	573	10	0.04	0.60608	1.00000	0.60608
C03	513	40	0.04	0.28333	1.00000	0.28333
C04	573	40	0.08	0.75518	0.91253	0.68912
C05	543	25	0.06	0.39844	1.00000	0.39844
C06	543	25	0.06	0.42651	1.00000	0.42651
C07	543	25	0.06	0.35051	1.00000	0.35051
D01	513	10	0.08	0.11293	1.00000	0.11293
D02	573	10	0.04	0.63648	1.00000	0.63648
D03	513	40	0.04	0.34286	1.00000	0.34286
D04	513	40	0.08	1.00000	0.83583	0.83583

D05	543	25	0.06	0.69799	1.00000	0.69799
D06	543	25	0.06	0.67429	1.00000	0.67427
D07	543	25	0.06	0.66875	1.00000	0.66875
E01	513	10	0.08	0.28840	1.00000	0.28840
E02	573	10	0.04	1.00000	0.05894	0.05894
E03	513	40	0.04	0.84797	0.47182	0.40009
E04	573	40	0.08	1.00000	0.00000	0.00000
E05	543	25	0.06	1.00000	0.26702	0.26702
E06	543	25	0.06	1.00000	0.24997	0.24997
E07	543	25	0.06	1.00000	0.26025	0.26025
F01	513	10	0.08	0.02942	1.00000	0.02942
F02	573	10	0.04	1.00000	0.00000	0.00000
F03	513	40	0.04	0.82609	0.10526	0.08696
F04	573	40	0.08	1.00000	0.00000	0.00000
F05	543	25	0.06	1.00000	0.01016	0.01016
F06	543	25	0.06	1.00000	0.01108	0.01108
F07	543	25	0.06	1.00000	0.01041	0.01041

C.2 Effects of Process Variables Runs

RUN	R	C	S	Y
		W/F=10 hr g-cat/g-mol methanol		
	T = 513 K			
I11	0.04	0.08854	1.00000	0.08854
I12	0.06	0.10416	1.00000	0.10416
I13	0.08	0.11270	1.00000	0.11270
I14	0.10	0.12485	1.00000	0.12485
	T = 533 K			
I21	0.04	0.20932	1.00000	0.20932
I22	0.06	0.21978	1.00000	0.21978
I23	0.08	0.23747	1.00000	0.23747
I24	0.10	0.24057	1.00000	0.24057
	T = 553 K			
I31	0.04	0.43201	1.00000	0.43201

I32	0.06	0.43891	1.00000	0.43891
I33	0.08	0.46875	1.00000	0.46875
I34	0.10	0.49758	1.00000	0.49758

T = 573 K

I41	0.04	0.63576	1.00000	0.63576
I42	0.06	0.64474	1.00000	0.64474
I43	0.08	0.74806	0.80828	0.60465
I44	0.10	0.74681	0.74745	0.55821

T = 593 K

I51	0.04	0.91535	0.90164	0.82532
I52	0.06	0.93020	0.70950	0.65997
I53	0.08	0.97863	0.67172	0.65737
I54	0.10	0.96842	0.66584	0.64481

W/F=20 hr g-cat/g-mol methanol

T = 513 K

J11	0.04	0.19301	1.00000	0.19301
J12	0.06	0.20668	1.00000	0.20668
J13	0.08	0.22542	1.00000	0.22542

J14	0.10	0.22803	1.00000	0.22803

T = 533 K

J21	0.04	0.32780	1.00000	0.32780
J22	0.06	0.36201	1.00000	0.36201
J23	0.08	0.37500	1.00000	0.37500
J24	0.10	0.39615	1.00000	0.39615

T = 553 K

J31	0.04	0.58920	1.00000	0.58920
J32	0.06	0.61397	1.00000	0.61397
J33	0.08	0.60390	0.88936	0.53708
J34	0.10	0.63197	0.89508	0.56567

T = 573 K

J41	0.04	0.91337	1.00000	0.91337
J42	0.06	0.94880	0.84312	0.79995
J43	0.08	0.94965	0.80105	0.76072
J44	0.10	0.98424	0.79174	0.77927

T = 593 K

J51	0.04	1.00000	0.90341	0.90341
J52	0.06	1.00000	0.69455	0.69455
J53	0.08	1.00000	0.68569	0.68569

J54	0.10	1.00000	0.67880	0.67880

W/F=30 hr g-cat/g-mol methanol

T = 513 K

K11	0.04	0.24638	1.00000	0.24638
K12	0.06	0.31463	1.00000	0.31463
K13	0.08	0.32432	1.00000	0.32432
K14	0.10	0.33244	1.00000	0.33244

T = 533 K

K21	0.04	0.49756	1.00000	0.49756
K22	0.06	0.51571	1.00000	0.51571
K23	0.08	0.52128	1.00000	0.52128
K24	0.10	0.54444	1.00000	0.54444

T = 553 K

K31	0.04	0.69311	1.00000	0.69311
K32	0.06	0.74096	1.00000	0.74096
K33	0.08	0.74195	0.90490	0.67140
K34	0.20	0.77006	0.88798	0.68380

T = 573 K

K41	0.04	1.00000	0.97553	0.97553
K42	0.06	1.00000	0.85017	0.85017
K43	0.08	1.00000	0.81414	0.81414
K44	0.10	1.00000	0.76048	0.76048

W/F=40 hr g-cat/g-mol methanol

T = 513 K

L11	0.04	0.35563	1.00000	0.35563
L12	0.06	0.39080	1.00000	0.39080
L13	0.08	0.40239	1.00000	0.40239
L14	0.10	0.41695	1.00000	0.41695

T = 533 K

L21	0.04	0.67070	1.00000	0.67070
L22	0.06	0.69051	1.00000	0.69051
L23	0.08	0.70881	1.00000	0.70881
L24	0.10	0.71918	1.00000	0.71918

T = 553 K

L31	0.04	1.00000	1.00000	1.00000
L32	0.06	1.00000	0.93007	0.93007
L33	0.08	1.00000	0.89201	0.89201
L34	0.10	1.00000	0.85471	0.85471

T = 573 K

L41	0.04	1.00000	0.83583	0.83583
L42	0.06	1.00000	0.73686	0.73686
L43	0.08	1.00000	0.71234	0.71234
L44	0.10	1.00000	0.67029	0.67029

Appendix D

Results of Regression

The results of the linear regression of the modelling are presented in this Appendix. Samples of plots of the model having the best fit are also presented.

Ra is the actual rate, g-mol/s

Rp is the predicted rate, g-mol/s

k_1 is the first-step rate constant, g-mol/g-cat s atm^2

k_2 is the second-step rate constant, g-mol/g-cat s atm

pre is the percent relative error

Model 1 m = 2 & n = 1

T=513 K

k1	k2
0.54E-02	0.19E-05

W/F	R	Ra	Rp	pre
10	0.04	0.7477E-06	0.7511E-06	-0.46
10	0.06	0.8796E-06	0.8997E-06	-2.29
10	0.08	0.9517E-06	0.9614E-06	-1.02
10	0.10	0.1054E-05	0.9928E-06	5.83
20	0.04	0.1630E-05	0.1472E-05	9.69
20	0.06	0.1745E-05	0.1756E-05	-0.60
20	0.08	0.1904E-05	0.1892E-05	0.62
20	0.10	0.1926E-05	0.1939E-05	-0.70
30	0.04	0.2081E-05	0.2097E-05	-0.79
30	0.06	0.2657E-05	0.2583E-05	2.80
30	0.08	0.2739E-05	0.2762E-05	-0.84
30	0.10	0.2807E-05	0.2846E-05	-1.39
40	0.04	0.3003E-05	0.2752E-05	8.36
40	0.06	0.3300E-05	0.3300E-05	0.01
40	0.08	0.3398E-05	0.3527E-05	-3.81
40	0.10	0.3521E-05	0.3655E-05	-3.80

T=533 K

k1	k2
1.95E-02	0.36E-05

10	0.04	0.1768E-05	0.1641E-05	7.17
10	0.06	0.1856E-05	0.1816E-05	2.15
10	0.08	0.2005E-05	0.1895E-05	5.49
10	0.10	0.2032E-05	0.1911E-05	5.95
20	0.04	0.2768E-05	0.2977E-05	-7.55
20	0.06	0.3057E-05	0.3330E-05	-8.94
20	0.08	0.3167E-05	0.3456E-05	-9.14
20	0.10	0.3345E-05	0.3545E-05	-5.98
30	0.04	0.4202E-05	0.4228E-05	-0.62
30	0.06	0.4355E-05	0.4654E-05	-6.87
30	0.08	0.4402E-05	0.4800E-05	-9.04
30	0.10	0.4597E-05	0.4934E-05	-7.31
40	0.04	0.5664E-05	0.5365E-05	5.27
40	0.06	0.5831E-05	0.5900E-05	-1.18
40	0.08	0.5986E-05	0.6150E-05	-2.75
40	0.1	0.6073E-05	0.6270E-05	-3.24

T=553 K

k1	k2
5.26E-02	0.70E-05

10	0.04	0.3707E-05	0.3346E-05	9.72
10	0.06	0.3741E-05	0.3597E-05	3.87
10	0.08	0.3918E-05	0.3737E-05	4.61
10	0.10	0.4148E-05	0.3852E-05	7.12
20	0.04	0.4975E-05	0.5258E-05	-5.67
20	0.06	0.5185E-05	0.5654E-05	-9.06
20	0.08	0.5100E-05	0.5709E-05	-11.95
20	0.10	0.5337E-05	0.5858E-05	-9.78
30	0.04	0.5853E-05	0.6339E-05	-8.30
30	0.06	0.6257E-05	0.6815E-05	-8.91
30	0.08	0.6265E-05	0.6923E-05	-10.49
30	0.10	0.6503E-05	0.7082E-05	-8.90

T=573 K

k1	k2
14.3E-02	1.24E-05

10	0.04	0.5369E-05	0.5415E-05	-0.86
10	0.06	0.5444E-05	0.5676E-05	-4.26

10	0.08	0.6317E-05	0.6275E-05	0.66
10	0.10	0.6306E-05	0.6291E-05	0.24
20	0.04	0.7713E-05	0.7562E-05	1.96
20	0.06	0.8012E-05	0.7957E-05	0.68
20	0.08	0.8019E-05	0.8051E-05	-0.40
20	0.10	0.8311E-05	0.8265E-05	0.56
30	0.04	0.8444E-05	0.8090E-05	4.19

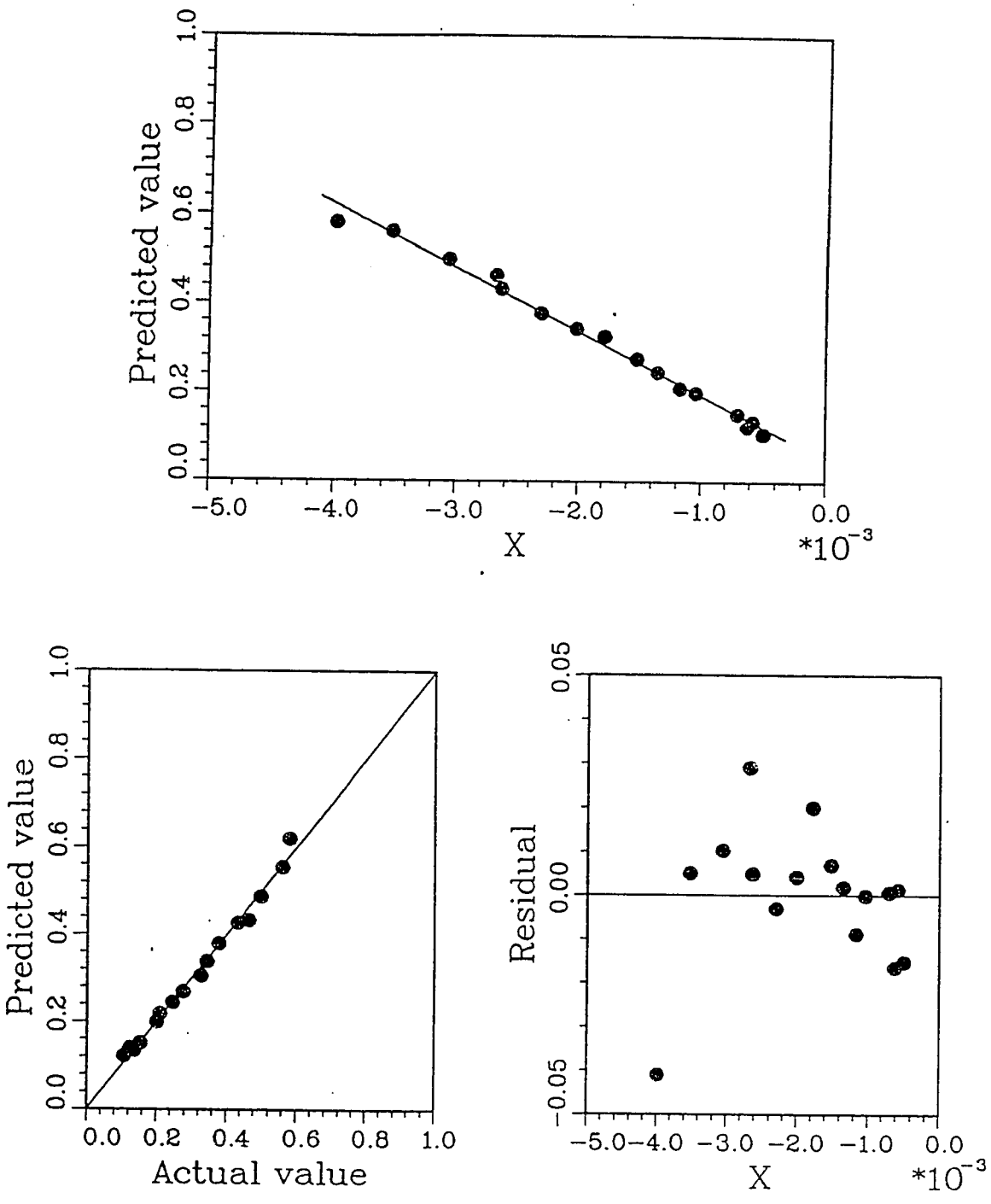

Figure D.1: Statistical analysis, m=2, n=1 at 513 K

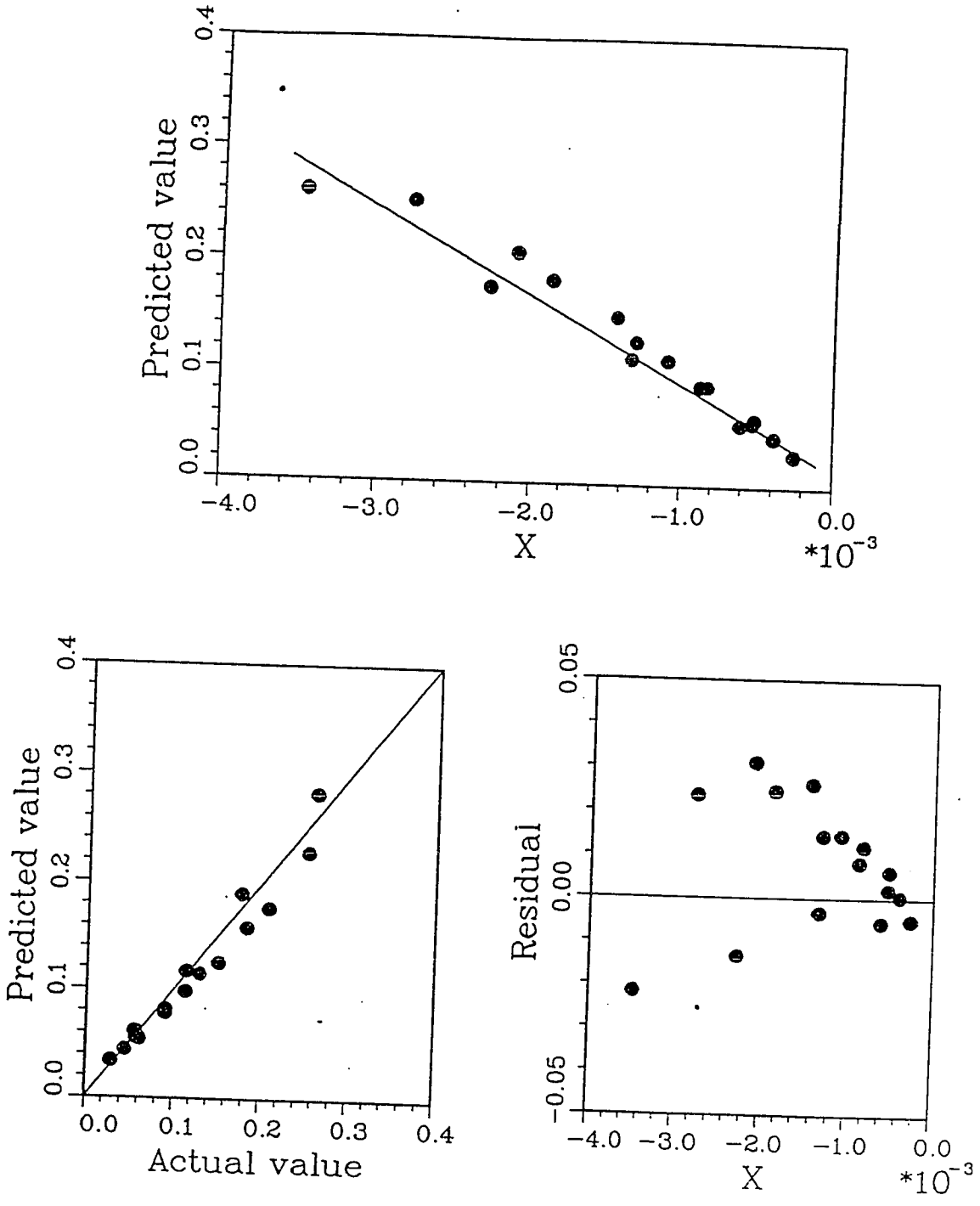

Figure D.2: Statistical analysis, m=2, n=1 at 533 K

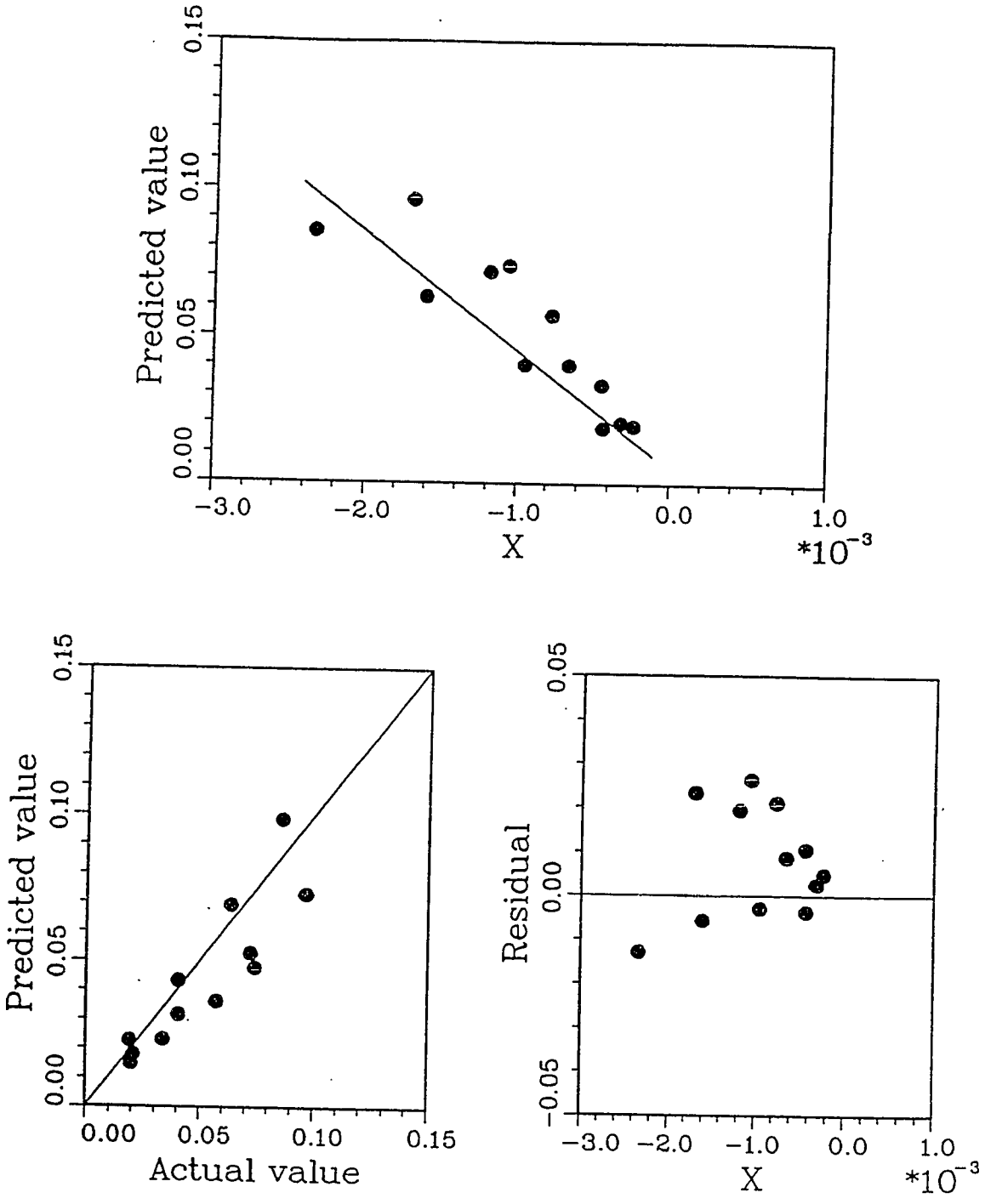

Figure D.3: Statistical analysis, m=2, n=1 at 553 K

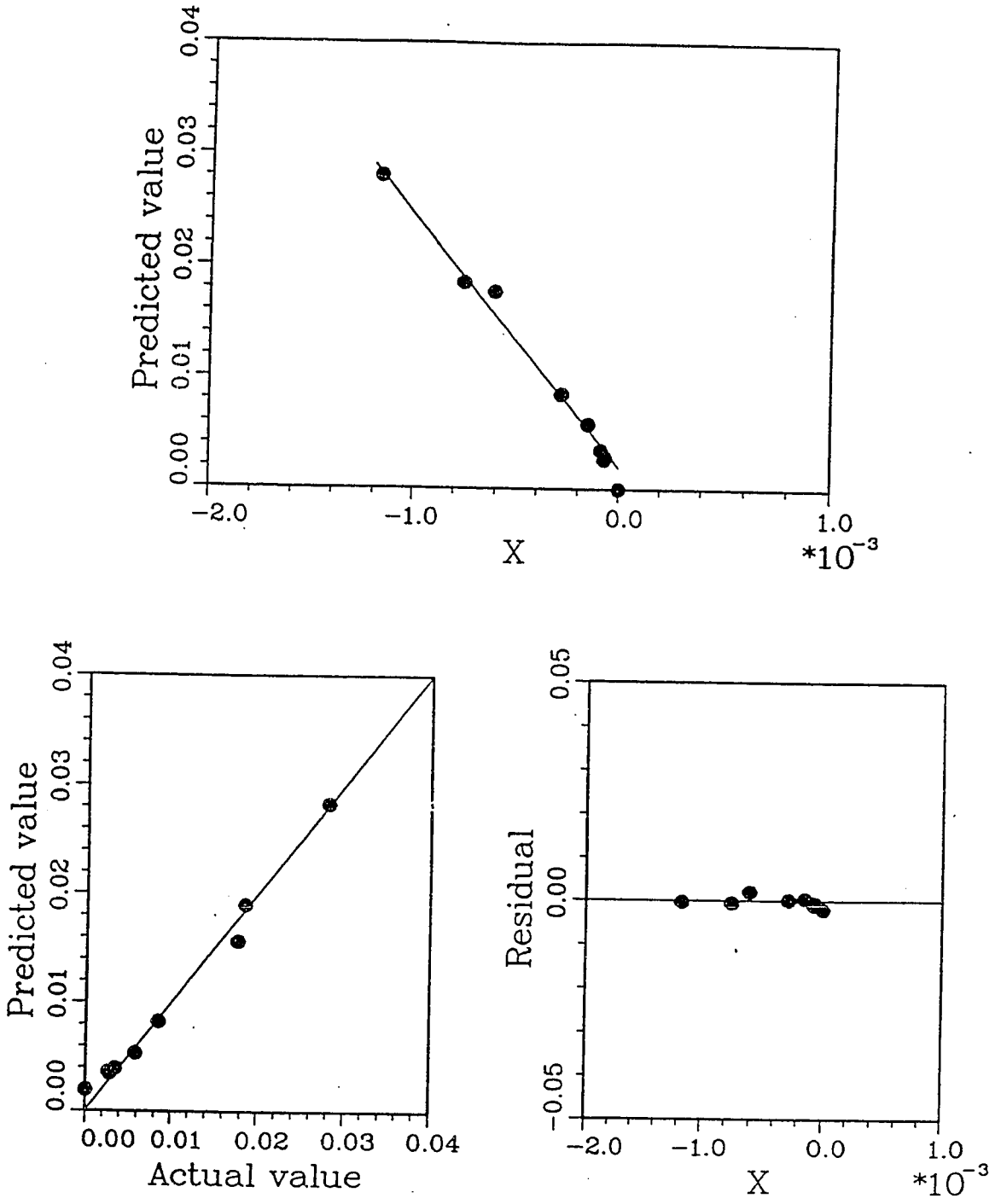

Figure D.4: Statistical analysis, m=2, n=1 at 573 K

Appendix E

Mass and Heat Transfer Effects

The calculations for the partial pressure drop between the main stream and the catalyst surface, as well as the calculations for the temperature drop from catalyst particle to ambient gas stream are presented in this appendix.

E.1 Mass Transfer Effects

The effects of mass transfer include the diffusion between the catalyst surface and the bulk fluid and the diffusion inside the pore itself.

E.1.1 External Diffusion

The estimation of the external diffusion is based on the method of Yoshida et al. [58]. The data for this estimation are taken from run L24. The conditions which apply for this run are as follows:

$$T = 533 \text{ K}$$

$$W/F = 40 \text{ hr g-cat/g-mol methanol}$$

$$R = 0.1 \text{ g-mol methanol/g-mol air}$$

$$W = 1.216 \text{ g}$$

ϕ = Shape factor (0.9 for irregular particles)

a_m =Surface area of catalyst per unit mass

=511649 cm^2/g

G_m =Molal mass velocity of gas based on the total cross section of the catalyst bed, g-mol/hr-cm^2

$=\frac{0.0304+0.304}{\pi(1.0/2)^2}=0.42577$

r_{mj} =Molal reaction rate per unit mass of the catalyst

r_{mM} $=\frac{(0.71918)(0.0304)}{1.216}=0.01798$ g-mol/hr g-cat

R_j =Dimensionless term of component j

$=\frac{r_{mj}}{a_m\phi G_m}$

R_M $=\frac{0.01798}{(511649)(0.9)(0.42577)}= 9.171 \times 10^{-8}$

$(y_j)_{in}$ =Mole fraction of component j in the feed

$(y_j)_{out}$ =Mole fraction of component j in the product

y_j =Mole fraction of component j at the interface

y_M $=\frac{0.0.91+0.028082}{2} = 0.059495$

$\frac{R_M}{y_M}$ $=\frac{9.171\times10^{-8}}{0.059495} = 1.541 \times 10^{-6}$

The value of $\frac{\Delta P_M}{P_M}$ is obtained from R_j versus $\frac{\Delta P_j}{P_j}$ given in Figure 2 by Yoshida et al. [58]. This value is much lower than 0.0001, hence the external diffusion effects are neglected. Note that M represents methanol in the above calculations. Similar

calculations were made for the other components, as shown in Table E.1, and all showed that $\frac{\Delta P_j}{P_j}$ is less than 0.0001.

Table E.1: Data for mass transfer effects

Component	$(y_j)_{in}$	$(y_j)_{out}$	y_j	r_{mj} $\frac{g-mol}{hrg-cat}$	R_j $\times 10^2$	$\frac{R_j}{y_j}$ $\times 10^8$	$\frac{\Delta P_j}{P_j}$ $\times 10^6$
O_2	0.194	0.156	0.175	0.91	4.61	0.263	$\ll$0.0001
CH_3OH	0.091	0.028	0.59	1.8	9.17	1.54	$\ll$ 0.0001
$HCHO$	0.0	0.063	0.032	1.8	9.18	2.9	$\ll$ 0.0001
H_2O	0.0	0.063	0.32	1.8	9.18	2.9	$\ll$ 0.0001

E.1.2 Internal Diffusion

Internal diffusion can be either molecular or pore diffusion.

Molecular Diffusion

The effect of molecular diffusion was verified by changing the feed velocity while keeping all the process variables constant. The effect of changing the feed velocity on conversion is shown in Table E.2

Table E.2: Variation of conversion with feed velocity

run number	temperature (K)	W/F	R	CH_3OH rate g-mol/hr	conversion (%)
P01	553	30	0.06	0.0152	49.76
P02	553	30	0.06	0.0304	51.57
P03	553	30	0.06	0.0752	52.13
P04	553	30	0.06	0.15193	50.51

Pore Diffusion

The effect of pore diffusion was studied by measuring the conversion of methanol at three runs of identical conditions but with different particle size. The results of these runs are shown in Table E.3. It was concluded that the pore diffusion is not controlling.

Table E.3: Variation of conversion with catalyst size

run number	temperature (K)	W/F	R	catalyst size (mm)	conversion (%)
Q01	553	30	0.06	0.2125	49.51
Q02	553	30	0.06	0.2735	51.31
Q03	553	30	0.06	0.3585	51.58

E.2 Heat Transfer Effects

Calculations of temperature drop from catalyst particle to ambient gas stream was carried out by using the method of Yoshida et al. [58]. The data of run K32 at W/F = 30 hr g-cat/g-mol feed were used for these calculations.

The heat capacities, C_p, of the product were estimated making use of the following equation

$$C_p = A + BT + CT^2 + DT^3 \tag{E.1}$$

The values of the constants A, B, C, and D are given in Table F.2

From standard thermodynamics

$$C_p = \sum_{j=1}^{n} C_{pj}\, y_j \tag{E.2}$$

thus

C_p at 553 K = 7.587 cal/g-mol K

Table E.4: Data for heat transfer effects

Component	A	B $\times 10^{-4}$	C $\times 10^{6}$	D $\times 10^{9}$	C_{pj} $\frac{cal}{g-mol\ K}$	y_j	ΔH_o^f $\frac{kcal}{g-mol\ K}$
O_2	6.713	-0.0088	4.170	-2.544	7.56	0.19	0.0
N_2	7.440	-32.4	6.40	-2.79	7.13	40.74	0.0
CH_3OH	5.052	169.4	6.179	-6.811	15.157	0.057	-48.08
$HCHO$	5.607	75.4	7.13	-5.494	11.03	0.021	-28.29
H_2O	7.701	4.595	2.521	-0.859	8.58	0.021	-57.8
CO	-	-	-	-	7.58	0.0	-26.41
CO	-	-	-	-	12.32	0.0	-94.05

The molal heat of reaction $-\Delta H$, per mole of methanol reacted was estimated using the group contribution Table E.4.

- Heat of reaction for formaldehyde production

$$\Delta H_1 = -57.8 - 28.28 + 48.08 + 0.0 = -38.01\ kcal/gmol$$

- Heat of reaction for formaldehyde conversion to CO

$$\Delta H_2 = -26.41 - 57.8 + 28.29 + 0.0 = -55.92\ kcal/gmol$$

- Heat of reaction for CO conversion to CO_2

$$\Delta H_3 = -94.05 - 57.8 + 28.29 + 0.0 = -123.56\ kcal/gmol$$

Since the selectivity is 100% for this case, the heat of reaction is:

$$-\Delta H = -\Delta H_1 = -38.01\ kcal/g-mol$$

The conditions that apply for this run are as follows:

T = 553 K

W/F = 30 hr g-cat/g-mol methanol

R = 0.06 g-mol methanol/g-mol air

W = 0.912 g

ϕ = Shape factor (0.9 for irregular particles)

a_m =Surface area of catalyst per unit mass

=511649 cm^2/g

G_m =Molal mass velocity of gas based on the total cross section of the catalyst bed, g-mol/hr-cm^2

$=\frac{0.0304+0.507}{\pi(1.0/2)^2}$=0.684239

r_{mj} =Molal rection rate per unit mass of the catalyst

r_{mM} $=\frac{(0.71918)(0.0304)}{0.912}$=0.0247 g-mol/hr g-cat

$$Q_M = \frac{-\Delta H\ r_{mM}}{a_m \phi C_p G_m} \tag{E.3}$$

$$Q_M = \frac{0.0247 \times 38.01}{511649 \times 0.9 \times 7.8586 \times 0.684239} = 3.93 \times 10^{-4}$$

From Figure 4 in the paper of Yoshida et al. [58], the value of ΔT that corresponds to this value of Q_M is less than 0.01 K, hence the catalyst surface temperature effect can be neglected.